1983

Cationic Ferritin Labeling Of Anionic Sites At Cellular Surfaces

Timothy Victor Brac

CANADIAN THESES ON MICROFICHE

I.S.B.N.

THESES CANADIENNES SUR MICROFICHE

National Library of Canada
Collections Development Branch

Canadian Theses on
Microfiche Service

Ottawa, Canada
K1A 0N4

Bibliothèque nationale du Canada
Direction du développement des collections

Service des thèses canadiennes
sur microfiche

NOTICE

The quality of this microfiche is heavily dependent upon the quality of the original thesis submitted for microfilming. Every effort has been made to ensure the highest quality of reproduction possible.

If pages are missing, contact the university which granted the degree.

Some pages may have indistinct print especially if the original pages were typed with a poor typewriter ribbon or if the university sent us a poor photocopy.

Previously copyrighted materials (journal articles, published tests, etc.) are not filmed.

Reproduction in full or in part of this film is governed by the Canadian Copyright Act, R.S.C. 1970, c. C-30. Please read the authorization forms which accompany this thesis.

THIS DISSERTATION
HAS BEEN MICROFILMED
EXACTLY AS RECEIVED

AVIS

La qualité de cette microfiche dépend grandement de la qualité de la thèse soumise au microfilmage. Nous avons tout fait pour assurer une qualité supérieure de reproduction.

S'il manque des pages, veuillez communiquer avec l'université qui a conféré le grade.

La qualité d'impression de certaines pages peut laisser à désirer, surtout si les pages originales ont été dactylographiées à l'aide d'un ruban usé ou si l'université nous a fait parvenir une photocopie de mauvaise qualité.

Les documents qui font déjà l'objet d'un droit d'auteur (articles de revue, examens publiés, etc.) ne sont pas microfilmés.

La reproduction, même partielle, de ce microfilm est soumise à la Loi canadienne sur le droit d'auteur, SRC 1970, c. C-30. Veuillez prendre connaissance des formules d'autorisation qui accompagnent cette thèse.

LA THÈSE A ÉTÉ
MICROFILMÉE TELLE QUE
NOUS L'AVONS REÇUE

NL-339 (r. 82/08)

Canada

CATIONIC FERRITIN LABELING OF ANIONIC SITES AT CELLULAR SURFACES

by

Timothy Victor Brac

Department of Zoology

Submitted in partial fulfillment
of the requirements for the degree of
Doctor of Philosophy

Faculty of Graduate Studies
The University of Western Ontario
London, Ontario
August, 1983

ABSTRACT

Cationic and anionic ferritins were used to map the distribution of charged sites on intracellular and extracellular surfaces. The distribution of tracers at cell surfaces and injected into live cells was examined by electron microscopy.

The distribution of microinjected ferritin, ranging in charge from anionic to highly cationic, showed that intracellular surfaces are negatively charged. Highly cationic ferritins (HCF > pI 9) were mostly bound to and caused swelling of the rough endoplasmic reticulum. Cationic ferritin (CF pI 7.0-8.0) and anionic ferritin (AF pI 4.0-4.4) caused no changes in morphology. Ferritin distribution in the cytoplasmic space varied with its charge. Significantly more CF was bound to surfaces than was found in the free cytoplasmic space. Conversely, there was significantly more AF in the free cytoplasmic space than close to surfaces. Comparison of the structures in the secretory pathway showed that there were no significant differences in the amount of CF (pI 7.0-8.0) bound. The Golgi complex beads were not distinguished by their charge. Differences in charge do not regulate membrane-membrane interactions in the secretory pathway.

The microinjection of cationic but not anionic molecules causes swelling of the rough endoplasmic

reticulum. Calcium buffers, lanthanum chloride, lysozyme, bovine serum albumin, highly cationic and anionic ferritin were microinjected into salivary gland cells and their effects observed by light and electron microscopy. Immediately after the microinjection of polycationic molecules, the cytoplasm changed from transparent to opaque as the rough endoplasmic reticulum became swollen. Binding of polycationic molecules to the rough endoplasmic reticulum may cause the membrane to become permeable to certain solutes and swell due to osmotic forces.

Clusters of anionic sites, labeled by HCF, are present throughout the basal lamina. The penetration of ferritins, with a range of charges from anionic to highly cationic, through the basal lamina into the spaces between fat body cells varies with the charge of the tracer. Cationic ferritins penetrated the basal lamina and bound to anionic sites on membrane surfaces. Little anionic ferritin was found in the spaces surrounding the fat body. The basal lamina therefore acts like a negatively charged sieve to control the composition of the fluid that bathes the fat body cells. More CF was bound to the membranes of the plasma membrane reticular system than to the lateral plasma membranes, suggesting that there are regional differences in surface charge.

HCF bound to the fat body plasma membrane and showed the fate of the membrane as it turned over. After

pinocytosis by coated vesicles, the first sites of intracellular accumulation were multivesicular bodies which became filled with HCF between 30-60 min after the cells were exposed to the tracer. By 60 min, the HCF was increasingly found in lamellar bodies that are presumed to form from multivesicular bodies. At no time during the experiments were any parts of the Golgi complex labeled with the tracer, ruling out direct membrane recycling. Since lamellar bodies occur in many other cell types, they may have a general role in membrane dynamics.

DEDICATION

I dedicate this thesis, with love, to Marg and Eric,

ACKNOWLEDGEMENTS

I thank my supervisor, Dr. Michael Locke, for providing an environment that challenged me to think and do this work. His probing mind and guiding direction have radically changed not only the way I view science but the rest of the world of which it is a part. The members of my advisory committee, Dr. S. Caveney and Dr. J. E. Steele provided guidance and much needed criticism during the course of this work.

I would like to thank Dr. H. G. Rennke for providing me with some of the tracers that made this work possible and also for the chance to visit his laboratory. Dr. R. Tanguay sent me many egg masses of Chironomus tentans to help start a culture. Dr. R. Podesta kindly read this thesis and I am grateful for all his suggestions.

Many people in the laboratory have influenced this work and I am grateful to them. Phil Huie, Helen Kirk, Lora Wilkie, Dr. David Brodie, Dave Webster, Jeff McClintock, Heather McDermid and Sylvia Franzl provided ideas, help and friendship.

I also thank N.S.E.R.C. and the Ontario government for financial assistance.

Finally, I thank the governments of the U.S.A and U.S.S.R. for giving me enough time to finish this work. I

hope that the mutual mistrust that pervades present attitudes will give way to agreements that halt the production, testing and stockpiling of the most serious threat to humankind, nuclear weapons.

TABLE OF CONTENTS

LIST OF TABLES

LIST OF FIGURES

LIST OF FIGURES (cont')

LIST OF FIGURES (cont')

LIST OF FIGURES (cont')

LIST OF FIGURES (cont')

LIST OF FIGURES (cont')

LIST OF FIGURES (cont')

CHAPTER 1. INTRODUCTION

The evolution and proliferation of life has been dependent on the ability of cells to control and segregate the reactions necessary for growth and differentiation. The development of limiting membranes was a necessary step in the origin of self-replicating cells (Alberts et al., 1983). The organization of molecules into structures for specific functions is governed by physicochemical principles that can be demonstrated in model systems. For example, the hydrophobic effect causes spontaneous aggregation of phospholipids into bilayers under the appropriate conditions (Tanford, 1979). The proliferation of interfaces at various levels of organization suggests that their properties may play an important role in the organization and function of cells. It is well established that the properties of surfaces differ enormously from the surrounding medium (Bangham, 1981) and in this way provide an environment for metabolic and regulatory activity. The charge at cellular interfaces plays a major role in determining its properties (Jones, 1975; McLaughlin, 1977; Sherbet, 1978) and in this way is of prime importance in the consideration of surface properties.

Surface charge of macromolecules and aggregates of macromolecules may have a role in cell function at several levels of organization. These include:

1) molecule/solution e. g. the electrophoresis of charged

proteins through intercellular bridges (Woodruff and Telfer, 1973; 1980),

2) molecule/ion, molecule/molecule, e. g. the binding of calcium by calmodulin (Cheung, 1980), the binding of histones to DNA (Busch, 1965; Earnshaw et al., 1980)

3) membrane/solution e. g. regulation of membrane bound enzymes (Wojtezak and Nalecz, 1979; Famulski et al., 1979; Nalecz et al., 1980), ion selectivity (Diamond and Wright, 1969; Diamond, 1975),

4) membrane/membrane, e. g. membrane fusion (Papahadjopoulos, 1978; Ekerdt et al., 1981), cell to cell contact (Deman et al., 1974; Wright et al., 1980), thylakoid stacking in photosynthesis (Barber, 1980),

5) extracellular matrix/solution e. g. permeability of the basal lamina (Rennke et al., 1975; 1978; Rennke and Venkatachalam, 1977).

In Chapter 1, the nature and function of surface charge will be examined and be related to the specific objectives of this thesis.

1.1 Anionic sites, surface charge and surface potential

The term surface layer refers to the three-dimensional region of contact between two homogenous phases in which molecules and ions can interact with either phase (Levine, 1978; James, 1979). The molecules and ions in this surface layer will show properties that differ from those

in the bulk phases (McLaughlin, 1977; James, 1979). The surface can be described as a series of shells that merge into one another in response to the molecular organization and properties of the cellular surface (James, 1979). The resulting interface is an ionic atmosphere held in the area by the ionic groups at the surface of the cell (James, 1979). The characteristics of interfaces can vary depending on the level of organization.

Cellular surfaces predominantly have a net negative charge which has an important influence on the properties of the interface (Weiss, 1969; McLaughlin, 1977; Sherbet, 1978). Anionic sites are the exposed functional groups of molecules that form the interface between two compartments. Charges may also be induced or altered by ion adsorption (Lis et al., 1981a, 1981b). Surface charge, which is measured in units of negative charge, is the net charge of the structure and is the result of the relative number of anionic and cationic sites (Sherbet, 1978). Surface potentials are the result of the redistribution of mobile charged ions and molecules at the interface caused by the surface charge. This unequal distribution of charge-carrying molecules results in an electrical potential difference between the bulk and surface phases of the solution, that is measured in millivolts (McLaughlin, 1977).

Biophysical techniques such as particle electrophoresis measure the surface potential and related properties (Sherbet, 1978; James, 1979). Charged tracers used for electron microscopy may be attracted or repelled by the surface potential and may bind electrostatically to charged sites (Burry and Wood, 1979; Feder and Glaever, 1980).

1.2 The ultrastructural localization of charged sites

Ultrastructural techniques give specific information about the distribution of charged groups and their relative contribution to membrane surface charge. Cationic electron-dense tracers such as ruthenium red (Luft, 1971a; 1971b), alcian blue (Behnke and Zelander, 1970) and ionic lanthanum (Shea, 1971; Shaklai and Tavassoli, 1982) have been used in tissue fixatives as markers for charged sites. It has been claimed that ruthenium red is a specific marker for acidic polysaccarides that contain sialic acid and hyaluronic acid (Dorscheidt-Kafer, 1979a; 1979b; Simonneau et al., 1980). The results of Luft (1971a, 1971b) show that ruthenium red, as a hexavalent polycation, binds to a large variety of polyanions by electrostatic interactions and is therefore not specific.

The labeling of the cell surface (Kahane et al., 1978) and the basal lamina (Cohn et al., 1977) with ruthenium red results in a layer or large clusters of dense amorphous

material. Quantitative analysis is not possible. A major drawback of ruthenium red is that is must be included in the fixative and subsequent preparative steps until the tissue is postfixed in osmium tetroxide (Luft, 1971a).

Ionic lanthanum has been used as an electron dense marker for anionic sites (Doggenweiler and Frenk, 1965; Heuser and Miledi, 1971; Morris and Schober, 1977) since it may mimic the binding of calcium (Weiss, 1974; Sauerheber et al., 1980). Lanthanum has a hydrated radius of 0.31 nm and is similar to that of calcium (0.28 nm) (Nayler and Harris, 1976). As with ruthenium red, lanthanum is usually included in the fixative and subsequent steps (Doggenweiler and Frenk, 1965). This suggests that the lanthanum may detach during processing for electron microscopy. Since ruthenium red and lanthanum must be included in the tissue fixative in order to localize anionic sites, their usefulness is limited.

Gasic et al. (1968) developed the use of colloidal iron, both positively and negatively charged, for detecting surface charge on prefixed cells at pH 1.8. It was shown that neuraminidase pretreatment removed most of the positive colloidal-iron binding of the cell surface (Gasic et al., 1968). Since the pKa of the sialic acid carboxyl groups not low enough for it to be negatively charged at pH 1.8 (Nordt, 1980), it is doubtful that the distribution of sialic acid was examined. Colloidal iron has also been

used to examine the charged sites on fractionated cellular surfaces (Virtanen and Wartiovaara, 1974; Feria-Velasco et al., 1976). The use of unphysiological pH in these investigations also make the results questionable. Therefore, results using colloidal iron can be questioned on the grounds that the cells were prefixed and labeling was done at low pH where most ionogenic groups would not be charged. Prefixation with glutaraldehyde can modify and redistribute charged sites (Grinnell et al., 1976; Burry and Wood, 1979).

The development of cationized ferritin (CF) by Danon et al. (1972) allowed the localization of anionic sites on living cells. Ferritin is an iron storage protein with a distinctive shape, a property which allows individual molecules to be recognized by electron microscopy. The size of ferritin is 11 nm in diameter with an iron core of 6 nm (Harrison et al., 1967). In addition, modification of the carboxyl groups with tertiary amines causes a change in the isoelectric point from 4.0-4.4 to 7-10 (Danon et al., 1972; Rennke et al., 1975) depending on the conditions of the reaction.

CF has been used to examine the distribution of anionic sites on cell surfaces (Pinto da Silva et al., 1973; Grinnell et al., 1975; Borysenko and Woods, 1979; Walker, 1981) and subcellular fractions (Abe et al., 1976; Eagles et al., 1976; Howell and Tyhurst, 1977). Since CF

binds to the cell surface it can act as a surface marker to trace the fate of the plasma membrane (Farquhar, 1978). However, the ability of anionic ferritin (AF) to detect cationic sites is disputed. Some researchers have reported that AF does not bind to the cell surface (Danon et al., 1972; King and Preston, 1977; Farquhar, 1978; Borysenko and Woods, 1979) while others have found consistent labeling (Burry and Wood, 1979; McNeil et al., 1981). It is possible that there is variation between different cell types but it is likely that under most conditons the net negative surface charge of cell membranes would repel AF and prevent binding to surface cationic sites.

Two important considerations in examining CF binding to cellular surfaces are:

1)what functional groups does CF bind

2)does the binding of CF cause a redistribution of anionic sites?

Some researchers (Abe et al., 1976; Sturgess et al., 1978) consider CF to act as a marker for sialic acid. In vitro tests of CF binding show that the reaction is non-specific with respect to the negatively charged group (Burry and Wood, 1979; Feder and Giaever, 1980). Using Sepharose-activated latex beads covered with substrate, CF was found to bind to sialic acid, the carboxyl groups of proteins and phosphate groups of phospholipids (Burry and Wood, 1979).

The binding of CF causes the redistribution of surface anionic sites at the cell surface (Ben-Ishay et al., 1975; Grinnell et al., 1975, Moller and Chang, 1978; Petty, 1980; Butman et al., 1980) but not on fractionated intracellular organelles (Eagles et al., 1976; Howell and Thyhurst, 1977). Mitochondrial outer, but not inner membranes are sensitive to CF-induced redistribution (Hackenbrock and Miller, 1975; Hochli and Hackenbrock, 1977). The fluidity of the membrane may regulate the clustering of surface anionic sites (Shinitzky and Henkart, 1979).

In interpreting the binding patterns of CF to surfaces it is important to note that electrostatic potentials of point charges in aqueous solutions are virtually reduced to zero at distances above 10 nm (Rand, 1981). CF binding reveals short-range electrostatic interactions and it therefore visualizes the distribution of clusters of anionic sites since one CF molecule may bind to many anionic groups (Danon et al., 1972; King and Preston, 1977). Examination of the pattern of ferritin binding using ferritins ranging in charge from anionic to cationic, can give information on the polarity and field strength of the surface charge.

1.3 Correlation of ultrastructural and biophysical methods of surface charge measurement

Biophysical techniques such as particle electrophoresis, isoelectric focussing, and two-phase aqueous partitioning are all influenced by net surface charge (Sherbet, 1978). While these techniques are sensitive, they can only give information about the net charge and not the physical distribution of the charged sites (Burry and Wood, 1979).

Order of magnitude comparisons of the number of anionic sites determined by CF binding and particle electrophoresis give comparable values (King and Preston, 1977; Walker, 1981). Similarly, the use of radioactively labeled CF has given results comparable to biophysical techniques (Grinnell and Hays, 1979).

1.4 Membrane surface charge may regulate membrane/membrane interactions

The likelihood of two membranes being able to come into contact can be estimated by applying the Derjaguin-Landau-Verwey-Overbeek (DLVO) theory of lyophobic colloidal particle interaction (Derjaguin and Landau, 1941; Verwey and Overbeek, 1948). There are detailed reviews on the applicability of this theory in biological systems (Parsegian, 1973; Dean, 1974; 1975; Dean and Matthews,

1975; Gingell and Ginsberg, 1978) but the main considerations are that the size and charge of the biological particles are in the right range for the application of DLVO theory.

The DLVO theory is based on studies of the interaction between the electrical double layers (also known as the Guoy-Chapman and Stern layer) that form at a charged interface in contact with a salt solution (Dean, 1974). Since most cellular surfaces have a net negative charge, the electrical double layer will consist of the attraction of counter ions (cations) and the repulsion of anions (Dean, 1974). The actual dimensions of the double layer depends inversely on the salt concentration (Dean, 1974). The rate of aggregation is governed by the interplay of repulsive and attractive forces between particles (Dean, 1974; Gingell and Ginsberg, 1978). The repulsive forces have their origin in the electrical double layer that surround the particles. No interaction occurs when the particles are far apart but on close approach of the two double layers, repulsion is encountered (Dean, 1974). Modulation of surface charge by divalent cations such as calcium may be important in regulating the repulsive forces (Dean and Matthews 1974, Papahadjopoulos, 1978).

Attractive forces arise from electrodynamic interactions involving long range London-Van der Waals forces which are a property of all molecules (Dean, 1974;

Parsegian, 1973). The total interaction energy is derived from the summation of repulsive and attractive energies (Parsegian, 1973; Dean, 1974; 1975). Since the concentration of charge-carrying ions is important in determining the structure of the surface double layer, it becomes a key consideration in DLVO theory.

Therefore, in the simplest situation, the physical factors that regulate the interaction of two charged surfaces will be London-Van der Waals forces of attraction and electrical double layer forces of repulsion. Reduction of the negative surface charge will reduce the repulsive forces and increase the probability of interaction. This is complicated by the fact that the London attractive energies are additive and operate at distances larger than electrostatic forces (Dean and Matthews, 1975). In the energy curves for the total interaction between particles repulsive forces have the feature of an exponential function with a range on the order of the thickness of the double layer (in the order of nanometers) (Dean and Matthews, 1975). Attractive forces decrease as an inverse power of the distance, and thus will predominate at very small and very large distances (Dean and Matthews, 1975). These electrostatic and electrodynamic forces have been recognized as playing an important role in membrane/membrane interactions such as vesicle/vesicle (Haynes et al., 1979; Morris et al., 1979), vesicle/cell

(Dean, 1975; Plattner, 1978) and cell/cell interactions (Deman et al., 1974; Wright et al., 1980).

Extensive work on the role of these forces in membrane interactions have been done using model phospholipid membranes where the results support the theory of the electrical double layer and its role in DLVO colloidal interactions (McLaughlin, 1977; Gingell and Ginsberg, 1978; Rand, 1981). However, more recent evidence suggests that the DLVO theory is untenable at close membrane contacts (<3 nm) where repulsive forces due to hydration barriers far outweigh electrostatic and electrodynamic forces (Rand, 1981).

At the cellular level, charge differences may play a role in the interaction between different surfaces. In the hierarchy of membrane interactions that are involved in the secretory pathway, higher negative surface charge may prevent some membranes from close contact and fusion. Attractive forces can arise between particles with non-identical surface charges (Bierman, 1955). Measurement of the isoelectric point of microsomes stripped of their ribosomes showed that they had a lower negative surface charge than the plasma membrane of Ehrlich ascites cells (Wallach et al., 1966). Comparison of the surface charge of fractionated liver cells by free flow electrophoresis gave the contradictory conclusion that microsomes without ribosomes did not differ significantly in surface charge

from plasma membrane vesicles (Blad-Holmberg, 1979).

The surface charge of synaptic vesicles and synaptosomes have been compared by free flow electrophoresis and electrophoretic light scattering (Ryan et al., 1971; Siegal and Ware, 1980). Free flow electrophoresis showed that the synaptosomes had a higher negative surface charge than the synaptic vesicles while electrophoretic light scattering showed that the synaptic vesicles had a higher negative surface charge.

Comparison of fractionated intracellular membranes of rat kidney proximal tubule cells showed that plasma membrane, microsomes and lysosomes migrated with different velocities in an electric field (Heidrich et al., 1972; Hannig et al., 1974). Since there was a large amount of overlap between membranes, it was not possible to interpret the surface charge of membranes in terms of the current model of membrane-membrane interactions in the secretory pathway (Hannig et al., 1974).

Since most studies to date have used fractionated cell membranes, with varying degrees of attention paid to the purity of the fractions used, it is difficult to make definitive conclusions on possible differences in surface charge. However, it is important to use different techniques to examine whether surface charge differences exist between intracellular membranes. Microinjection of

ferritin, ranging in charge, into whole cells has not been used but it offers a novel way of examining the charge of intracellular surfaces.

1.5 The basal lamina may act as a charged sieve

The basal lamina is a connective tissue layer, common to both vertebrates and invertebrates, that surrounds all cells except blood cells (Heathcote and Grant, 1981). Its location at the surface of the cell that synthesizes it, suggests the basal lamina has an important role in cell and tissue scaffolding (Banerjee et al., 1977; Bernfield and Banerjee, 1978). The presence of anionic sites in the basal lamina have been demonstrated in cells of the kidney glomerulus (Rennke et al., 1975; Caulfield and Farquhar, 1976; Kanwar and Farquhar, 1979a), wax moth neural lamella (Dybowska and Dutkowski, 1977) and fat body (Dutkowski, 1977), mouse salivary glands (Cohn et al., 1977), pancreas and intestinal mucosa (Simionescu et al., 1982) and cultured cells (Leivo, 1983).

The function of the anionic sites has been demonstrated clearly for the kidney glomerulus where they act as a charge barrier to prevent anionic plasma proteins from entering the forming urine (Deen et al., 1983). It is not clear if this is a general function of anionic sites on the basal lamina or a case of specialization to fill a specific function.

The anionic sites of kidney glomerular basal lamina have been identified as heparan sulfate by enzyme digestion (Kanwar and Farquhar, 1979b) and isolation from tissue fractions (Kanwar and Farquhar, 1979c). The presence of glycosaminoglycans in basal laminae have been shown in insects (Ashhurst, 1982; Telfer et al., 1982), rat duodenum and incisor tooth (Laurie et al., 1982) and rat salivary gland (Bernfield and Banerjee, 1972). Because of the physical properties of glycosaminoglycans, there may result an unequal distribution of ions between the basal lamina and the fluid surrounding it. The glycosaminoglycans have a net negative charge, high charge density and gel-like consistency because of their large branched structure and negatively charged sulfate groups (Chakrabarti and Park, 1980). Therefore, the glycosaminoglycans are well suited to influence the electrical properties of tissues (Laurent, 1977; Comper and Laurent, 1978).

One consequence of the presence of immobilized charged molecules in basal laminae is that they introduce a Donnan type of ion distribution between compartments (Comper and Laurent, 1978; Dow et al., 1981). The concentration of cations will be greater in the basal lamina as compared to the fluid in which it is bathed. Electron-microprobe analysis has shown higher concentrations of potassium in the basal lamina of Calliphora salivary glands than in the

fluid on either sides of the basal lamina (Gupta et al., 1977). The polyanionic properties of basal laminae may act like ion exchange resins and therefore affect the distribution of charged molecules available to cells

The physiological significance of the electric potential differences, arising from the redistribution of ions between the basal lamina and the fluid in which it is bathed, has not been studied. Cell attachment and migration may be influenced by basal laminae (Nardi, 1983) since cell surface charge is important in the locomotion of cells on substrates (Ebbesen and Guttler, 1979; Weinberger and Brick, 1980). It is important to examine the distribution of anionic sites and to determine their function. The results of work on the basal lamina (Rennke et al., 1975; 1978; Rennke and Venkatachalam, 1977) have clearly shown that the anionic sites act as a charged sieve in the movement of charged proteins. It is not known whether this is a general function of the basal lamina. The fat body is an ideal cell type to examine the distribution and function of anionic sites of the basal lamina since this cell is involved in protein secretion and uptake (Dean et al., 1984).

1.6 Thesis Aims

In order to correlate cell structure and function with interfacial charge properties, I have used the charged

tracer ferritin as a marker for surface charge. The distribution and function of charged sites at several levels of organization were examined.

The aim of this thesis will be to answer the following questions:

1) Can microinjection of charged tracers be used to examine the distribution of charged sites at intracellular interfaces?

2) Does the charge of the tracer molecule affect its distribution in the cytoplasmic space?

3) Do different surfaces of the secretory pathway have different charges?

4) What effect does the binding of the charged tracers have on the structure of the intracellular surfaces?

5) What is the distribution of charged sites at the external cell surfaces, such as the plasma membrane and basal lamina, and are there regional specializations?

6) What is the function of the charged sites on the basal lamina?

7) Can the binding of tracers to the plasma membrane be used to examine the fate of the membrane as it is turned over?

The experiments examining the intracellular charge distribution were done using the salivary gland cells of Chironomus tentans (Diptera:Chironomidae) since they were an ideal system for in vitro studies and microinjection

(Lambert and Daneholt, 1975; Grossbach, 1977). Experiments examining the distribution of charged sites at the cell surface were done on the fat body of fifth instar larvae of Calpodes ethlius (Lepidoptera:Hesperiidae).

CHAPTER 2

THE DEVELOPMENT OF A TECHNIQUE FOR THE MICROINJECTION OF TRACERS INTO CELLS WHILE MAINTAINING THEIR VIABILITY

2.1 Introduction

The distribution and nature of charged sites at biological interfaces plays an important role in determining surface properties (Jones, 1975; McLaughlin, 1977). In order to determine whether it is possible to examine the intracellular distribution of charged sites I have developed a simple method for the microinjection of the secretory cells of the salivary gland of *Chironomus tentans*.

The tracer horseradish peroxidase (HRP) can be visualized by the light and electron microscope, thus facilitating identification of microinjected cells for electron microscopy (Straus, 1964; Graham and Karnovsky, 1966). Although commercial preparations contain a variety of isozymes ranging in charge (Rennke and Venkatachalam, 1979), HRP has been reported to bind to surface anionic sites (Bock, 1972; Kenny and Shivers, 1974; Kessel and Ganion, 1979). However, Davies *et al.* (1981) found that neither native or cationic horseradish peroxidase bound to the cell surface of cultured endothelial cells.

The results show that the HRP reaction product diffused in the cytoplasm of the injected cell and was not found in any adjacent cells. Examination by electron microscopy showed that the reaction product was bound to the intracellular surfaces. Although these results show that it is possible to microinject tracers inside intact cells, the diffusion of the reaction product may limit conclusions about the actual distribution of the HRP.

2.2. Materials and Methods

(a) Rearing C. tentans

Eggs rafts of C. tentans were allowed to hatch in plastic tubs filled with tap water containing a layer of sand and ground filter paper. The larvae were fed twice weekly on ground fish food. Under an 18 hour day / 6 hour night cycle, the larvae reached the adult stage in 6 to 8 weeks.

(b) Culturing of salivary glands

Salivary glands of the fourth larval instar were used in all experiments. The salivary gland cells are large polytene cells that specialize in the synthesis of secretory proteins (Grossbach, 1977; Hertner et al., 1980; Mahr et al., 1980). The secretory proteins form a gelatinous substance that is used to trap food particles

and make tubes in which the larvae live (Lambert and Daneholt, 1975). The large size (100-200 um in diameter) of Chironomus salivary gland cells has facilitated studies using microdissection (Edstrom and Lonn, 1976; Lonn and Edstrom, 1976; Vincent and Tanguay, 1979), microinjection (Paine, 1975) and the analysis of the components involved in the synthesis of the secretory proteins (Lamb and Daneholt, 1979; Andersson et al., 1980; Edstrom et al., 1980; Olins et al., 1980; Rylander and Edstrom, 1980; Rylander et al., 1980).

Large larvae (20 to 30 mm in length and dark red in colour) living in tubes were selected. Larvae were washed in tap water and placed in a drop of culture medium (87 mM NaCl, 2.7 mM KCl, 1.3 mM $CaCl_2$, 10 mM HEPES, pH 7.1). When the head was pulled off, the large paired salivary glands came out of the body attached to the salivary gland ducts. The glands were transferred rapidly to a fresh drop of culture medium in a Falcon 1004 petri dish (Falcon, Oxnard, CA). The salivary glands adhered tightly to clean plastic, thus facilitating microinjection.

(c) Tracers

HRP (Worthington Enzymes, pI 7-8) was suspended in injection buffer (100 mM KCl, 5 mM HEPES, pH 7.0) to a final concentration of 1 mg/ml as determined spectrophotometrically using the standard that 1 mg/ml has

an absorbance of 2.275 at a wavelength of 403 nm (Rennke and Venkatachalam, 1979).

(d) Microinjection

A 50 ml plastic syringe, filled with paraffin oil, was connected to polyethylene tubing by a 20 gauge needle. Micropipettes pulled for electrophysiology were modified by breaking the tip with a pair of fine tweezers. These were filled with tracer and connected to the polyethylene tubing, excluding all air bubbles. The micropipette was attached to a Prior micromanipulator (Prior Instruments, England). The volume of HRP injected was estimated by measuring the size of a drop of tracer appearing in paraffin oil under the same conditions used to inject cells. From 50,000 to 100,000 μm^3 was injected into each cell. This corresponds to 5-10% of the cell volume (Paine, 1975; Egyhazi et al., 1980).

Salivary glands were viewed at a total magnification of 100 in darkfield illumination of a Zeiss photomicroscope. The tip of the micropipette was put into the same focal plane as the basal surface of the cell. The micropipette was slowly advanced until it penetrated the plasma membrane and the tip became visible within the cytoplasm. The tracer was then injected and the micropipette withdrawn. The injected cell was identified on a map of the salivary gland.

(e) Fixation and Processing

From 5 to 30 minutes after microinjection, the culture medium was removed and the gland was flooded with ice cold 5% glutaraldehyde in 0.1 M phosphate buffer, pH 7.4, and fixed for 1 hour. After rinsing in the same buffer, the gland was washed in Tris-HCl buffer pH 7.6. The tissue was incubated in 0.03% diaminobenzidene free base in 0.1 M Tris-HCl pH 7.6 on a rotary shaker at room temperature. After 10 min, 30% H_2O_2 was added to make the solution 0.03% in concentration (Locke and Collins, 1968). The tissue was shaken for a further 6 min. After washing in Tris buffer, the glands were photographed with a Zeiss photomicroscope and then processed for electron microscopy.

The glands were postfixed in a vial containing 1% osmium tetroxide in 0.1 M phosphate buffer, pH 7.4 for 1 hour on ice. The gland was carefully washed in buffer and then in distilled water. It was then dehydrated in a graded series of alcohols, washed in propylene oxide and embedded in Araldite (R. P. Cargille Laboratories, Inc., Cedar Grove, NJ).

(f) Electron Microscopy

Thin sections of gray interference colour were cut on a diamond knife and mounted on 400 mesh copper grids. For photography, sections were viewed without further

enhancement of contrast or stained in in uranyl acetate (Locke and Huie, 1980) for 5 minutes. Micrographs were taken on a Philips EM 300 at 80 kV.

2.3 Results

(a) Cell viability after microinjection

Microinjected cells excluded trypan blue dye when tested for viability. The stucture of injected cells was a more sensitive indicator of the effects of microinjection since cells that showed changes suggesting damage (such as swollen rough endoplasmic reticulum) continued to exclude trypan blue dye (see Chapt. 4).

(b) Localization of HRP

HRP-injected cells were identified by the dark black reaction product in the cytoplasm. When cells were injected with a large amount (about 20-30% of the cell volume the reaction product filled the entire cytoplasm (Fig. 1). Injection of HRP into the gland lumen outlines the shape of the individual cells (Fig. 2). When HRP was injected into the nucleus and left for 30 min before fixation, the reaction product was confined to the nucleus (Fig. 3).

Fig. 1. HRP-injected cell in Chironomus tentans salivary gland. After pressure microinjection of about 25% of cell volume with 1 mg/ml HRP solution, the cell was fixed and reacted with diaminobenzidene-H_2O_2. The dense reaction product fills the cytoplasm. Bar=50 µm, x165.

①

Fig. 2. Microinjection of HRP into the salivary gland lumen. A large excess of 10 mg/ml HRP solution was injected into the lumen of the salivary gland, fixed and reacted diaminobenzidene-H_2O_2. The reaction product outlines the individual cells. Bar=100 μm, x90.

Figs. 3-5. Diffusion of HRP reaction product in the nucleus and cytoplasm.

Fig. 3. HRP was microinjected into the nucleus and left for 30 min before fixation and reaction with diaminobenzidene-H_2O_2. The reaction product is confined to the nucleus. Bar=100 μm, x160.

Fig. 4. A cell that has been microinjected with 10% of its volume and fixed 30 sec later shows the reaction product mainly around the point of injection. Bar=50 μm, x380.

Fig. 5. A cell that has been microinjected with 10% of its volume and fixed 30 min later shows the reaction product dispersed throughout the entire cytoplasm. Bar=50 μm, x380.

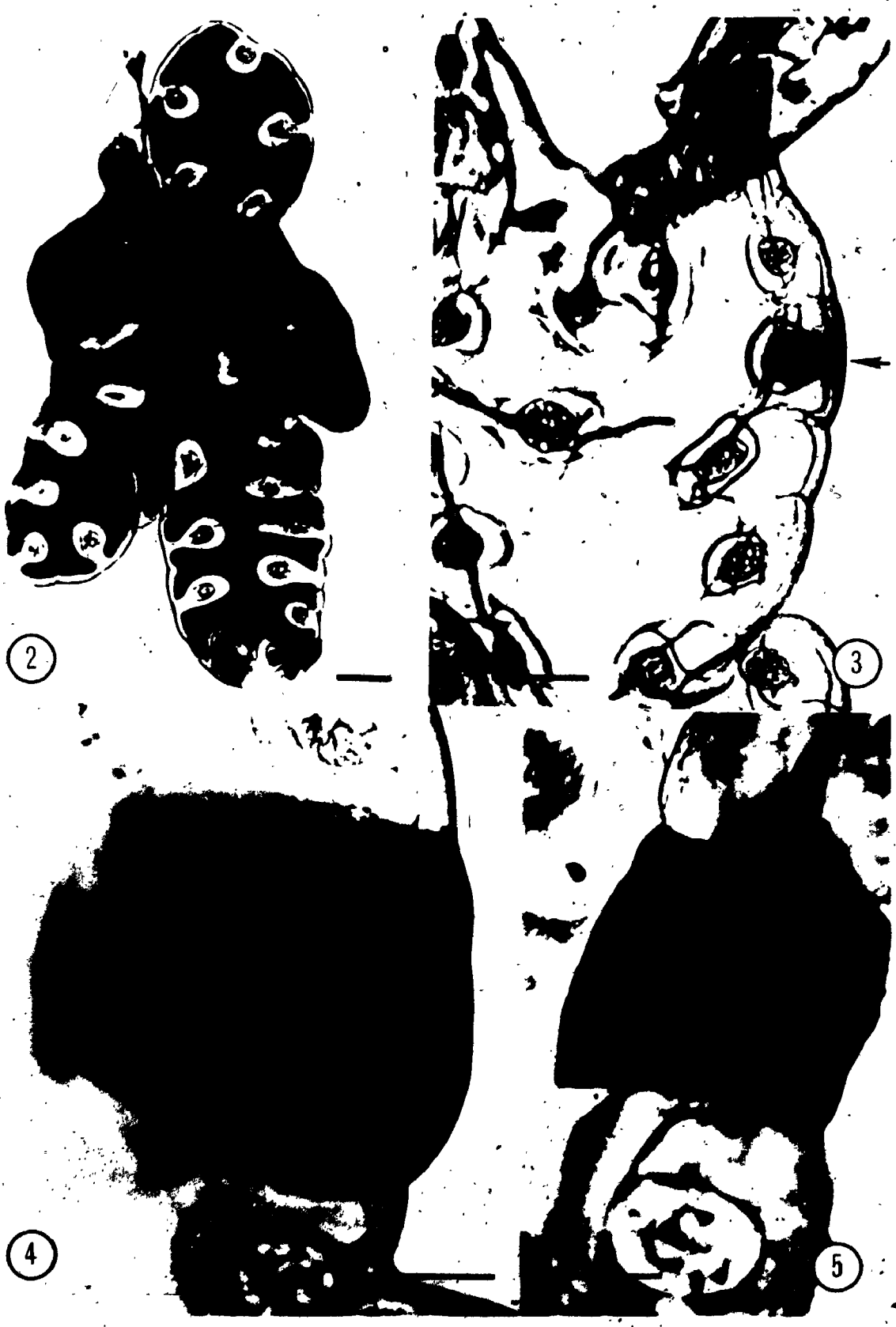
2
3
4
5

Injection of smaller amounts of HRP (5-10% of cell volume) are seen as localized reaction product around the injection site when fixation follows within 30 sec after injection (Fig. 4). When a cell that has been microinjected with HRP is left in culture for 30 min before fixation, the reaction product is distributed through the entire cytoplasm (Fig. 5). At no time was any reaction product seen in any adjacent cells.

HRP can be pressure-microinjected into salivary gland cells and the protein or its enzymatic product diffuses in the cytoplasm. Since the reaction product is osmiophilic, it can be localized by electron microscopy.

(c) HRP reaction product is bound to intracellular surfaces

Microinjected cells could easily be identified in unstained sections because of their increased contrast. Examination of HRP-injected cells by electron microscopy showed that the reaction product was surface bound (Fig. 6). The plasma membrane, ribosomes and endoplasmic reticulum are outlined by the osmiophilic reaction product (Fig. 6, 7). Unstained sections of HRP-injected cells appear as though stained by uranyl acetate except that in stained cells the contents of the lumen of the endoplasmic reticulum were stained while only the intracellular surfaces appeared stained in HRP-injected cells (compare Fig. 8 and 9). The surface localization of the reaction

Figs. 6, 7. HRP reaction product is bound to intracellular surfaces. Salivary gland cells were microinjected with about 10% of their volume of 10 mg/ml of HRP, and fixed 30 min later. The tissue was reacted with diaminobenzidene-H_2O_2. RER rough endoplasmic reticulum, R ribosomes, Cont non-injected cell, M mitochondria, cv coated vesicle. Bar=0.2 μm.

Fig. 6. Comparison of injected and control cell shows that the injected cell has greatly increased contrast due to the HRP reaction product. The reaction product is adsorbed to membranes (arrows) and ribosomes. There is little or no reaction product in the cytoplasmic space, x150,000.

Fig. 7. The basal surface of a injected cell shows the reaction product adsorbed to ribosomes and membranes and a coated vesicle, x80,000.


Cont
R
R
6
7
M

Figs. 8, 9. Cells that have been injected with HRP resemble control cells that have been section stained. Cells, prepared as described in Fig. 6 (Fig. 8) were compared to control cells that had been section stained (Fig. 9). The surface localization of the HRP reaction product resembles the staining of the uranyl ion. Fig. 8 unstained (HRP), Fig. 9 uranyl acetate section stained (UA), bar=0.5 μm, x42,000.


8
9

product was not obscured when increased amounts of HRP were injected (Fig. 10).

While the HRP reaction product is surface bound, the uniformity and diffusion of the reaction product does not make it possible to compare the distribution of the actual HRP molecules.

2.4 Discussion

The localization of HRP depends on the generation of highly insoluble polymers that are osmiophilic and homogenous when viewed by electron microscopy (Essner, 1974). Diffusion of the products of enzyme reactions give a questionable localization of the protein in question (Cornelisse and Van Duijn, 1973a; 1973b) unless there is a membrane limiting the diffusion. While it is possible that the actual HRP molecules diffused and were bound to cytoplasmic surfaces (Bock, 1972; Seligman et al., 1973) it is more likely that the reaction product diffused and was adsorbed to surfaces (Novikoff et al., 1972; Novikoff, 1980).

The appearence of injected cells suggests a similarity in staining with uranyl salts. It has been shown that the uranyl ion is positively charged and binds to anionic sites of surfaces in model systems (D'Arrigo, 1975; Ting-Beal, 1979; Degens and Ittekkel, 1982). The HRP reaction

Fig. 10. The surface localization of the HRP reaction product is not an artifact of the injection of small amounts of HRP. Cells that were injected with about 30% of their volume were examined by electron microscopy. The reaction product is surface bound (arrows), but the rough endoplasmic reticulum is swollen. RER rough endoplasmic reticulum, R ribosomes. Unstained, bar=0.2 μm, x135,000.


RER
RER
10

product may be acting in a similar way.

HRP has been used widely as an intracellular tracer for marking cells in neurobiology (Muller and McMahan, 1976; Neale et al., 1978; Crow et al., 1979), but little attention has been paid to the actual localization in the cytoplasmic space. This could be due to the fact that cells tend to be overloaded with HRP and while this marks the cell clearly, it obscures the intracellular localization of the reaction product (Bock, 1972; Eckert and Boschek, 1980).

Microinjection of charged molecules into live cells may alter salt and water movements by disrupting the normal Donnan equilibria. It is possible that such changes may alter ion binding at surfaces and thus the surface potentials. However, if changes do occur they do not noticeably affect cell ultrastructure or cell viability.

In conclusion, it is possible to microinject tracers into Chironomus salivary gland cells without killing them. The diffusion of the reaction product limits the procedure since the location of the HRP can only be inferred from the reaction product. The use of direct non-enzymatic tracer molecules, such as cationic ferritin, to examine the distribution of anionic sites should allow a direct test of the hypothesis that intracellular surfaces are negatively charged.

CHAPTER 3

THE CHARGE DISTRIBUTION IN THE ROUGH ENDOPLASMIC RETICULUM/ GOLGI COMPLEX TRANSITIONAL AREA INVESTIGATED BY MICROINJECTION OF CHARGED TRACERS

3.1 Introduction

While much is known about the morphological correlates of the steps of intracellular transport of secretory proteins, little is known about the factors that regulate interaction between different membranes (Palade, 1975; Jamieson and Palade, 1977; Farquhar and Palade, 1981). There is a series of fission-fusion events in the secretory pathway which makes a hierarchy of membrane interaction (Palade, 1975). Physical differences between membranes in the secretory pathway may be the basis for the specificity of their interaction. This study attempts to detect differences in surface charge between membranes of the endoplasmic reticulum/Golgi complex transitional area of the secretory pathway.

Particle electrophoresis (Dean, 1975; Hannig and Heidrich, 1974), isoelectric point determination (Wallach et al., 1966) and binding of charged molecules (Hackenbrock and Miller, 1975; Abe et al., 1976; Eagles et al., 1976; Bittiger and Heid, 1977; Howell and Tyhurst, 1977; Virtanen, 1978) have shown that isolated sub-cellular

structures have a net negative charge. Since like charges repel, the resulting electrostatic force may play an important role in repulsion at distances of 2.5 to 10 nm under physiological conditions (Parsegian et al., 1979; Rand, 1981).

While it has been suggested that the negative surface charge may simply provide a barrier to close approach (Plattner, 1978) it is possible that the surface charge of membranes plays a fundamental role in regulating surface to surface interactions and fusion (Dean, 1975; Poste and Pasternak, 1978; Gad et al., 1982). The modulation of surface charge, perhaps involving calcium, may be the way that membrane-membrane fusion is brought about (Douglas, 1974; Papahadjopoulos, 1978; Duneic et al., 1979; Haynes et al., 1979a, 1979b; Morris et al., 1979; Portis et al., 1979; Wagner et al., 1980).

The Golgi complex beads (Locke and Huie, 1975; 1976a) are situated at the base of forming transitional vesicles and may be the morphological correlate of the postulated "lock-gate" at the level of the endoplasmic reticulum/Golgi complex transitional area (Palade, 1975). Depletion of ATP collapses the bead ring structure and is also correlated with a halt in protein transport (Brodie, 1981). Bead arrangement is not affected by treatments that disrupt the cytoskeleton (Brodie, 1982a). Bismuth binding to the beads may be through phosphate groups (Locke and Huie, 1977;

Brodie et al., 1982). If the phosphate groups cause a negative surface charge on the beads, then it may have a role in vesicle formation. A high negative charge on the beads may prevent negatively charged membrane proteins on the cytoplasmic surface from entering the area of vesicle formation. Differences in surface charge between two faces of a membrane can cause instability and vesicle formation (Allan et al., 1976; Hope and Cullis, 1979).

It is therefore important to compare the surface charge of structures in the secretory pathway to see if sequential changes in charge are detectable and to see if the Golgi complex beads are highly charged. Approaches such as particle electrophoresis that have been used, are limited in resolution and depend on fractionated organelles.

Highly cationic ferritin (HCF) has been used as a marker for surface charge on cell surfaces (Danon et al., 1972; Grinnell et al., 1975; Burry and Wood, 1979), subcellular fractions (Eagles et al., 1976; Howell and Tyhurst, 1977) and freeze-fracture (Pinto da Silva et al., 1981). To examine the distribution of charged sites inside intact cells this study uses ferritins modified to have anionic to highly cationic charges (Rennke et al., 1975). Five types of charged ferritin were separately microinjected into secretory cells of the salivary gland of Chironomus tentans and their intracellular distribution

quantified in an attempt to answer the following questions:

1) Can variously charged ferritins be used to map charge differences on intracellular structures as well as external surfaces?

2) Does the charge on the tracer molecule affect its distribution in the cytoplasmic space?

3) Do structures in the secretory pathway differ in their surface charge?

4) Can any specific charge be detected on the Golgi complex beads?

The results show that the distribution of ferritin molecules in the cytoplasmic space varies with their charge, with the positively charged ferritins being bound by intracellular structures (Brac, 1981). The membranes of the rough endoplasmic reticulum were not significantly different from those in the Golgi complex. The Golgi complex beads were not distinguished by their charge.

3.2 Materials and Methods

(a) Rearing *C. tentans*

Larvae of *C. tentans* were used in all experiments. They were raised as described in Chapt 2.2 (a).

(b) Culturing of salivary glands

Salivary glands of the fourth larval instar were used in all experiments. The salivary glands were cultured as described in Chapt. 2.2 (c).

(c) Tracers

AF (pI 4.0-4.4) (from Sigma Chemical Co., St. Louis, MO) and two types of HCF (HCF2 pI 8.5-9.4, HCF3 pI 9.5-10.1) (from Polysciences Inc., Warrington, PA and Sigma Chemical Co.) were dialyzed against distilled water for 24 hours to remove all salts. The isoelectric points were determined by the isoelectric precipitation method (Rennke et al., 1975). The ferritin was diluted in injection buffer (100 mM KCl, 5 mM HEPES, pH 7.0) to a final concentration of 10 mg/ml as determined spectrophotometrically using the standard that 10 mg/ml has an absorbance of 79.9 at a wavelength of 270 nm (Rennke et al., 1975).

CF of intermediate positive charge (CF1 pI 7.0-8.0 and CF2 pI 7.9-9.1) were provided by Dr. H. G. Rennke (see Rennke et al., 1975).

The basis of the conversion of anionic (native) ferritin to the cationic derivative is the use of carbodiimide hydrochloride as an activator and 1,3-propanediamine or 1,6-hexanediamine (depending on the source) as nucleophile to replace the carboxyl groups

(Hoare and Koshland, 1967; Danon et al., 1972; Rennke et al., 1975).

(d) Microinjection

Microinjection of the salivary gland cells was carried out as described in Chapt. 2.2 (d). Injected cells were identified by making a map of the salivary gland.

(e) Fixation and processing

At 30 minutes after microinjection, the culture medium was removed and the gland was flooded with ice cold 5% glutaraldehyde in 0.1 M phosphate buffer, pH 7.4, and fixed for 1 hour. After rinsing in the same buffer, the gland was transferred to a vial containing 1% osmium tetroxide in 0.1 M phoshate buffer, pH 7.4, and postfixed for 1 hour on ice. The gland was carefully washed in buffer and then in distilled water. It was then dehydrated in a graded series of alcohols, washed in propylene oxide and embedded in Araldite (R. P. Cargille Laboratories, Inc., Cedar Grove, NJ).

Bismuth staining of tissue before osmication is the method of choice for the localization of beads in arthropod tissue (Locke and Huie, 1976a). The beads can be seen in uranyl acetate stained tissue (Locke and Huie, 1976b) and especially after tannic acid mordanting in the initial

fixative (Brodie, 1982b). Bismuth staining of tissue was not used for microinjected cells because it obscured the ferritin localization.

(f) Electron microscopy

Thin sections of dark gray interference colour were cut on a diamond knife and mounted on 400 mesh copper grids. Sections were stained with bismuth for 30 minutes to increase the contrast of the ferritin (Ainsworth and Karnovsky, 1972) or in uranyl acetate (Locke and Huie, 1980) for 5 minutes. Micrographs were taken on a Philips EM 300 at 80 kV.

(g) Quantitation of ferritin distribution

The strategy for measuring surface charge with microinjected ferritin was to see 1) if there were obvious differences between structures or, 2) if differences could be measured by counting ferritin particles bound to different surfaces. Between 1000 to 1500 ferritin particles were counted within each injected cell. This number of particles was found in 7 micrographs.

Comparison of the rough endoplasmic reticulum and Golgi complex was carried out on the selected micrographs. The Golgi complex was defined as the structure that consists of the smooth face of the endoplasmic reticulum

where transition vesicles form, the transitional area adjacent to the forming face of the Golgi saccules, the Golgi saccules and the secretory vesicles at the mature face of the Golgi saccules. This area was marked with a wax pencil on the micrographs and three sub-categories of cell space defined within it: 1) cisternal space of the rough endoplasmic reticulum and other components of the vacuolar system not available to the ferritin, 2) the space within 15 nm of surfaces where ferritin particles are assumed to be bound to that surface, and 3) the remaining space further than 15 nm from surfaces where the ferritin is assumed to be free.

(h) Measurement of total cytoplasmic space

A transparent overlay sheet with a 2.5 cm lattice of 80 dots was placed on the micrograph to estimate the total cytoplasmic space. The number of dots in the cytoplasmic space of the endoplasmic reticulum and Golgi complex was counted. The area value of one point at a magnification of 138,500 is equal to

$$(2.5 \text{ cm} \times 10{,}000 \ \mu\text{m/cm})^2 / 138{,}500^2$$

$$= 3.26 \times 10^{-2} \ \mu\text{m}^2.$$

The total cytoplasmic space of a particular area is given by the number of dots over that area multiplied by $3.26 \times 10^{-2} \ \mu\text{m}^2$.

(i) Measurement of the surface cytoplasmic space.

A transparent overlay sheet ruled with lines 6.5 mm apart and total length of 7723 mm was placed on the micrograph where the lengths of membrane profiles were to be measured. Only sections of gray interference colour (approximately 60 nm thick) were used for membrane profile measurements. The number of times a line crossed membrane profiles, normal in section and that could be clearly identified, was counted. It has been shown that the number of times a surface is cut by a line is directly related to the profile length (Williams, 1977). If L equals the total length of lines (in mm) on a micrograph that has an area A (in mm^3) and if I equals the number of times that lines cut the profile in question, then

contour length = $I/2L \times A$.

When the contour length of a given structure was determined in one micrograph, the length was converted to micrometers. The surface cytoplasmic space was determined by multiplying the contour length by 1.5×10^{-2} µm. This distance was chosen to represent the cytoplasm within which ferritin particles were considered to be bound. This takes into account the size of the ferritin particle which is approximately 11 nm in diameter.

The transition vesicles have a high radius of curvature because of their size (about 50 nm). Because of

the sampling method, the transition vesicles are prone to the error of underestimating their surface cytoplasmic space. This was corrected by calculating and graphing the measured and true surface membrane length (Fig. 11), and using it to correct the surface cytoplasmic space of transition vesicles.

(j) Determination of free cytoplasmic space

Since the total cytoplasmic space is defined as the sum of the surface cytoplasmic space plus the free cytoplasmic space, and the total and surface cytoplasmic spaces have been measured, the free cytoplasmic space could be calculated.

(k) Counting ferritin particles

The results from a series of micrographs from each microinjected cell were converted to mean number of ferritin particles per square micrometer plus or minus the standard deviation, to allow direct comparison.

(l) Comparison of different surfaces

The mean density of ferritin particles in the surface cytoplasmic space of the rough endoplasmic reticulum, transition vesicles, Golgi saccules and secretory vesicles was compared within each individual cell. Since a variable

Fig. 11. Correction of membrane surface length measurement is related to vesicle diameter. The measurement of membrane lengths is necessary to calculate the cytoplasmic space classified as bound. For vesicles under 1000 nm, the apparent surface cytoplasmic space is underestimated. Transition vesicles are about 50 nm and would be underestimated by 30%. This hypothetical curve was derived by comparing the difference between the area adjacent a straight and curved membrane.

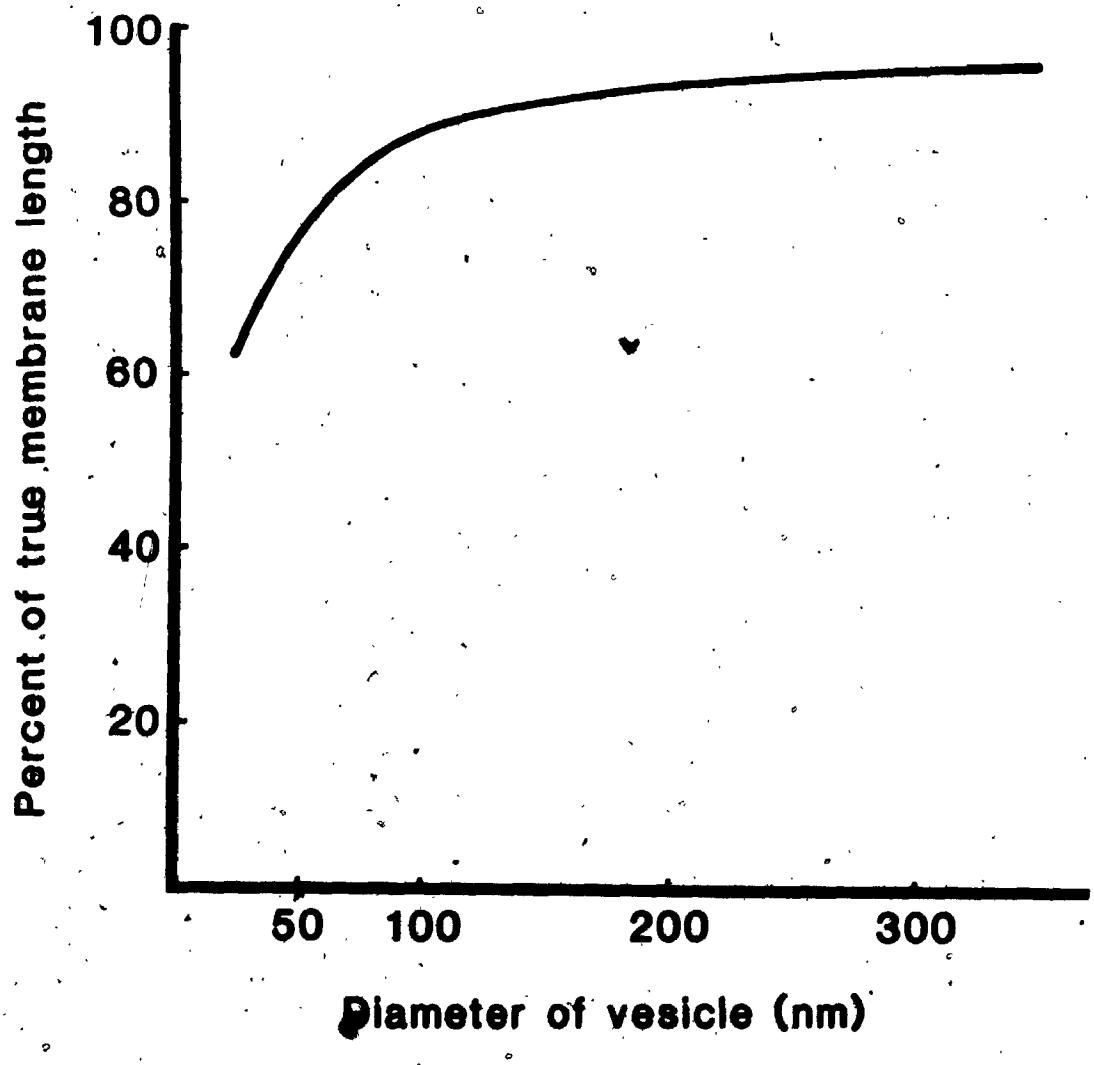
100
80
60
40
20
Percent of true membrane length
50
100
200
300
Diameter of vesicle (nm)

number of ferritin particles was injected into each cell, comparisons could only be made within each injected cell. Results were compared statistically by analysis of variance followed by the Student Newman-Keuls test for multiple rank ordering (Zar, 1974).

The ferritin distribution was examined in more than 200 micrographs from 25 microinjected cells.

3.3 Results

(a) Structural changes and cell viability after microinjection

Microinjection of AF (pI 4.0-4.4) and CF (pI 7.0-8.0) did not cause structural damage, while injection of HCF1 (pI 7.9-9.1.) and HCF2 (pI 8.5-9.4) caused the rough endoplasmic reticulum to swell (Figs. 12-15). HCF3 (pI 9.5-10.1) bound to intracellular surfaces causing damage and did not diffuse from the injection site (Fig. 16). Since CF (pI 7.0-8.0) and AF (pI 4.0-4.4) diffused throughout the cytoplasm and did not cause the rough endoplasmic reticulum to swell, they were used to examine the surface charge on intracellular surfaces.

Microinjected cells that were tested for viability consistently excluded trypan blue dye. The structure of injected cells was a more sensitive indicator of the

Figs. 12-16. The distribution of microinjected ferritin, which ranged in its charge from anionic to highly cationic, in the cytoplasmic space. The bar is equal to 0.2 μm in all figures. F ferritin, ER endopasmic reticulum.

Fig. 12. AF (pI 4.0-4.4) is predominantly found in the free cytoplasmic space. Bismuth stained, x145,000.

Fig. 13. CF (pI 7.0-8.0) is distributed in the free cytoplasmic space and also bound to surfaces. Bismuth stained, x145,000.

Fig. 14. HCF1 (pI 7.9-9.1) is mostly bound to surfaces and has caused some morphological changes to the rough endoplasmic reticulum. Bismuth stained, x90,000.

Fig. 15. HCF2 (pI 8.5-9.4) is bound to surfaces and has caused gross swelling of the endoplasmic reticulum. Unstained, x90,000.

Fig. 16. HCF3 (pI 9.5-10.1) is bound to the endoplasmic reticulum and has caused gross changes in morphology. It has not diffused from the injection site. Unstained, x90,000.

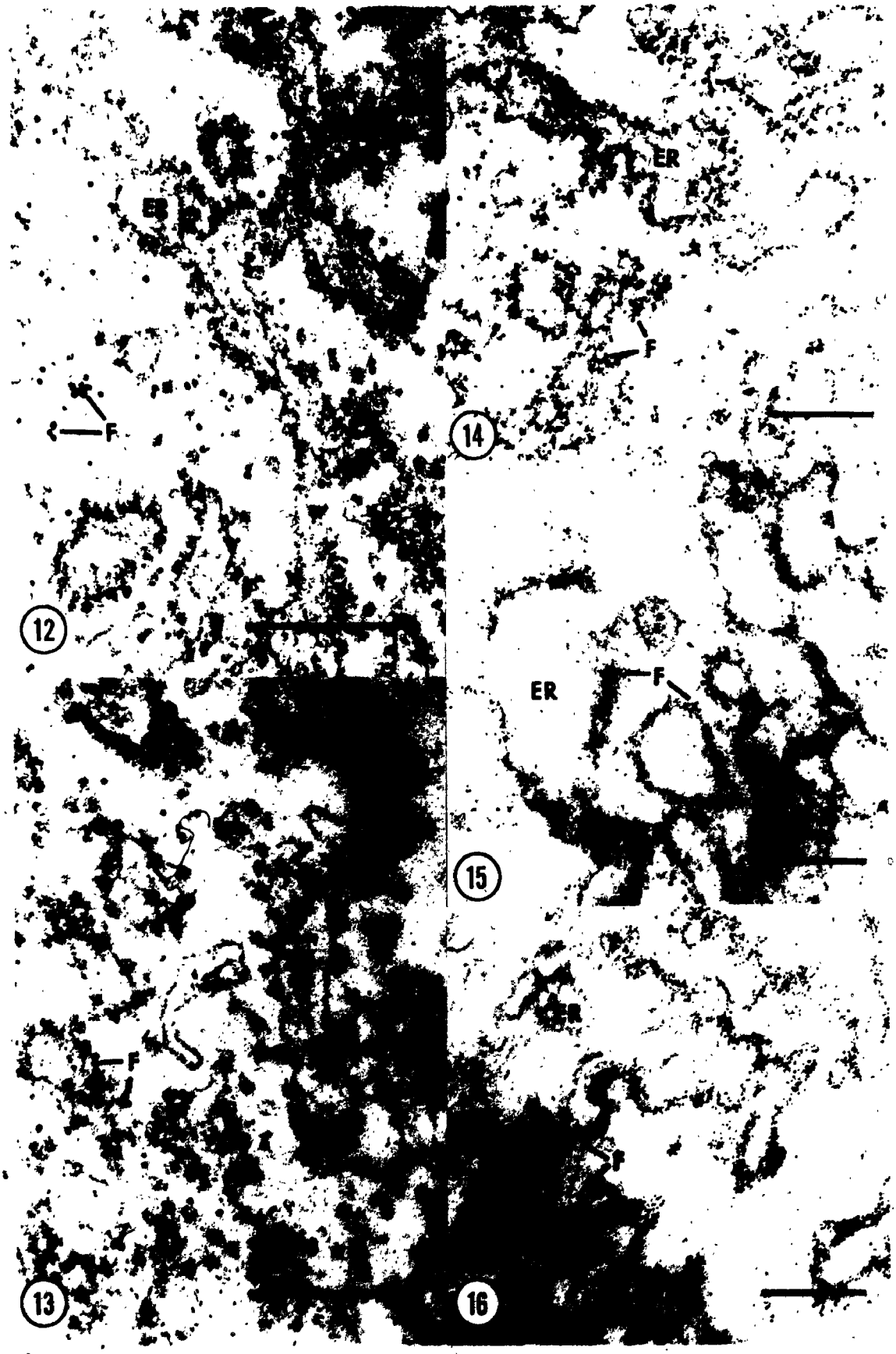
ER
F
14
12
ER
F
15
F
13
16

effects of the tracer molecules than trypan blue dye exclusion since cells with swollen rough endoplasmic reticulum excluded trypan blue.

(b) Distribution of microinjected ferritin in the cytoplasmic space

Microinjected ferritin was found in the cytoplasmic space of injected cells (Fig. 12-16). Analysis of AF distribution showed significantly more free than bound ferritin (Table 1). The ratio of bound to free ferritin is a measure of the affinity of the ferritin for a surface. A ratio of 1 shows equal numbers of bound and free ferritin. The ratio of bound to free AF was 0.5 and therefore it interacts weakly with membrane surfaces. This ratio was reversed for CF with significantly more bound than free ferritin. In three separate experiments, the ratios of bound to free CF were 2.0, 2.6 and 2.8 (Table 1). This shows that the CF interacts strongly with intracellular surfaces relative to AF.

The ratio of bound to free HCF1 (pI 7.9-9.1) was 3.8 (Table 1) but it caused some swelling of the rough endoplasmic reticulum (Fig. 13). Both HCF1 and HCF2 (pI 8.5-9.4 and pI 9.5-10.1) were strongly bound to cytoplasmic surfaces (Figs. 14, 15). The ratio of bound to free HCF2 was 6.7 (Table 1). Thus, increases in the isoelectric point of ferritin is correlated with an increase in the

Table 1: Location of microinjected cationic and anionic ferritins in the cytoplasmic space.

	Ferritin particles/$\mu m^2 \pm SD$				
	Free	Bound	Bound / Free	H_0 Free = Bound *	n
Anionic Ferritin	548±123	29.2±8.3	0.5	p<.001	7
Cationic Ferritin 1.	177±64	350±83	2.0	p<.01	5
Cationic Ferritin 2.	118±37	306±70	2.6	p<.001	7
Cationic Ferritin 3.	78±31	219±56	2.8	p<.001	7
Highly Cationic Ferritin one	202±63	912±224	4.5	p<.001	7
Highly Cationic Ferritin two	309±114	2040±343	6.6	p<.001	7
Highly Cationic Ferritin three	highly bound ♦				

* Student's t-test

♦ Morphological damage prevented detailed analysis

proportion of bound to free ferritin.

Since CF was surface bound its distribution relative to intracellular structures can be used to compare the surface charge of different structures.

(c) Distribution of CF in the endoplasmic reticulum/Golgi complex transitional area

The distribution of CF bound to the rough endoplasmic reticulum, transition vesicles, Golgi saccules and secretory vesicles was examined (Figs. 17, 18). Since there were no obvious differences between the structures (Fig. 17, 18), the distribution of CF was quantitated to see if significant differences existed. The mean density of CF was significantly greater in the Golgi complex than in the rough endoplasmic reticulum (Table 2). There was no significant difference in the amount of free ferritin in the cytoplasmic space between the Golgi complex and rough endoplasmic reticulum.

Comparison of the different surfaces in the secretory pathway showed that there were no significant differences between the surfaces. Similar results were found in three separate experiments (Table 2).

The Golgi complex beads could be identified in thin sections but they were not distinguished by their binding of CF (Fig. 17). Therefore if the phosphate groups impart

Figs. 17, 18. The distribution of microinjected CF in the rough endoplasmic reticulum and Golgi complex. The distribution of CF in two different cells used to compare ferritin binding is shown. CF is bound to the surfaces of the secretory pathway F ferritin, ER endoplasmic reticulum, TV transition vesicles, arrowhead to Golgi complex beads, GS Golgi saccules, SV secretory vesicles. Bismuth stained, x155,000.

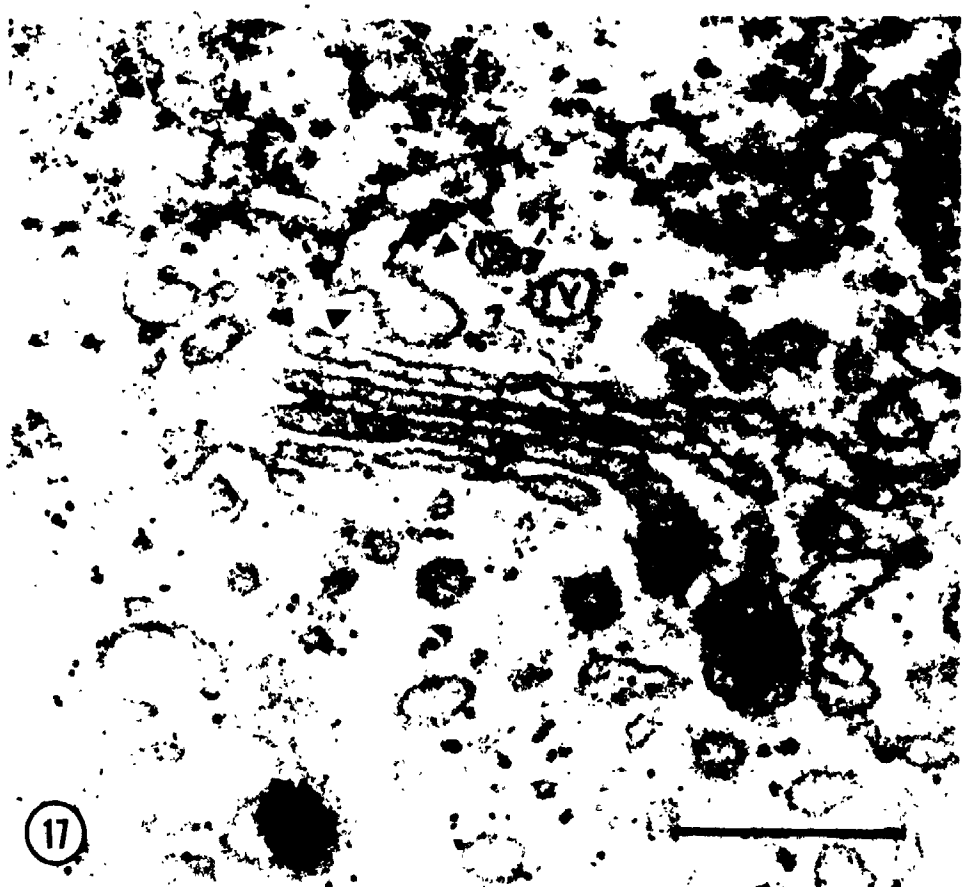

17

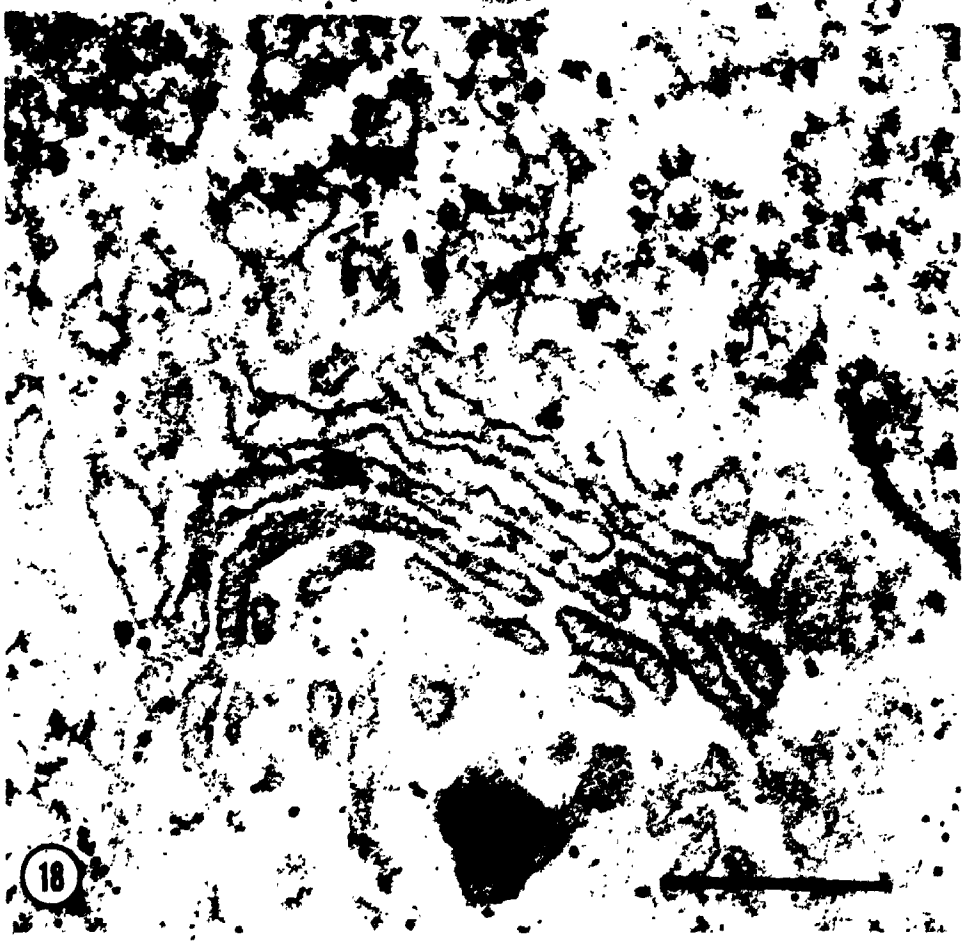

18

Table 2. Distribution of microinjected cationic ferritin in the secretory pathway.*

	Ferritin particles/μm^2 ±SD			
	Endoplasmic Reticulum	Transition Vesicles	Golgi Saccules	Secretory Vesicles
Total Ferritin	1. 127±41		1. 181±49 ✱	
	2. 197±41		2. 285±83 ✱	
	3. 207±55		3. 311±110 ✱	
Bound Ferritin	1. 203±57	253±80	159±62	230±98 §
	2. 276±69	388±164	214±96	208±112 §
	3. 301±30	599±294	399±173	430±282 §
Free Ferritin	1. 73±33		1. 92±39 ‖	
	2. 109±39		2. 146±65 ‖	
	3. 158±57		3. 221±65 ‖	

*The distribution of microinjected cationic ferritin was examined as described in the Materials and Methods. Since comparisons are based on the average number of ferritin particles/μm^2, the sum of the bound and free ferritin does not necessarily equal the total ferritin unless the total area is taken into account. Different amounts of ferritin were injected into each cell. The numbers 1, 2 and 3 refer analyses from individual cells (1 n=7, 2 n=7, 3 n=5).

✱ There is significantly more ferritin/μm^2 in the Golgi than in the endoplasmic reticulum, $p<.05$ Student's t-test.

§ The amount of bound ferritin of the structures compared was not significantly different.

‖ The amount of free ferritin/μm^2 found in the Golgi complex and the endoplasmic reticulum was not significantly different.

a net negative surface charge, it cannot be detected with this technique.

(d) Distribution of AF in the endoplasmic reticulum/Golgi complex transitional area

The distribution of bound AF was examined in the secretory pathway using the same criteria that were used for CF (Fig. 19). There was no significant difference between the Golgi complex and rough endoplasmic reticulum in the amount of AF in the free, surface or the total cytoplasmic space (Table 3). The Golgi complex beads were not characterized by AF binding (Fig. 19).

3.4 Discussion

(a) Microinjection of ferritin can be used to map surface charge.

Microinjection of ferritins (CF and AF) used to examine the surface charge in salivary gland cell does not affect cell morphology or viability. Experiments on fractions of intracellular membranes have shown that they have a net negative charge (Wallach et al., 1966; Hannig and Heidrich, 1974; Bittiger and Heid, 1977). In intact cells we should therefore expect that tracers would be distributed according to their charge. Positively charged tracers should be bound to anionic sites on intracellular

Fig. 19. The distribution of microinjected AF in the rough endoplasmic reticulum and Golgi complex. Most AF (pI 4.0-4.4) particles are in the free cytoplasmic space. F ferritin particle, ER endoplasmic reticulum, TV transition vesicles, GS Golgi saccules, SV secretory vesicles. Bismuth stained, x150,000.

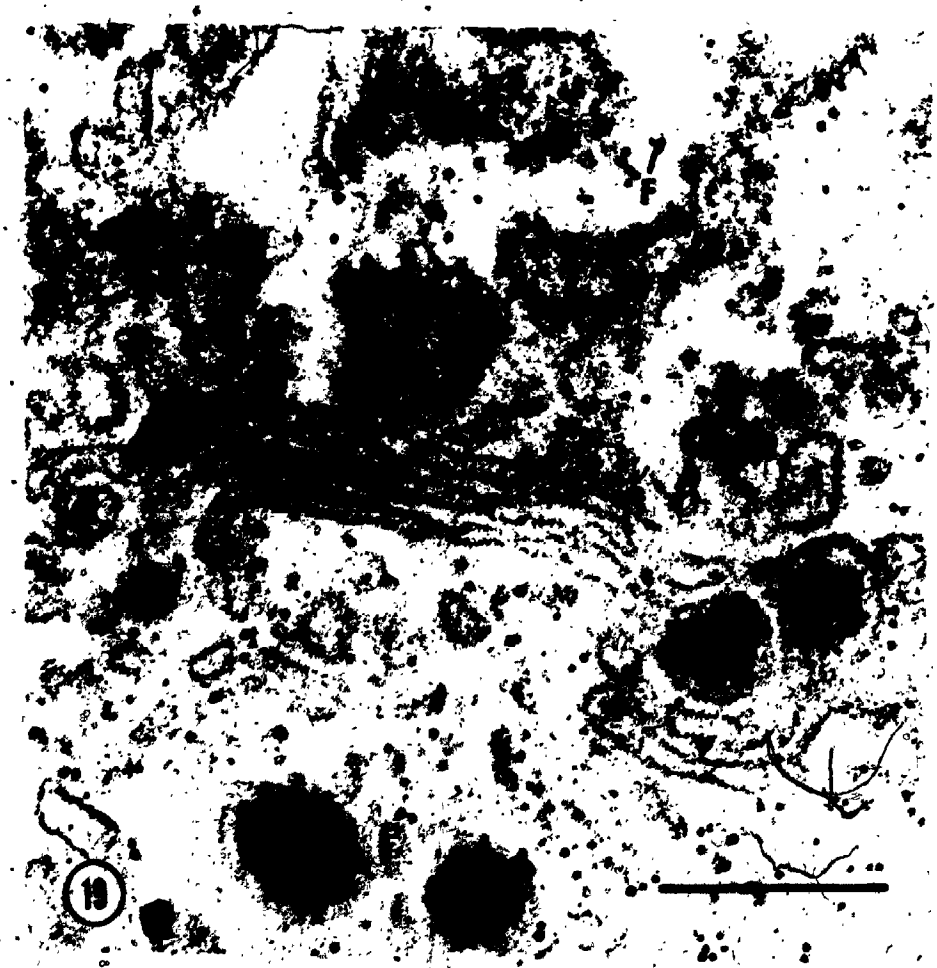
19

Table 3. Distribution of microinjected anionic ferritin in the secretory pathway.*

	Ferritin particles/μm^2 ±SD			
	Endoplasmic Reticulum	Transition Vesicles	Golgi Saccules	Secretory Vesicles
Total Ferritin	436±125	410±92 ♦		
Bound Ferritin	277±92	268±140	151±53	303±186 §
Free Ferritin	548±152	612±270 ‖		

*The distribution of microinjected anionic ferritin was examined as described in the Materials and Methods. Since comparisons are based on the average number of ferritin particles/μm^2, the sum of the bound and free ferritin do not necessarily equal the total ferritin unless total area examined is taken into account. These comparisons are from one microinjected cell, n=7.

♦ There is no significant difference in the total ferritin/μm^2 between the Golgi complex and endoplasmic reticulum.

§ There are no significant differences between the amount of bound ferritin in the structures examined.

‖ The amount of free ferritin/μm^2 found in the Golgi complex and the endoplasmic reticulum is not significantly different.

surfaces and negatively charged tracers should be repelled. The distribution of microinjected ferritins was consistent with this view. As the isoelectric point of the ferritins increased, the proportion of bound to free ferritin also increased. There was more AF in the free cytoplasmic space than bound to surfaces. However, there was some bound AF therefore not only is net charge important but also the distribution of charged sites. Otherwise, absolutely no AF could be bound.

The microinjection of HCF1, HCF2 and HCF3 resulted in most of the molecules being bound to intracellular surfaces. The most positively charged ferritins caused swelling of the rough endoplasmic reticulum and they did not diffuse from the injection site. The finding that cationic but not anionic molecules can cause changes in organelle size suggests that binding to the anionic sites alters solute and water equilibria. It also shows that the distribution of molecules is strongly influenced by surface charges.

The microinjected ferritin can be considered to be in equilibrium between being free in the cytoplasmic space or bound to surfaces. The charge on the ferritin molecule will determine its distribution between the surface and free cytoplasmic spaces. It is possible that the molecules are bound in the free cytoplasmic space to structures that cannot be visualized in thin sections. Nevertheless, the

differential distribution of the ferritin tracers clearly shows that surfaces are more negatively charged than the free cytoplasmic spaces, within the intact cell.

(b) Accuracy of the method

There are two possible sources of error that might affect the quantification of ferritin distribution. These are (1) all ferritin particles can be seen because of their density but not the organelle to which they may be bound, and (2) surfaces tend to be underestimated because of image loss effects. First, ferritin that is categorized as free may in fact be bound to a surface which cannot be seen in the micrograph. This would lead to an underestimate of the amount of bound ferritin. Second, the surface area may be underestimated because of image loss effects which lead to overestimates of bound ferritin. For example, the surface area of the endoplasmic reticulum is usually underestimated since the presence of membranes cut obliquely are not identified as surfaces (Williams, 1977). Correction is not possible without estimating the amounts of image loss. Since the underestimation of surface area cannot be accurately determined, correction is of limited value. It has been suggested that these two effects may cancel out and corrections should not be attempted (Williams, 1977). It is therefore unlikely that these errors would influence the results in a meaningful way.

(c) Comparison of the surface charge in the endoplasmic reticulum/Golgi complex transitional area

Surface charge is important in membrane-membrane interactions since modulation by calcium can affect repulsion and attraction between surfaces (Haynes et al., 1979a, 1979b; Portis et al., 1979). Finding no significant differences between the surfaces of membranes involved in intracellular transport suggests that major differences in surface charge are not the mechanism of regulating membrane-membrane interaction. If differences exist, they cannot be detected with this technique. Comparison of the electrophoretic mobility of fractionated intracellular rat kidney showed no significant differences between the membranes involved in secretion (Hannig and Heidrich, 1974).

Transition vesicles connect two distinct compartments of the vacuolar system. Locke (1983) emphasized the division of membranes of the vacuolar system into pre- and post-transition compartments. Pre-transition membranes are derived solely from the endoplasmic reticulum while the post-transition compartment receives membrane from the plasma membrane and the endoplasmic reticulum. If the Golgi complex beads are involved in maintaining the sharp discontinuity between these two compartments (Brodie, 1982b), then their charge is not important in this role.

CHAPTER 4

INTRACELLULAR POLYCATIONIC MOLECULES CAUSE REVERSIBLE SWELLING OF THE ROUGH ENDOPLASMIC RETICULUM

4.1 Introduction

Swelling of the endoplasmic reticulum has been reported to be a sign of death in various cells (Pilar and Landmesser, 1976; Eggleton and Norkin, 1981; Smith and Nijhout, 1983). Since polycationic molecules cause lipid bilayers to become leaky (Chwang et al., 1979; Hammoudah et al., 1979; DeKruijff et al., 1980; Mandersloot et al., 1981), swelling of the rough endoplasmic reticulum (RER) may be due to the increased cytoplasmic concentration of cationic molecules. Microinjected highly cationic, but not anionic, ferritin binds to intracellular surfaces and causes the RER to swell even though the cells remain viable (Chapt. 3).

In order to determine whether the charge of the molecule is related to RER swelling; the effects of microinjected molecules with a range of charges have been observed on the integrity of cell organelles. The light and electron microscope observations reported here show that polycations cause swelling of RER but not other organelles.

4.2 Materials and Methods

(a) Microinjection of molecules into salivary gland cells

The salivary glands of late fourth instar larvae of *C. tentans* were used in this study. The larvae were reared and the salivary glands were maintained *in vitro* as described in Chapt. 2. Briefly, the glands were cultured in media consisting of 87 mM NaCl, 2.7 mM KCl, 1.3 mM $CaCl_2$, 10 mM HEPES, pH 7.1 in Falcon 1004 petri dishes. The salivary glands adhered tightly to clean plastic, thus facilitating microinjection. The glands were observed and microinjected in darkfield microscopy using a Zeiss photomicroscope. Experiments were performed after the glands had been *in vitro* 15-30 min. Test molecules were pressure-microinjected with micropipettes which were connected to a sealed plastic syringe filled with paraffin oil. The volume of tracer injected was estimated by measuring the size of a drop of tracer appearing in paraffin oil under the same conditions used to inject cells. About 50,000 to 100,000 μm^{-3} were injected per delivery. This corresponds to 5-10% of the cell volume (Paine, 1975; Egyhazi *et al.*, 1980).

(b) Tracers

The following molecules were microinjected in buffer (100 mM KCl, 5 mM HEPES pH 7.0) at the concentrations

shown.

1) Calcium-EGTA buffer (calcium concentration 10 μM, see Rose and Rick, 1978)

2) Lanthanum chloride (0.1 mM)

3) Lysozyme (10 mg/ml; pI 11, Sigma Chemical Co.)

4) Highly cationic ferritin (10 mg/ml, pI 8.5-9.4, Polysciences Inc.)

5) Cationic ferritin (10 mg/ml, pI 7.9-9.1)

6) Anionic ferritin (10 mg/ml, pI 4.0-4.4 Sigma Chemical Co.)

7) Bovine serum albumin (10 mg/ml, pI 4.6 Sigma Chemical Co.)

8) control buffer (100 mM KCl, 5 mM HEPES pH 7.0)

Some cells were injected with two different types of test molecules e.g. micrpinjection of bovine serum albumin followed by injection of lysozyme. Injected cells tested for viability by trypan blue vital dye consistently excluded dye.

(c) Tissue processing for electron microscopy

After microinjection, the culture medium was removed and the salivary gland was flooded with ice-cold 5% glutaraldehyde in 0.1 M phosphate buffer, pH 7.4, and fixed for 1hr. After rinsing in the same buffer, the gland was transferred to a vial containing 1% osmium tetroxide in 0.1 M phosphate buffer, pH 7.4, and postfixed for 1 hr on ice.

The gland was carefully washed in buffer and then distilled water. The gland was then dehydrated in a graded series of alcohol, rinsed in propylene oxide and embedded in Araldite.

Thin sections were cut on a diamond knife and mounted on copper grids. For photography, sections were stained in bismuth for 30 min to enhance the contrast of ferritin (Ainsworth and Karnovsky, 1972) or uranyl acetate for 5 min (Locke and Huie, 1980). Micrographs were taken on a Philips EM 300 at 80 kV.

4.3 Results

(a) In vitro morphology of salivary gland cells

The large salivary gland cells of C. tentans are convenient experimental cells for microinjection studies. The cytoplasm is normally transparent when cultured in vitro (Fig. 20). Microinjection of control solution (containing 100 mM KCl, 5 mM HEPES pH 7.0), did not cause any noticeable change in the cytoplasm (Fig. 21). Injection of the same cell with lanthanum chloride (0.1 mM) caused the cytoplasm to go opaque immediately after injection (Fig. 22), and stay this way (Fig. 23). Since lanthanum but not potassium caused the cytoplasm to go opaque, it is probably due to the positive charges of the lanthanum molecule. It should therefore be possible to

Figs. 20-23. Microinjection of control solution into the cell does not cause the cytoplasm to change. Live preparation in darkfield, bar=50 µm, x400.

Fig. 20. The normal morphology of the salivary gland cell that has been *in vitro* for 30 min. The cytoplasm is transparent.

Fig. 21. Microinjection of 3 pulses of injection buffer (containing 100 mM KCl) does not affect the cytoplasm.

Fig. 22. Microinjection of the same cell as in Fig. 21 with 1 pulse of lanthanum chloride (0.1 mM) caused the cytoplasm to go opaque.

Fig. 23. The cytoplasm remains opaque 15 min after injection.

Figs. 24-25. A cell that has been pre-injected with an anionic protein goes opaque when microinjected with a cationic protein. Live preparation in darkfield, bar=50 µm, x400.

Fig. 24. A cell that has been injected with 3 pulses of bovine serum albumin (10 mg/ml, pI 4.6) has no visible change in the cytoplasm immediately after injection.

Fig. 25. The same cell as in Fig. 24, was microinjected with 4 pulses of lysozyme (10 mg/ml, pI 11) which causes the cytoplasm to go opaque.

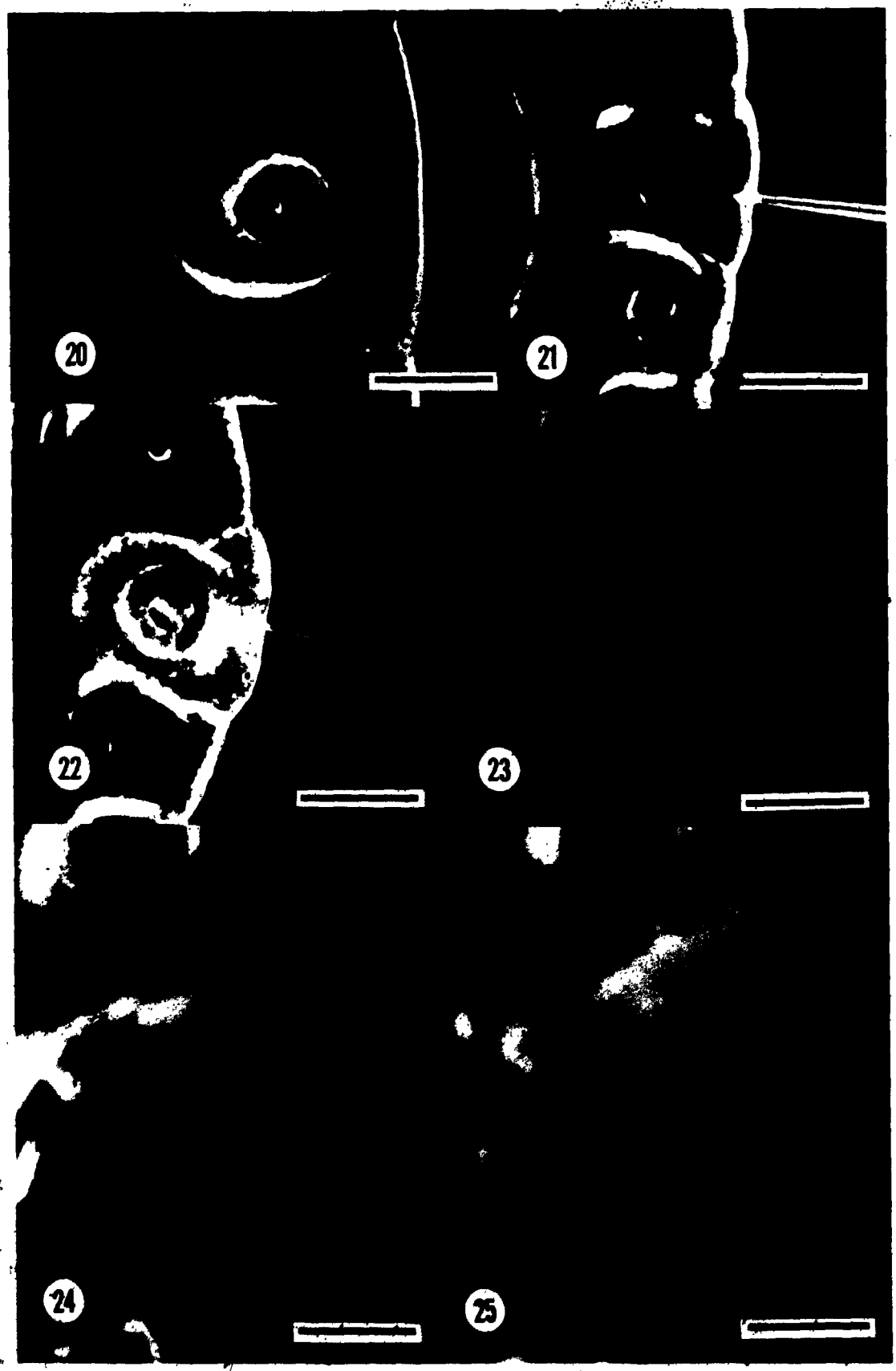
20
21
22
23
24
25

cause the same change by injection of other polycationic molecules.

(b) Injection of cationic but not anionic molecules causes a change in cell transparency

Microinjection of anionic proteins such as bovine serum albumin (10 mg/ml, pI 4.6) caused no change to the cytoplasm (Fig. 24) but a second injection into the same cell of the highly cationic protein lysozyme (10 mg/ml, pI 11) caused most of the cytoplasm to become opaque (Fig. 25). Control injections of lysozyme alone caused similar changes in cell transparency. The change in transparency due to the injection of lanthanum and lysozyme were both irreversible during the experiment (60 min) although the cells continued to exclude trypan blue. Both lanthanum and lysozyme are highly cationic molecules. It was therefore of interest to determine if cationic molecules such as calcium could cause similar changes when microinjected.

(c) Calcium causes reversible changes in cell transparency

Microinjection of calcium-EGTA buffer consistently caused the cytoplasm to go from transparent to opaque immediately after microinjection (Figs. 26-30). These changes were not a result of cell death since cells that had been injected with test molecules continued to exclude trypan blue. Injection of calcium buffer showed zones of

Figs. 26-28. Microinjection of calcium-EGTA buffer into a salivary gland cell causes it to go from transparent to opaque. Live preparation in darkfield, bar=50 μm, x400.

Fig. 26. Three injections of calcium-EGTA (calcium 10 μM)into the cytoplasm causes the cytoplasm to become opaque.

Fig. 27. Ten min after injection the cytoplasm has returned to normal.

Fig. 28. Same cell injected ten times causes the cytoplasm, but not the nucleus, to go opaque.

Figs. 29-30. There is a graded change in opaqueness during microinjection of calcium-EGTA into the cytoplasm. Live preparation in darkfield, bar=100 μm, x220.

Fig. 29. One pulse of calcium-EGTA (calcium 10 μM) causes a small change in the cytoplasm near the tip of the micropipette.

Fig. 30. Three more pulses of calcium-EGTA (calcium 10 μM) causes a definite change in the cytoplasm but not in the nucleus. The zone of opaqueness partially surrounds the nucleus.

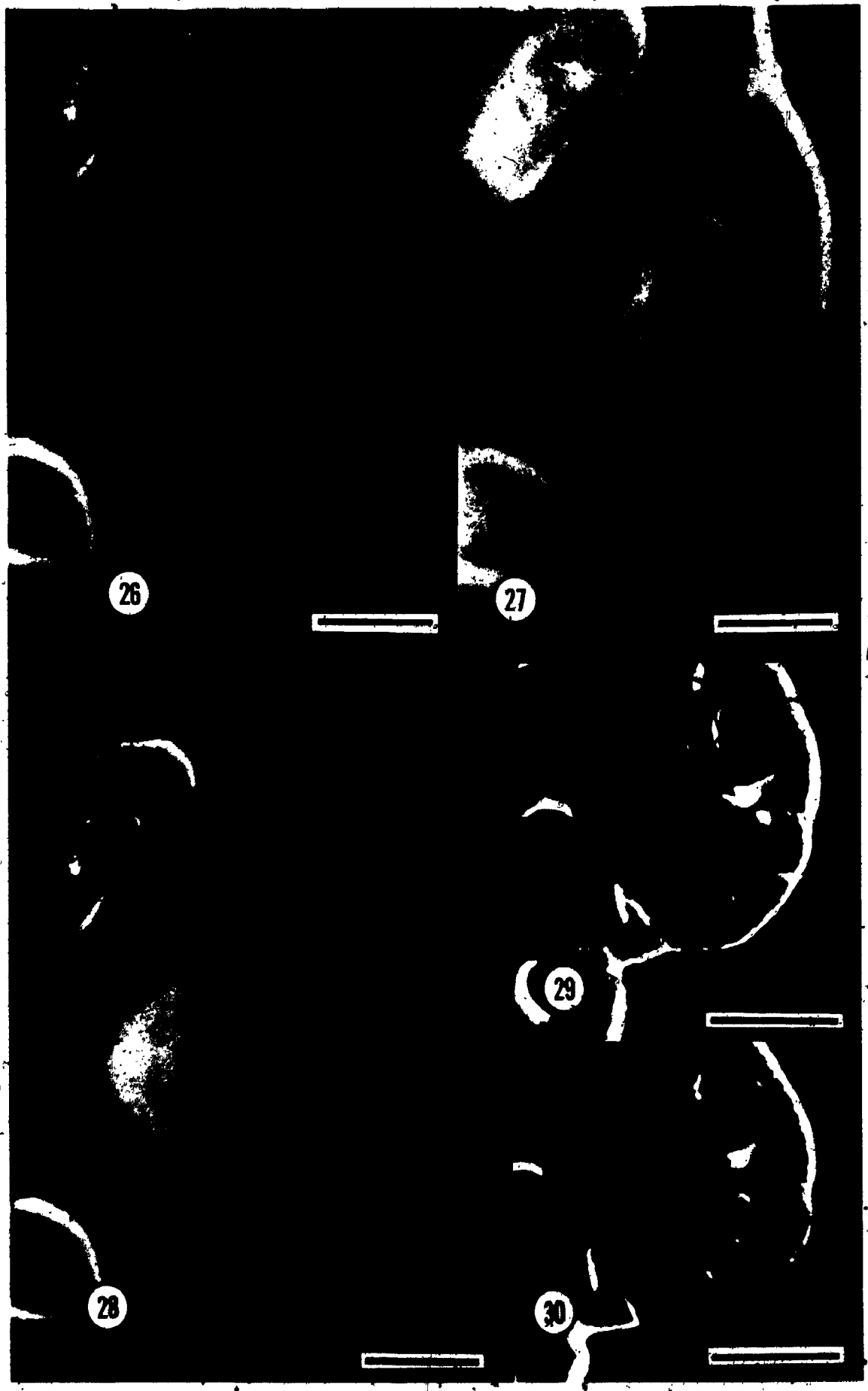
26
27
29
28
30

2 OF/DE 2

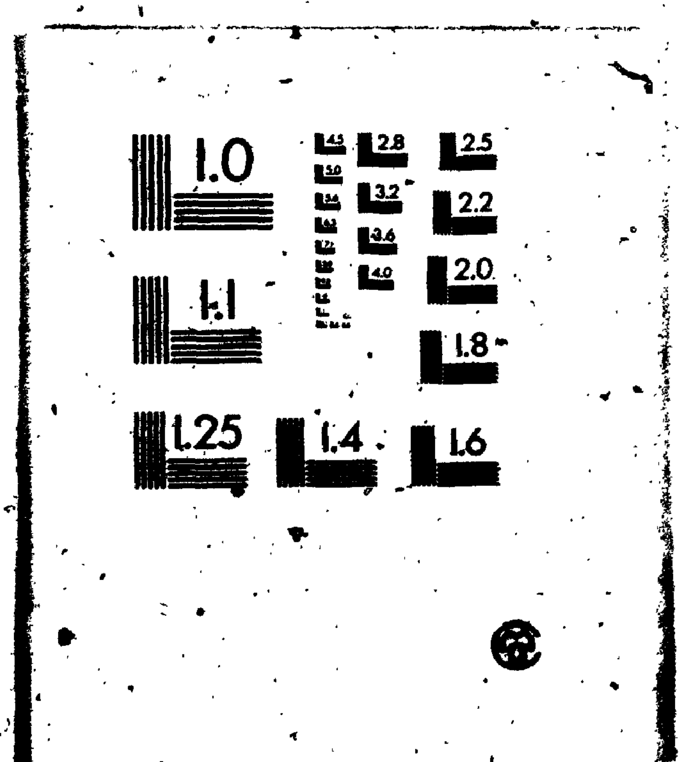

opaqueness near the micropipette tip (Fig. 26), which were only visible in the cytoplasm and not the nucleus. Microinjection into the nucleus did not cause any observable changes. These effects on the cytoplasm were graded and reversible. When small amounts (10-20% of the cell volume of 10 μM calcium-EGTA) were injected (Fig. 26) the cytoplasm returned to normal within 10 min (Fig. 27) but when massively injected, the cell would remain opaque (Fig. 28). Increasing amounts of calcium buffer caused larger areas of opaqueness when injected into the cytoplasm (Figs. 29, 30). Since polycations consistently caused changes in the transparency of the cytoplasm, injected cells were examined by electron microscopy to see what changes had occurred.

(d) Injected polycationic molecules cause the RER to swell

Salivary gland cells cultured <u>in vitro</u> but not injected, showed the normal RER characteristic of this cell type (Fig. 31). Most membranes are part of the RER with numerous Golgi complexes. The transient or permanent opacity observable by light microscopy was correlated with swelling of the RER (Fig. 32). While the RER has swollen, other organelles such as secretory granules have not (Fig. 32).

Since injection of polycationic molecules causes the RER to swell it is possible that the injected molecules

Figs. 31-32. Control and microinjected salivary gland cell structure. Uranyl acetate stained, bar=2 μm, x8,000

Fig. 31. The structure of a control salivary gland which had been *in vitro* for 30 min. The endoplasmic reticulum is the normal size.

Fig. 32. The structure of a cell that had been injected and gone opaque has swollen RER cisternae. In order to examine the ultrastructure of a cell that had gone opaque, the cell from Figs. 26-28 was fixed and processed for electron microscopy. The RER has swollen enormously but the other membranes have not. RER=rough endoplasmic reticulum, Nu=nucleus, SV=secretory vesicle.

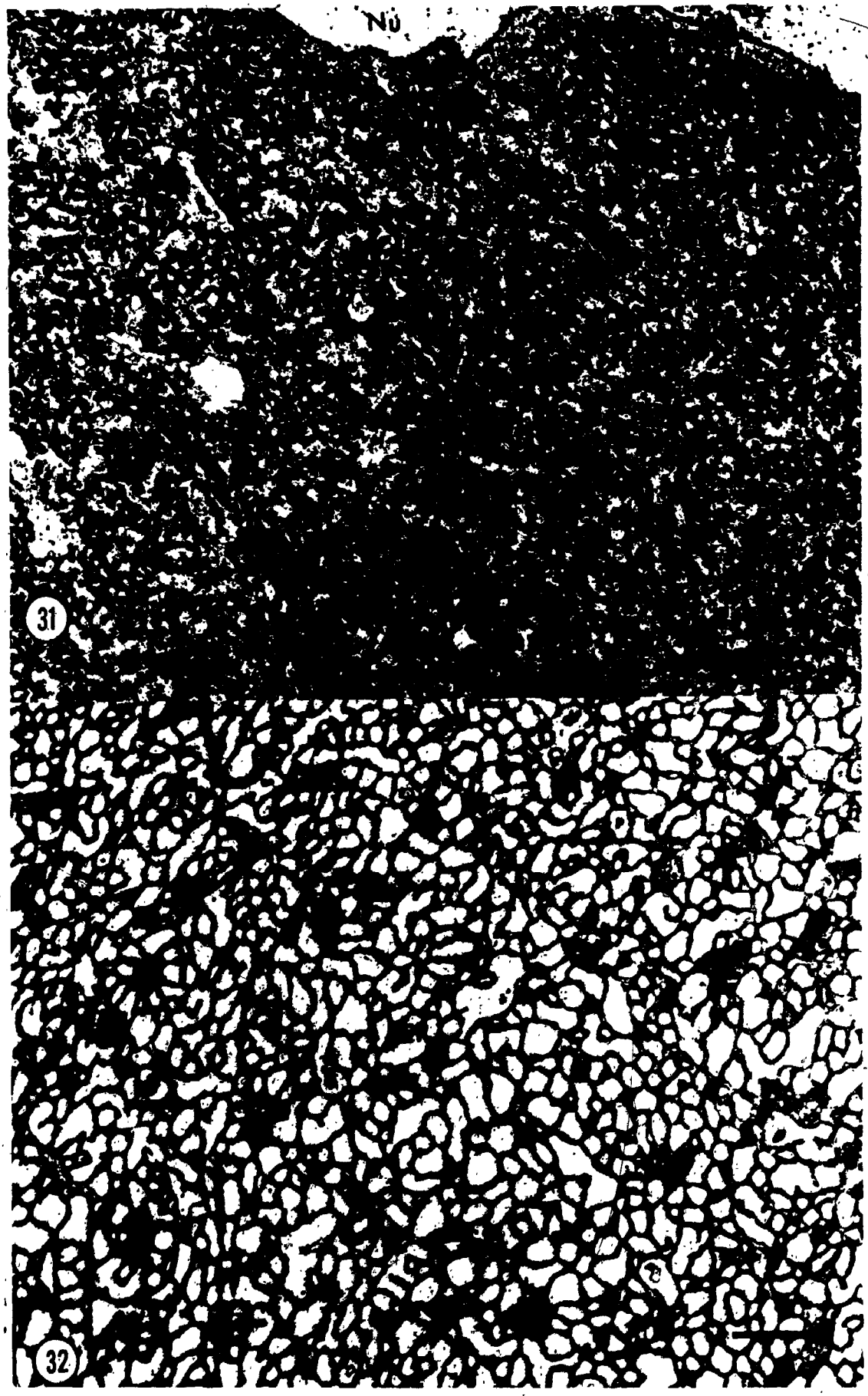
Nu
31
32

bind to the RER surface. Microinjection of highly cationic ferritin (pI 8.5-9.4) consistently caused gross swelling of the RER (Figs. 33). This was correlated with its charge since cationic ferritin (pI 7.9-9.1) caused noticeable disruption of the morphology but not as great swelling (Fig. 34) while anionic ferritin (pI 4.0-4.4) did not cause the RER to swell and was localized mainly in the free cytoplasmic space (Fig. 35). Only the RER swelled as a result of cationic ferritin injection. Other organelles such as secretory vesicles, Golgi saccules, and transition vesicles did not swell although they did bind cationic ferritin. Swelling as a response to polycation binding is thus a specific response of the RER rather than a general membrane response.

4.4 Discussion

Microinjection of polycationic molecules consistently caused changes in the opacity of the cytoplasm which could be seen with the light microscope. The opacity was correlated with a striking increase in size of the RER cisternae but not other organelles. The changes are not an artifact of the injection process since they could not be induced by control injections with potassium buffer, anionic ferritin or bovine serum albumin.

It has been shown that the charge of the ferritin molecule directly affects its distribution in the

Figs. 33-35. Microinjection of cationic but not anionic ferritin causes the RER to swell. Bar=0.2 μm.

Figs. 33. Microinjection of highly cationic ferritin (pI 8.5-9.4) causes the RER to swell at a concentration of 10 mg/ml. Unstained, x80,000.

Fig. 34. Microinjection of cationic ferritin of intermediate positive charge (10mg/ml, pI 7.9-9.1) causes swelling of the RER but not as great as the highly cationic ferritin. Bismuth stained, x140,000.

Fig. 35. Microinjection of anionic ferritin (10 mg/ml, pI 4.0-4.4) does not cause any morphological changes to the cytoplasmic membranes. Bismuth stained, x140,000. RER=rough endoplasmic reticulum, GC=Golgi complex, F=ferritin particle(s).


RER
RER
33
F
RER
34
35

cytoplasmic space (Chapt. 3). Cationic molecules are bound to surfaces while anionic molecules are predominantly in the free cytoplasmic space. Since increased positive charge led to increased surface binding and increased positive charge also led to greater swelling of the RER, it seems likely that binding is necessary for the swelling to occur. The common factor shared by the molecules that caused RER swelling is that they are polycations and likely to interact with negatively charged surfaces.

While little is known about solute concentration differences across the endoplasmic reticulum inside the cell, it is known that microsomes, which are composed mainly of endoplasmic reticulum fragments, are osmotically active and will swell *in vitro* due to osmotic differences (Tedeschi *et al.*, 1963). The fact that the endoplasmic reticulum swells *in vivo* when polycationic molecules bind to it suggests that a concentration difference exists across it and that the binding of positively charged tracers causes a change in RER permeability.

It has been shown that calcium and other polycations that bind to anionic phospholipids in model systems can change the configuration from a bilayer to a non-bilayer structure such as the hexagonal phase (Cullis and DeKruijff, 1979; DeKruijff and Cullis, 1980). These interactions are electrostatic (DeKruijff and Cullis, 1980), suggesting that the charge of the molecules is

important. The change from bilayer to non-bilayer structure causes the membrane to lose its ability to act as a permeability barrier and to become leaky to monovalent cations such as potassium (Mandersloot et al., 1981). While the function of non-bilayer structures in membranes is still in question, there is evidence for non-bilayer structures in microsomes which is the result of the action of certain endogenous proteins (DeKruijff et al., 1980).

The evidence suggests that the microinjection of polycationic molecules may cause a permeability change in the endoplasmic reticulum by binding to anionic phospholipids and causing the formation of non-bilayer structures. The reason that the RER but not other membranes swell so greatly relates either to its luminal composition or the nature of the phospholipids in its membranes. Comparison of the phospholipid composition of intracellular membranes shows that RER and Golgi complex are very different but there is much overlap between Golgi complex and plasma membrane (Meldolesi et al., 1978; Boggs, 1980). The difference in phospholipid composition of the RER may make it more sensitive to polycation-induced swelling.

If the cisternae of the endoplasmic reticulum are topologically equivalent to the extracellular space, then ionic differences that exist across the plasma membrane may also exist across the membranes of the endoplasmic

reticulum. It has been shown that the endoplasmic reticulum in many cell types accumulates calcium as part of a calcium homeostatic mechanism (Black et al., 1981; Wick and Hepler, 1980). Since intracellular potassium is high and extracellular potassium low, a great concentration difference would exist if this was also true for the membranes of the RER. The permeability to potassium may be a key factor in the swelling of the RER.

CHAPTER 5

CHARGED SIEVING BY THE BASAL LAMINA AND THE DISTRIBUTION OF ANIONIC SITES ON THE EXTERNAL SURFACES OF FAT BODY CELLS

5.1 Introduction

In all tissues, except blood cells, the basal lamina is the primary barrier between the tissue and the fluid in which it is bathed. The permeability of the basal lamina to macromolecules will depend both upon its porosity and the nature of the charge upon the channels that make up the structural components of the sieve (Ashhurst, 1982). The surface charge of the basal lamina should directly affect the movement and distribution of charged molecules in the tissue it surrounds. For example, in Calpodes ethlius, the size of the major hemolymph proteins (10-11 nm in size) (Webster, 1982) and their charge (ranging from anionic to cationic) (Mussett, 1977), may play a role in the movement of proteins from the hemolymph to the lymph spaces of the fat body.

The basal lamina of fat body cells separates the hemolymph, in which the fat body is suspended, from the lymph spaces that surround the fat body cells themselves. At the fat body surface there is a system of plasma membrane infolds forming lymph spaces called the plasma

membrane reticular system (PMRS) (Locke, 1984). Lateral intercellular lymph spaces are formed by the apposing membranes of different cells (Locke, 1984; Dean et al., 1984).

To examine the role of the basal lamina in the movement of charged molecules to the fat body, ferritins, ranging in charge from anionic to highly cationic, were injected into larvae of Calpodes. The distribution of these ferritins was examined with respect to the basal lamina, the lymph spaces around the cells, the membranes of the lymph spaces and intracellular vacuoles. The results show that there are clusters of anionic sites in the basal lamina. These prevent anionic but allow cationic ferritins into the lymph spaces of the fat body and could therefore affect the distribution of variously charged hemolymph proteins. Furthermore, the membranes of the PMRS are differentiated from the membranes of the lateral intercellular spaces by more anionic sites.

5.2 Materials and Methods

(a) Test animals

Larvae of C. ethlius were reared as previously described (Locke, 1970). Mid-fifth stage larvae were used in this study because their fat body is metabolically active at this stage (Locke and Collins, 1968). After

injection with tracer solution, larvae were kept in a 22° C incubator with a 12 hr light, 12 hr dark cycle and were allowed to feed normally.

b) Tracers

The net charge of four different types of ferritin (ranging from anionic to highly cationic) were characterized by isoelectric precipitation (Rennke et al., 1975). Native (anionic) ferritin (AF1) was obtained from Sigma Chemical Co., highly cationic ferritin (HCF) was obtained from Miles Biochemicals. Anionic ferritin (AF2) and cationic ferritin (CF), were synthesized and kindly donated by Dr. H. Rennke (see Rennke et al., 1975 for modification procedure). The tracers were diluted with Grace's medium (Gibco Chemical Co.) and 40 µl was then injected into larvae weighing 1.6-1.8 gr. The hemolymph of these larvae has a volume of approximately 300 µl so that the effective concentration of the tracer exposed to the fat body was diluted by a factor of 8.5. The two anionic and cationic ferritins had a final hemolymph concentration of 4.7 mg/ml. HCF had a hemolymph concentration of 1.2 mg/ml.

c) Fixation and Processing

After incubation for 30 or 60 min, larvae were ligated and inflated with ice cold 5% glutaraldehyde in 0.1 M

phosphate buffer pH 7.4 with 2% sucrose. After immersion in fresh fixative for 1 to 2 hr, the tissue was washed in 0.1 M phosphate buffer pH 7.4 with 2% sucrose. The tissue was postfixed in osmium tetroxide in 0.1 M phosphate buffer pH 7.4 with 2% sucrose on ice for 1 hr. The tissue was washed carefully in ice cold buffer and then in distilled water. After dehydration in a graded series of alcohols, the tissue was rinsed in propylene oxide and embedded in Araldite.

d) Electron Microscopy

Thin sections of gray interference colour were cut on a diamond knife and mounted on 300 mesh copper grids. Sections were stained in bismuth for 30 min to increase the contrast of the ferritin (Ainsworth and Karnovsky, 1972), or uranyl acetate for 5 min (Locke and Huie, 1980). Micrographs were taken on a Philips EM 300 at 80 kV. The results are based on observations of 40 animals and several hundred micrographs.

(e) Quantitation of CF Distribution

The amount of CF bound to the plasma membrane of the PMRS and the lateral intercellular spaces was compared at 30 and 60 min of incubation. Micrographs at the same magnification and appropriate location (4-6 samples per location per animal) were taken and the length of membrane in micrometers was measured with a cartographer's wheel. Only sections of gray interference colour (approximately 60 nm thick) and membrane profiles normal in section were used for calculating ferritin densities. Ferritin particles within 15 nm of a surface were considered to be bound. All results are given as ferritin particles per square micrometer plus or minus the standard deviation (i.e. the density of ferritin within the area 15 nm of the membrane). Densities were compared statistically by the Student's t-test (Zar, 1974).

5.3 Results

(a) The time course of ferritin penetration

Uptake of ferritin particles into intercellular spaces from the hemolymph was in equilibrium by 30-60 min of incubation, since analysis of ferritin binding (see Results section "Quantitation of CF bound to the membranes of the PMRS and lateral intercellular spaces") at these times showed no differences. All micrographs presented were from

the animals exposed for 60 min.

b) The labeling of the basal lamina by ferritin

HCF (pI 8.5-9.5) intensely labeled the basal lamina of fat body cells (Fig. 36). Large clusters of HCF were found on the membrane of the PMRS, while smaller clusters of HCF were localized on the membranes of the lateral intercellular spaces (Figs. 37, 38). A slightly oblique section through the basal lamina showed discrete clumps of ferritin particles throughout the thickness of the basal lamina (Fig. 37). Higher magnification resolved clusters of particles separated by unlabeled areas (Fig. 38).

If ferritin binds to the structural components of the basal lamina, then it should be associated with the structures that are visible when contrasted with uranyl acetate. Analysis of sections stained with uranyl acetate showed that HCF was bound only to the uranyl acetate staining portions of the basal lamina (Fig. 39). Analysis of the other ferritins (AF1, AF2 and CF) showed that these were also found in the same location of the basal lamina (Figs. 40-44). Decrease of the positive charge on the ferritin molecule led to much less binding to the basal lamina.

The appearance of clustering by HCF and CF to the electron dense portions of the basal lamina may be due to

Figs. 36-38. HCF labels the basal lamina.

Fig. 36. HCF labels the anionic sites of the fat body basal lamina. Large clusters of HCF are found in the PMRS and lateral intercellular spaces. Bismuth stained, bar=0.2 μm in all figures, x73,000.

Fig. 37. An oblique section shows clusters of HCF throughout the basal lamina. There are large aggregates of ferritin in the PMRS. Unstained, x45,000.

Fig. 38. The distribution of HCF closely corresponds to the portion of the basal lamina that is stained with uranyl acetate. There are few particles in the electron-lucent areas. Uranyl acetate stained, x175,000. PMRS=plasma membrane reticular system, Bl=basal lamina, Hy=hemolymph F=ferritin, LS=lateral intercellular space.

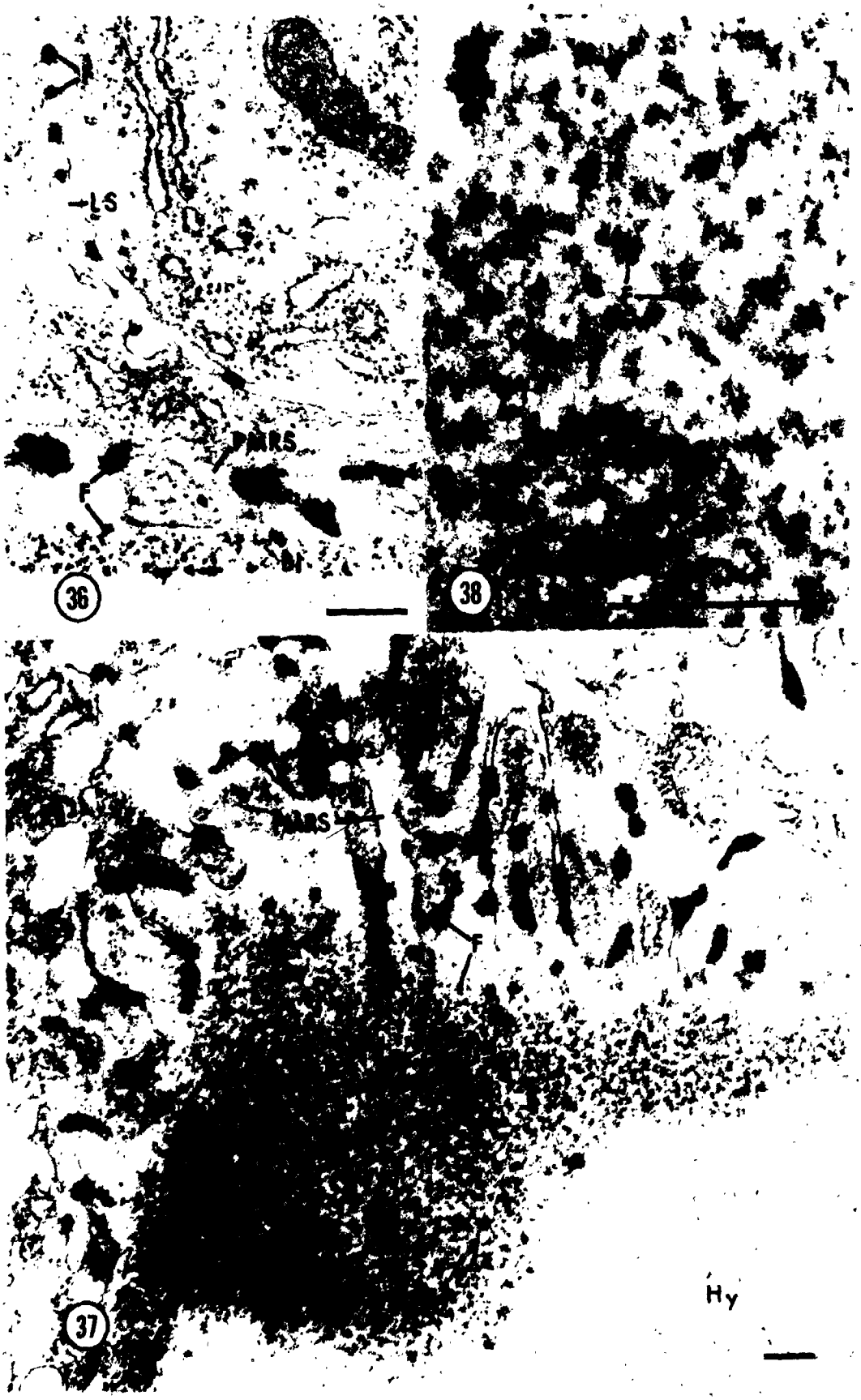
LS
PMRS
F
36
38
PMRS
37
Hy

Figs. 39, 40. Comparison of the distribution of HCF and CF in the basal lamina. Oblique sections of the basal lamina show that for HCF (Fig. 39) and CF (Fig. 40) the electron-dense portion of the basal lamina has bound the ferritin. An elastic fiber has a dense array of bound HCF (Fig. 39). Uranyl acetate stained, x175,000. Bl=basal lamina, F=ferritin, FB=fat body, Ef=elastic fiber.

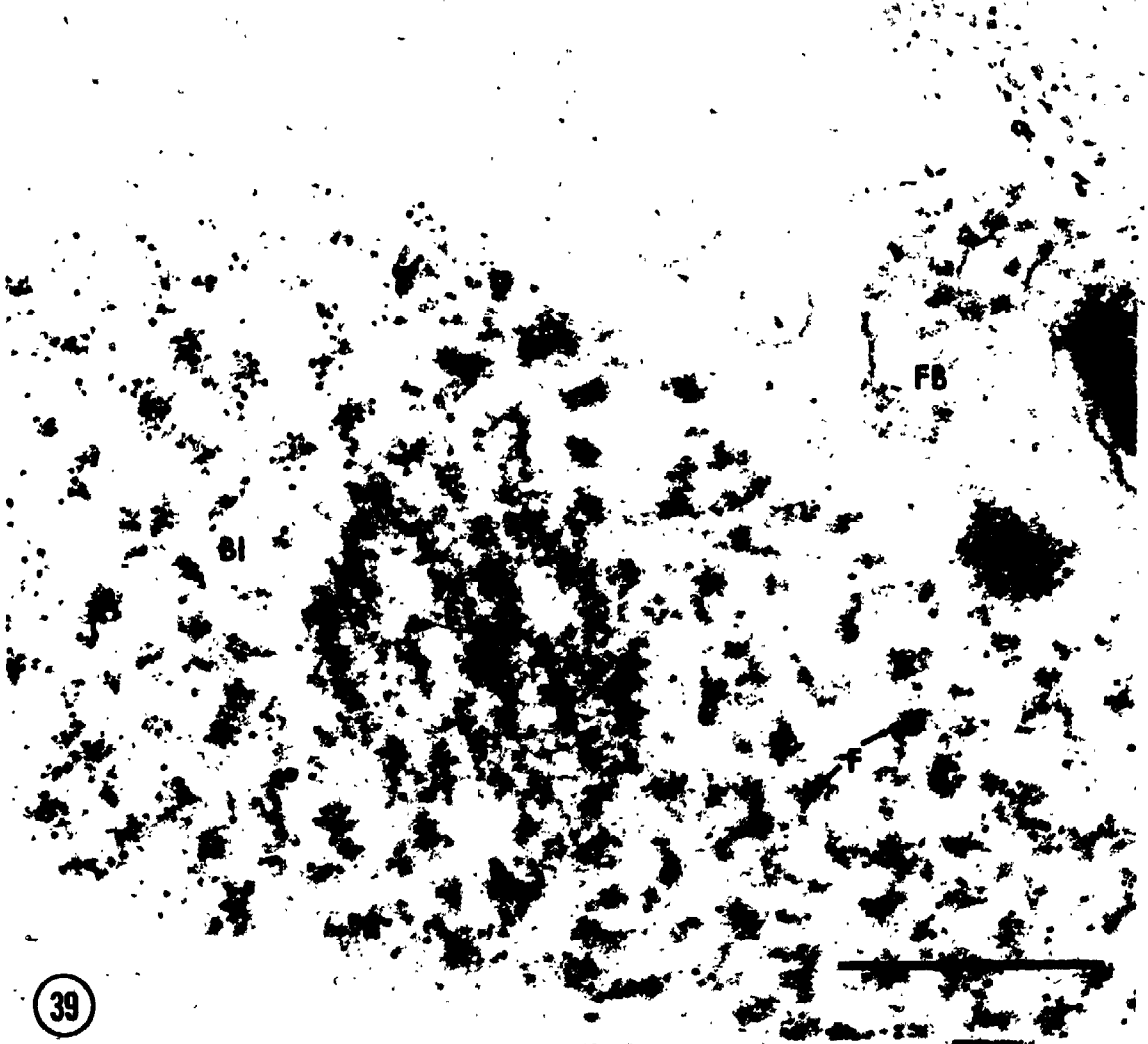

39

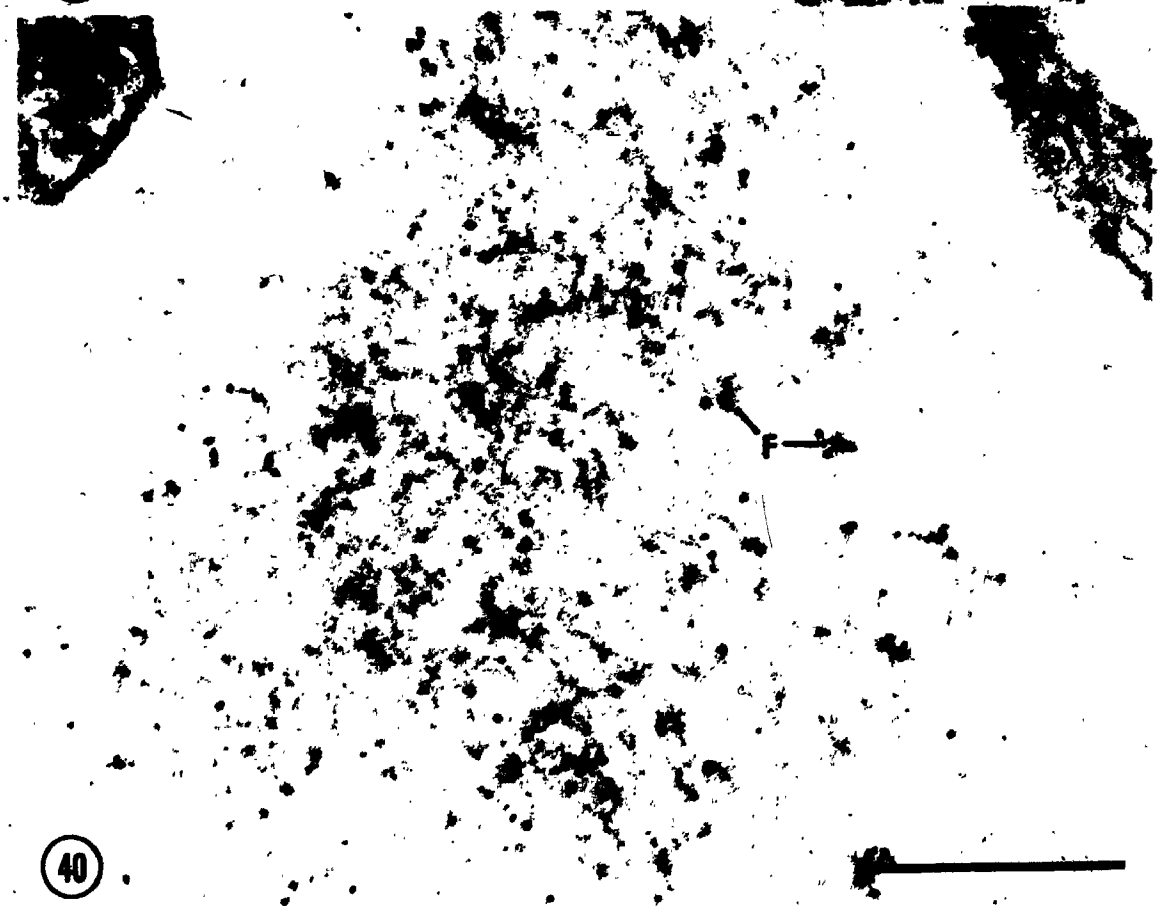

40

Figs. 41, 42. Transverse sections of the basal lamina show that cationic ferritins bind to the electron-dense areas. Both HCF (Fig. 41) and CF (Fig. 42) bind to the uranyl-staining portion of the basal lamina. Much more HCF than CF is bound to the basal lamina. While both types of cationic ferritin bind to the cell surface HCF (Fig. 41) shows dense aggregates while CF (Fig. 42) is not aggregated. Uranyl acetate stained, x175,000. Bl=basal lamina, F=ferritin, FB=fat body.

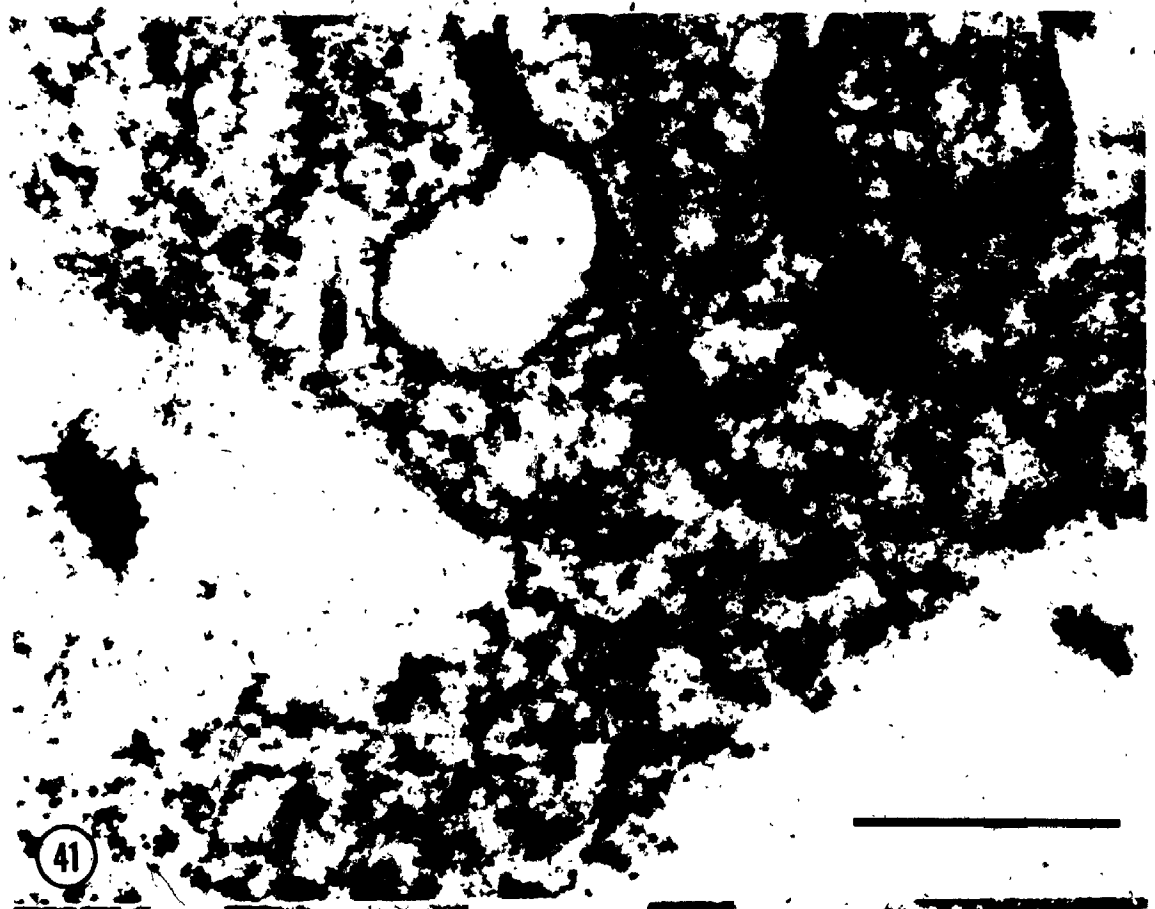

41

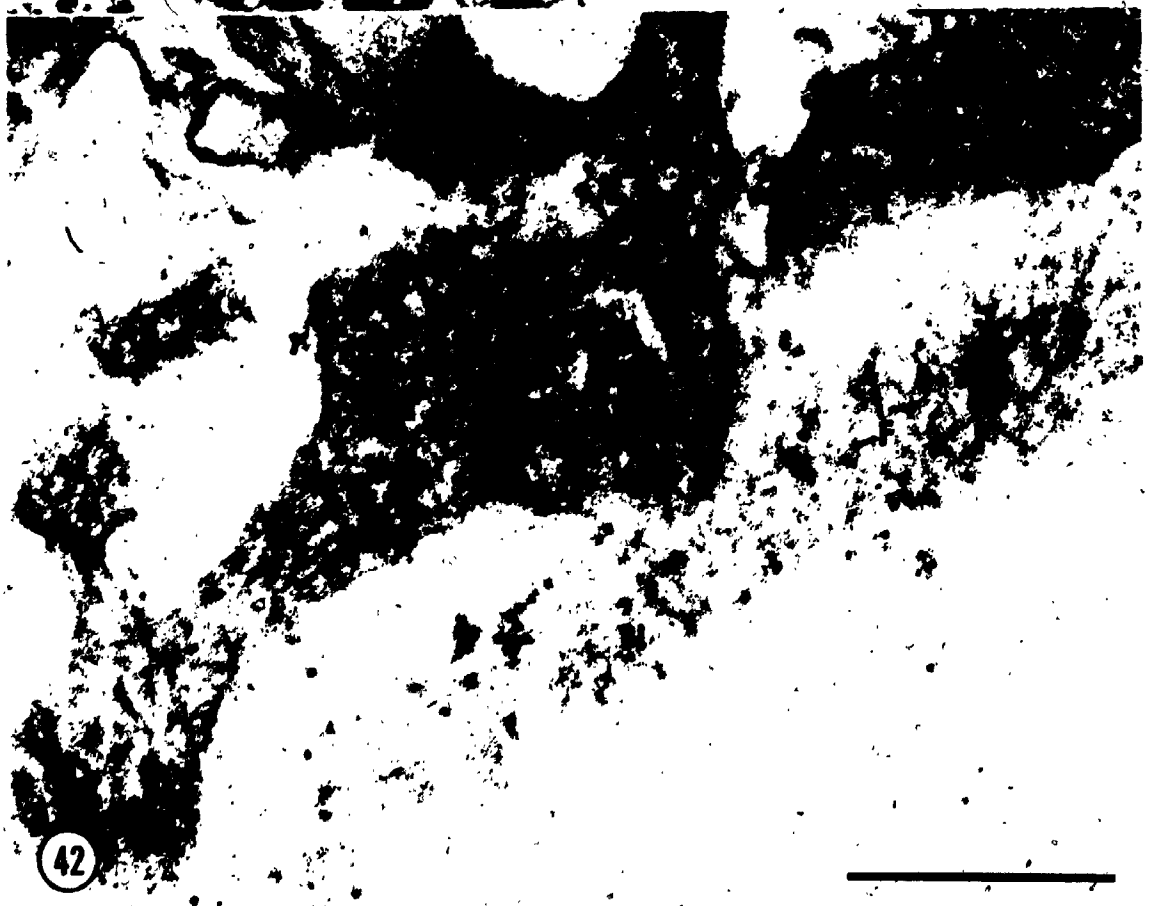

42

Figs. 43, 44. Distribution of anionic ferritins in the basal lamina. Transverse sections of cells labeled with AF1 (Fig. 43) and AF2 (Fig. 44) also shows that the ferritin particles are bound to the uranyl-staining portion of the basal lamina. The amount of ferritin bound is much less than with the cationic ferritins. Uranyl acetate stained, x175,000. Bl=basal lamina, F=ferritin, FB=fat body.

(43)

(44)

artifactual shrinkage during fixation. The binding of polycationic molecules, such as HCF, can neutralize anionic groups, which in turn can cause collapse or denaturation of the macromolecules to which they bind (Skutelsky et al., 1978; Skutelsky and Bayer, 1979). This puts into question the existence of the pore-like structures in the basal lamina where the ferritin does not bind (Fig. 38-40). All ferritins regardless of charge were bound to the staining portion of the basal lamina but the amount of ferritin varied greatly.

The binding of HCF suggested that the basal lamina might be negatively charged and that it could act as a negatively charged sieve to affect the distribution of charged molecules between hemolymph and the lymph spaces.

(c) The penetration of ferritin through the basal lamina to the PMRS

Although the concentration of AF1 (pI. 4.0-4.4) was higher than HCF, very few particles of AF1 were found in the PMRS at the surface of the fat body (Fig. 45). Some amorphous material (possibly protein) had ferritin particles associated with it. Almost no ferritin particles were found in the region of the basal lamina.

AF2 (pI 5.5-6.5) sparsely labelled the basal lamina and there were few particles in the PMRS (Fig. 46). Most

Figs. 45-48. Penetration of ferritin into the PMRS is related to the charge of the molecule. Bismuth stained, x90,000.

Fig. 45. AF1 does not bind appreciably to the basal lamina, and few particles are found in the lymph spaces.

Fig. 46. AF2 is present in very small numbers in the PMRS and basal lamina.

Fig. 47. CF sparsely labels the basal lamina. The membranes of the PMRS are labelled with clusters of CF particles.

Fig. 48. HCF is present in large aggregates in the PMRS which appear to be surface bound. PMRS=plasma membrane reticular system, Bl=basal lamina, Hy=hemolyph, F=ferritin.


PMRS
Bl
F
Hy
45
PMRS
Bl
F
Hy
46
PMRS
F
F
Bl
Hy
47
PMRS
F
F
Hy
48

of the particles in the spaces were bound to the plasma membrane (Fig. 46).

Particles of CF (pI 7.0-8.0) were clustered at the surface of the PMRS (Fig. 47). The basal lamina was sparsely labelled (Fig. 47).

Large clusters of HCF were found at surfaces of the PMRS and lateral intercellular spaces (Fig. 48). Large clusters of particles which exhibited close packing were bound to membranes of the lymph spaces (Fig. 48).

There is thus a dramatic difference between the density of the anionic and cationic derivatives of ferritin on the lymph side of the basal lamina. AF was not removed from the hemolyph during the experiment since fixation and examination of the hemolyph showed much more AF than in the lymph spaces (data not shown).

The basal lamina presumably prevents the penetration of negatively charged ferritins but allows positively charged ferritins into the lymph of the PMRS.

d) The penetration of ferritin into intercellular spaces

Very few AF1 and AF2 particles were found in the intercellular spaces between fat body cells (Figs. 49, 50). CF showed sparse labelling of the lateral intercellular spaces (Fig. 51). HCF was found in the

Figs. 49-52. Penetration of ferritin into intercellular spaces. Bismuth stained, x92,000.

Figs. 49, 50. Very few particles of AF1 (Fig. 49) or AF2 (Fig. 50) are found in the intercellular spaces.

Fig. 51. CF is found sparsely labelling the membranes of the lateral intercellular spaces.

Fig. 52. HCF is bound in aggregates in the lateral intercellular spaces. LS=lateral intercellular space, F=ferritin.


F
LS
49
F
LS
50
LS
F
LS
51
52

intercellular spaces, in tightly packed aggregates bound to the membrane (Fig. 52).

The distribution of ferritins in intracellular vacuoles was also dependent upon the charge of the ferritin molecules. Multivesicular bodies contained large clusters of HCF but AF was very difficult to find and only few vacuoles contained AF particles (Figs. 53, 54). AF was not found in any other intracellular vacuoles in the fat body. The large clusters of HCF in the multivesicular bodies may correspond to the clusters of HCF that were observed at the surface of the cell (Figs. 36, 37, 48).

These results show that negatively but not positively charged ferritins are excluded from the fat body spaces, presumably by the basal lamina.

(e) The quantitation of CF bound to the membranes of the PMRS and lateral intercellular spaces

Comparison of the amount of CF bound by membranes of the PMRS and the lateral intercellular spaces showed that the membranes of the PMRS consistently bound more CF at both 30 and 60 min of incubation ($p<.001$ t-test) (Table 4). There was no significant difference between 30 and 60 min for the PMRS or the lateral plasma membrane binding (Table 4).

Figs. 53, 54. Multivesicular bodies contain aggregates of HCF (Fig. 53) but little AF (Fig. 54). Fig. 53 is bismuth stained, Fig. 54 is unstained, x85,000. MVB=multivesicular body, F=ferritin.

Fig. 55. CF labels the basal lamina of tracheoles, which penetrate the fat body at approximately the same density as the basal lamina at the fat body surface. Bismuth stained, x90,000. Bl=basal lamina, Tr=tracheole, FB=fat body, F=ferritin.

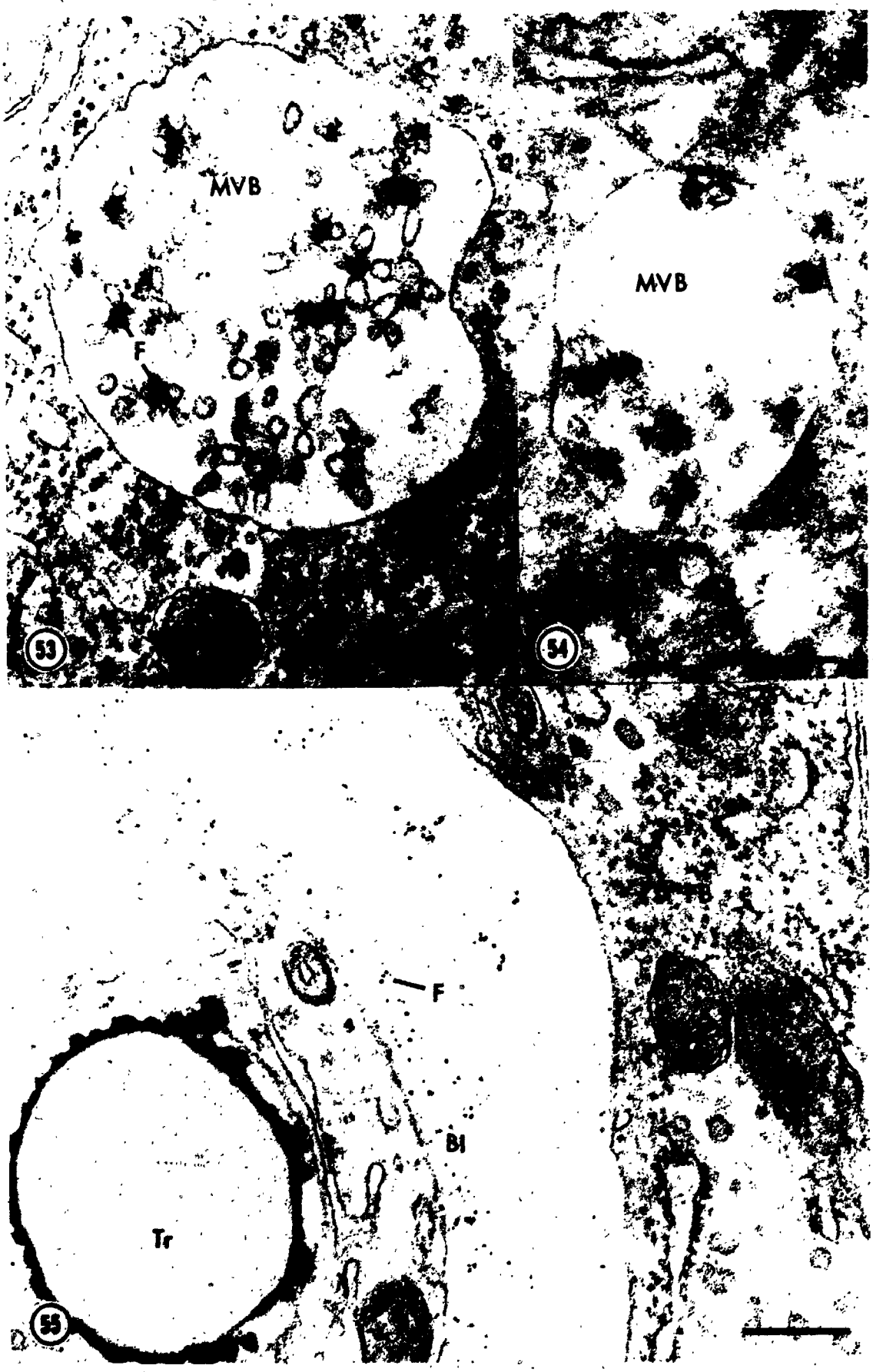
MVB
F
MVB
53
54
F
Bl
Tr
55

Table 4. Quantitation of cationic ferritin binding to the membranes of the Plasma Membrane Reticular System and lateral intercellular space.*

membrane	30 min	n	60 min	n
PMRS	176±43 ✱	10	169±33 ✱	10
lateral intercellular space	39±26	8	40±27	8

*Experimental details are given in the Materials and Methods section. All measurements are in ferritin particles/μm^2 ±SD.

✱At both 30 and 60 min the number of cationic ferritin particles bound to the membranes of the PMRS is significantly greater than the amount bound to the membranes of the lateral intercellular space ($p < .001$ t-test).

The differential labeling of the PMRS was not due to concentration differences since the basal laminae of tracheoles that penetrate the fat body had similar amounts of bound CF as did the basal lamina at the fat body surface (Fig. 55). This suggests that the membranes of the PMRS may have significantly more anionic sites than the membranes of the lateral intercellular spaces.

5.4 Discussion

The anionic sites of the basal lamina of the fat body act as a barrier to anionic but not cationic derivatives of the protein ferritin. The specialized case of the kidney glomerular basal lamina has clearly shown that the anionic sites of the basal lamina (Rennke et al., 1975; Kanwar and Farquahar, 1979a) play an important role in the movement of charged proteins across it (Rennke and Venkatchalam, 1977; Rennke et al., 1978). Loss of anionic sites from the basal lamina, whether through enzyme digestion (Kanwar et al., 1980) or pathological condition (Caulfield and Farquahar, 1978; Olson et al., 1981), causes changes in glomerular basal lamina permeability to charged proteins. Clusters of anionic sites have also been found on the basal lamina of the endothelium in capillaries and it is proposed that these may also have a role in regulating the movement of charged molecules across the endothelium (Simionescu et al., 1982). The anionic sites of basal laminae may have a

general role in determining the permeability to charged proteins.

The anionic sites on the plasma membrane of fat body cells may play a role in the movement of the tracers into fat body spaces. Cationic tracers, after diffusing through the basal lamina, bind to anionic sites of the PMRS or the plasma membrane of the lateral intercellular spaces. The PMRS has more anionic sites as determined by CF binding, than the lateral plasma membrane. It has been proposed that the PMRS may form the reaction chamber for the loading and unloading of lipophorin (Locke, 1984). The regional differentation of surface charge may play a role in this function.

Since major hemolymph proteins of Calpodes have been found to be the same size (10 to 11 nm) as ferritin and approximately the same charge as the anionic ferritins used in this study (Mussett, 1977; Webster, 1982), the charge of the basal lamina may play a role in regulating protein entry into the spaces surrounding fat body cells. It has been shown that the fat body synthesizes and secretes these proteins into the hemolymph and then at a later time may resorb them (Locke and Collins, 1968; Locke et al., 1982; Webster, 1982). A modification of the charge differences between the basal lamina and proteins may be necessary for this change.

Anionic sites of the basal lamina may also affect the distribution of smaller molecules and ions. The redistribution of ions by fixed polyanionic groups would result in a Donnan potential (Comper and Laurent, 1978). X-ray microanalysis has shown that the basal laminae of insect epithelial cells sequester potassium and exclude sodium and chloride (Gupta et al., 1977; Gupta and Hall, 1979). The high levels of proteoglycans containing sulphur and phosphorus could be responsible for this discrimination (Dutkowski, 1977; Dybowska and Dutkowski, 1977; Kanwar and Farquahar, 1979b). The anionic sites of the basal lamina labeled by HCF may affect the transport of both large and small molecules from the hemolymph to create the lymph bathing the cells.

CHAPTER 6

Lamellar bodies are the intracellular site of membrane turnover in the fat body

6.1 Introduction

The fat body is the main tissue for hemolymph protein synthesis in insects (Wyatt, 1980). In Calpodes ethlius there is a dramatic increase in the amount of hemolymph protein during the last larval stadium (Locke and Collins 1968), that is correlated with an increase in ecdysteroid titre (Dean et al., 1980). The secretion of hemolymph proteins by the fat body would mean an increase in the plasma membrane area if there were no mechanisms to deal with the excess (Palade, 1959; 1975).

The pathways of plasma membrane turnover have been examined in cells by the use of highly cationic ferritin which binds to the plasma membrane and marks the membrane compartments involved (reviewed in Steinman et al., 1983). In some cell types, surface membrane has been traced back into the secretory pathway (Golgi saccules and secretory granules) thus providing evidence for membrane recycling (Farquhar, 1978; Herzog and Miller, 1979; Ottosen et al., 1980; Thyberg, 1980; Thyberg et al., 1980) even though some studies showed minimal amounts of tracer in the Golgi complex (Denef and Ekholm, 1980; Nielsen et al, 1981;

Nilsson et al., 1983). Other studies have found that plasma membrane could be traced to multivesicular bodies (MVB) and lysosomal compartments and not the Golgi complex (Tartakoff et al., 1981; Van Deurs et al., 1981; Van Deurs et al., 1982; Van Deurs and Nilausen, 1982; Williams, 1982; King, 1982).

In order to map the pathway of plasma membrane turnover in the fat body of Calpodes, the uptake of highly cationic ferritin (HCF) and its distribution at various times after injection, was examined. The basal lamina that surrounds the fat body of Calpodes acts as a charge selective barrier preventing anionic but allowing cationic derivatives of the protein ferritin into and around the cells (Chapt. 5). The results show that after uptake by coated vesicles at the cell surface, the first sites of accumulation were the MVBs but soon after the ferritin was found in lamellar bodies that formed from the MVBs. No evidence for direct membrane recycling to the secretory pathway was found.

6.2 Materials and Methods

(a) Test animals

Larvae of C. ethlius were reared as previously described (Locke, 1970). Mid-fifth stage larvae were used in this study because their fat body is metabolically active at this stage (Locke and Collins, 1968). After injection with tracer solution, larvae were kept in a 22° C incubator with a 12 hr light, 12 hr dark cycle and were allowed to feed normally.

(b) Time course of HCF uptake

HCF (pI 8.5-9.5) was obtained from Miles Biochemicals. Cationic ferritin (CF pI 7.0-8.0) was synthesized and kindly donated by Dr. H. Rennke (see Rennke et al., 1975 for modification procedure). The tracers were diluted with Grace's medium (Gibco Chemical Co.) and 40 µl was then injected into larvae weighing 1.6-1.8 gr. Concentration of the tracer exposed to the fat body was diluted by a factor of 8.5 because of the volume of hemolymph. HCF had a hemolymph concentration of 1.2 mg/ml, while CF had a concentration of 4.7 mg/ml.

Larvae were injected with the tracer solution and then fixed at 30 sec, 10, 30, 60 and 240 min.

(c) Fixation and Processing

After the appropriate incubation period, larvae were ligated and inflated with ice cold 5% glutaraldehyde in 0.1 M phosphate buffer pH 7.4 with 2% sucrose. The tissue was processed as described in section 5.2 (c).

(d) Electron Microscopy 

Thin sections of gray interference colour were cut on a diamond knife and mounted on 300 mesh copper grids. Sections were viewed unstained, or stained in bismuth to enhance ferritin contrast (Ainsworth and Karnovsky, 1972) or uranyl acetate (Locke and Huie, 1980). Micrographs were taken on a Philips EM 300 at 80 kV. The results are based on observations of of at least 3 animals for each time period in 2 separate experiments.

6.3 Results

(a) Uptake of ferritin at the fat body cell surface

At the shortest period of incubation (30 sec), HCF was bound to the fat body plasma membrane (Fig. 56). When the plasma membrane was normal to the plane of the section, the particles were in a single row bound to the membrane and separated by a particle to membrane spacing of 4-5 nm. Even at the earliest time, some HCF was found in clusters

Figures 56-59. Uptake of ferritin at the fat body cell surface. The time course of HCF uptake was examined in larvae 30 sec, 10, 30 and 60 min after injection. The plasma membrane reticular system (PMRS) is a specialization at the surface of fat body cells where much pinocytosis was observed. Bar=0.2 μm in all figures, x85,000.

Fig. 56. At 30 sec after injection, single rows and clusters of HCF (F) are bound to the plasma membrane. There is no evidence of pinocytosis. The basal lamina (Bl) has few bound ferritin particles. Unstained.

Fig. 57. 10 min after injection numerous pinocytic vesicles (designated by arrowheads) are taking up aggregates of HCF. Clusters of HCF (F) are also bound to the cell surface. The basal lamina (Bl) is labeled with many particles of HCF. Bismuth stained.

Fig. 58. At 30 min after injection, pinocytic vesicles (arrowheads) are still present, as well as many clusters of HCF bound to the plasma membrane. The basal lamina (Bl) and a thickened portion of an elastic fiber (Ef) have groups of bound HCF. Bismuth stained.

Fig. 59. After 60 min, clusters of HCF are still present on the cell surface. A slightly oblique section shows a cluster of densely packed HCF (arrow) particles bound to the membrane. The basal lamina has numerous clusters of bound ferritin particles. Bismuth stained.

56

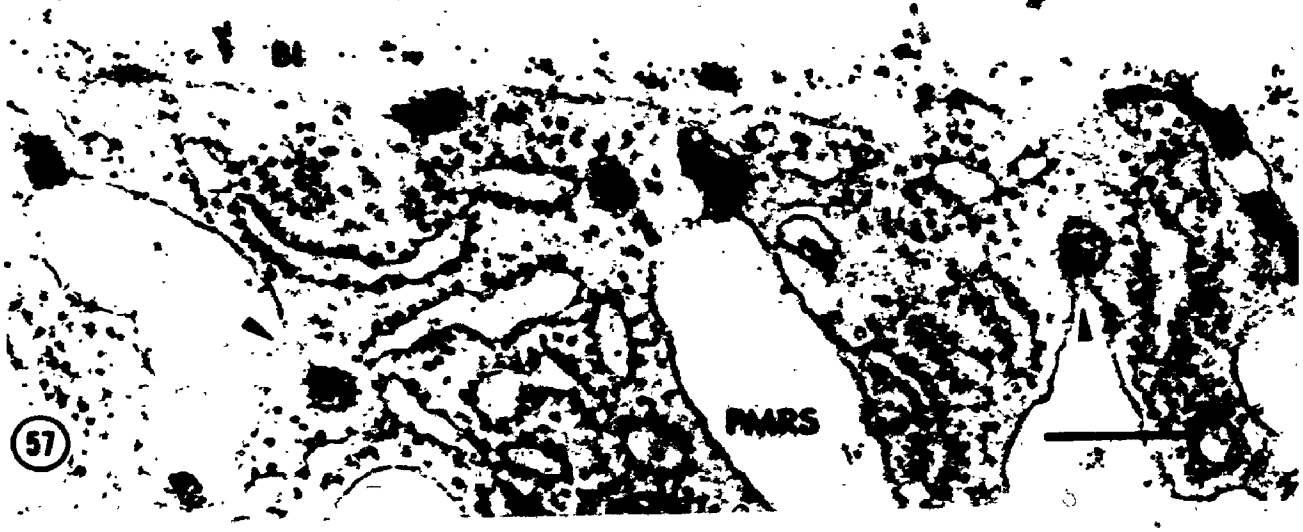

57

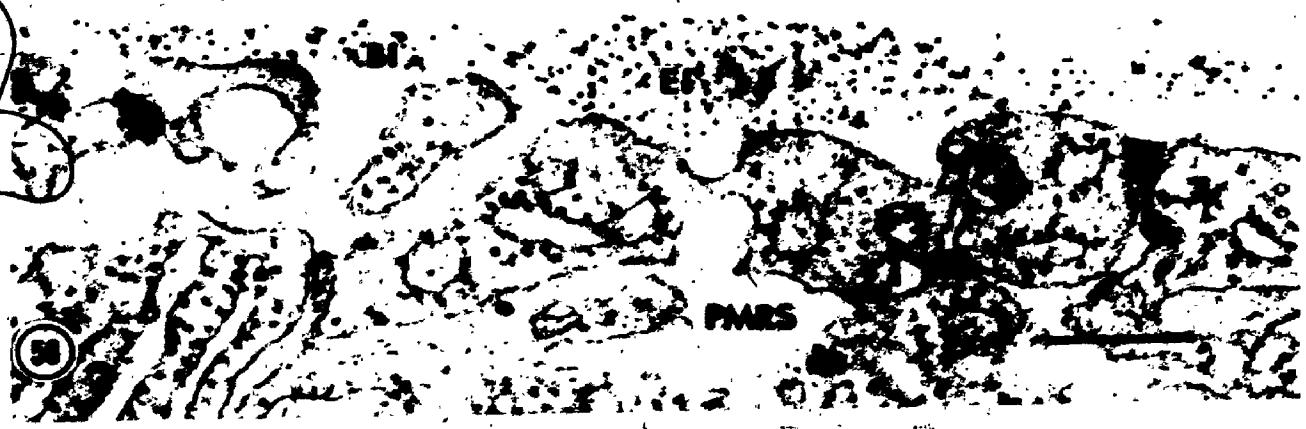

58

59

at the membrane surface. There were only a few HCF particles bound to the basal lamina (Fig. 56).

By 10 min of incubation, coated vesicles were pinocytosing HCF at the cell surface (Fig. 57). Large clusters of HCF were bound to the plasma membrane. After 30 min of incubation pinocytic vesicles were still taking up HCF at the PMRS (Fig. 58). At 60 min, there were aggregates of HCF on the plasma membrane (Fig. 59). Between 10 and 60 min the basal lamina was consistently labeled with HCF (Figs. 57-59).

Membrane-bound ferritin was taken up by fat body cells by pinocytosis. The distribution of the ferritin inside the vacuolar system can therefore be used as a marker for the fate of the membrane.

(b) Intracellular distribution of pinocytosed HCF

Examination of intracellular structures at 10 min showed no HCF in MVB or any other organelle (Figs. 60, 61). After 30 min the first site of HCF accumulation was the MVB (Fig. 62). At this time no other structures (excluding pinocytic vesicles) had any HCF. Not all MVBs had HCF after 30 min (Fig. 62). Lamellar bodies did not contain HCF after 30 min of incubation (Fig. 63-65). HCF occurred in clusters at the periphery of MVB suggesting that these had been delivered by pinocytic vesicles (Fig.

Figs. 60, 61. Intracellular distribution of HCF after 10 min. No HCF was found in any organelles 10 min after injection. The "light" and "dark" MVBs (l-MVB and d-MVB respectively) and the tubular stuctures (t) had no HCF (Fig. 60). Lamellar bodies (LB), MVBs and tubular structures (t) are frequently found together. They contain no HCF at this time (Fig. 61). The electron-dense particles in one vesicle (arrowhead) are not ferritin since they are much smaller and have a different shape. Unstained, x85,000.


MVB
d-MVB
60
61

Fig. 62-66. MVBs are the first organelle to contain HCF.

Fig. 62. 30 min after injection, clusters of HCF (F) are found in MVB lumen close to the limiting membrane. A "dark" MVB (dMVB) contains no HCF. Unstained, x81,000.

Fig. 63. A lamellar body (LB) has no HCF at 30 min after injection. Unstained, x90,000.

Fig. 64. At 30 min after injection, a MVB has clusters of HCF (F) at the periphery. The small lamellar body (LB) beside the MVB has no ferritin in it. Unstained, x85,000.

Fig. 65. A lamellar body (LB) contains no HCF in its lumen. Several tubular structures (t) are found at one end. Uranyl acetate stained, x85,000.

Fig. 66. A "light" MVB (lMVB) with few vesicles in its lumen, has clusters of HCF (F) bound to the membrane and contents in the lumen. Uranyl acetate stained, x85,000.


d-MVB
MVB
F
F
MVB
62
63
64
65
66

62, 64, 66).

At 60 min of incubation another major structure, the lamellar body, was labeled with HCF (Fig. 67). While all MVBs were labeled with HCF some but not all lamellar bodies contained HCF (Figs. 67-69). This suggests that the lamellar bodies are a subsequent step in the uptake of ferritin. The Golgi complex and other post-transition vacuolar compartments did not at any time in these experiments, contain HCF (Fig. 67).

MVBs and lamellar bodies were frequently found in close association with each other (Fig. 67). Dark-staining tubules, that contain ferritin and may be either breakdown products of lamellar bodies or connecting tubules, were found between MVBs and lamellar bodies (Fig. 67). Different types of MVBs which have previously been classified according to the density of their contents may be at different stages of maturation. Lamellar bodies may be terminal stages in this sequence since they accumulate HCF after it first appears in the MVBs. If this is so one should be able to find intermediate stages in their formation.

(c) Lamellar Bodies develop from MVBs

After 60 min of incubation with HCF, all MVBs contained HCF in their lumen, while some lamellar bodies

Figs. 67-69. Lamellar bodies are labeled with HCF

Fig. 67. Lamellar bodies (LB) are labeled with HCF (F) after 60 min of incubation. A MVB and several tubular structures (t) which also contain HCF are in close association with a lamellar body (LB). The Golgi complex (GC) contains no ferritin. Unstained, x90,000.

Fig. 68. While most lamellar bodies (LB) are labeled, there are some which do not contain ferritin. Unstained, x85,000.

Fig. 69. Both MVBs contain HCF (F) after 60 min of incubation. Uranyl acetate stained, x85,000.


MVB
67
68
MVB
69

had HCF and others did not. The various types of MVBs found at 60 min suggests a possible developmental sequence for the formation of lamellar bodies.

MVBs with an electron lucent matrix invariably have fewer vesicles and less HCF, suggesting that they may have been formed from fewer pinocytic vesicles (compare Fig. 66 with Figs. 70 and 71). Intermediates between lamellar bodies and MVBs showed that as the vesicles declined the lamellae increased to form ferritin-containing lamellar bodies (Figs. 72-74).

The distribution of HCF in the fat body after 4 hr was not different from the pattern found at 60 min (data not shown). Since the HCF was injected into the hemolymph in excess, there would be a constant source of HCF during the experiment.

Similar results for the time course and destination were obtained with cationic ferritin of lower positive charge (pI 7.0-8.0) (data not shown).

These results suggest that there are continuous cycles of MVB formation by pinocytic vesicles derived from the fat body plasma membrane which become lamellar bodies filled with HCF. This interpretation is shown in Figure 75.

Figs. 70-74. Lamellar bodies develop from MVBs. After 60 min of incubation, there are various intermediates between MVBs and lamellar bodies (LB) which suggest a developmental sequence. Figs. 70, 72 are bismuth stained; Figs. 71, 73 and 74 are uranyl acetate stained, x85,000.

Fig. 70. As the MVB fills up with vesicles and HCF (F) the lumen becomes increasingly dense. The smaller MVB has a vesicle (arrow) that appears to be fusing with the limiting membrane. Tubules (t) around the MVBs also contain ferritin (F).

Fig. 71. A MVB is densely packed with vesicles and HCF. It is closely associated with tubules (t) and a lamellar body (LB) that contains HCF.


F
MVB
F
VP
70
F
MVB
71

Fig. 72. A MVB of intermediate density has much HCF within the luminal contents that include vesicles (ve) and few membrane lamellae (lm).

Fig. 73. As the density of the MVB increases the vesicles (ve) decrease while the lamellae (lm) increase. The ferritin (F) is still visible between the lamellae and around the vesicles.

Fig. 74. The final stage of lamellar body (LB) formation consists of the elimination of vesicles and the lumen filling with parallel arrays of membranes (lm) which are filled with ferritin (F). Tubules (t) surround the lamellar body.


72
73
LB
74

Fig. 75. An interpretation of the uptake and fate of HCF in the fat body. HCF is pinocytosed at the fat body cell surface and delivered first to MVBs which become lamellar bodies via intermediate stages. The role of the tubules which are found frequently between MVBs and lamellar bodies and contain ferritin is not known.

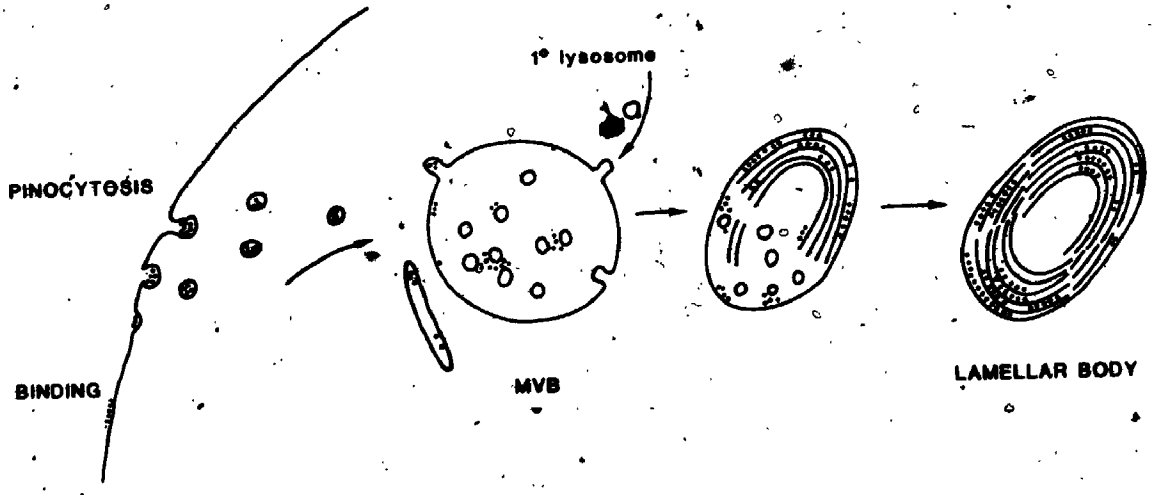
1° lysosome
PINOCYTOSIS
BINDING
MVB
LAMELLAR BODY

6.4 Discussion

HCF binds to the fat body plasma membrane anionic sites and is pinocytosed into the cell, acting as a marker for the surface to which it is bound. Analysis of the intracellular distribution of HCF shows that MVBs are the first site of ferritin accumulation and that they become lamellar bodies. At no time was any HCF found in the Golgi complex or other components of the secretory pathway. This supports the finding that cells vary in the way that they deal with excess surface membrane (see references in Introduction sect. 6.1). Division of the cells with respect to the method of secretion (continuous, non-regulated secretion e. g. fibroblasts, plasma and fat body cells as compared to discontinuous, hormone-regulated secretion e. g. pituitary, thyroid cells and macrophages) suggests that the membrane recycling may be related to the method of secretion. Cells that continuously secrete do not recycle membrane directly to the secretory pathway while cells that secrete periodically do. This may reflect the necessity of cells that have sudden massive secretion to reutilize directly their secretory membranes.

The novel finding in this study is that there is a direct link between endocytosed HCF and the formation of lamellar bodies from MVB. Previous work has shown the sequence of "light" to "dark" MVB maturation using HCF as a tracer (Van Deurs et al., 1981) but no lamellar body was

identified in this sequence. Membrane turnover in the compound eyes of tipulid flies may involve lamellar bodies as a final step (Williams and Blest, 1980) but studies with membrane tracers are lacking.

The role of MVBs in the uptake of tracers from the cell surface has been shown to be important in many cell types (Friend and Farquhar, 1967; Locke and Collins, 1967, 1968; Holtzman and Dominitz, 1968; Locke, 1969; Locke and Krishnan, 1973; Larsen, 1976). These studies have used horseradish peroxidase as a tracer, which may or may not be a membrane marker depending on the type of enzyme and the conditions of use. MVBs are heterophagic since they have the lysosomal marker acid phosphatase (Locke and Sykes, 1975). It has been generally concluded that MVBs are an important site of membrane turnover (Holtzman, 1976; Locke and Collins, 1980).

Lamellar bodies have been described in many different cell types but there has been little evidence to suggest a general function. The time of occurrence and the similarity of lamellar body and plasma membrane thickness suggested that lamellar bodies are involved in the uptake of the excess membrane after the release of tyrosine-storage vacuoles in Calpodes fat body (McDermid and Locke, 1983). Since a MVB intermediate was not described in this sequence, it may be possible that in some cases lamellar bodies form directly from endocytosed

membrane. This supports the generalization that lamellar bodies are concerned with membrane turnover. Since the lamellar bodies of Calpodes are acid phosphatase positive (McClintock, 1982) they may be part of the lysosomal system. Published micrographs have shown "dense bodies" with lamellar arrays of membrane (Arstila et al., 1971; Sohal et al., 1976, 1977; Harrod and Kastritsis, 1972) suggesting that these stuctures have largely been ignored in many cell types.

Organelles called lamellar bodies, which have the same basic multilamellar-membrane appearence, have been described in specialized cells such as type II alveolar cells (Gil and Reiss, 1973; Stratton, 1978), and also schistosome parasites (McDiarmid et al., 1982) and the compound eye of tipulid flies (Williams and Blest, 1980). In the case of lamellar bodies in lung and parasites, most studies have focussed on these stuctures' role in the production of phospholipid to be added to the cell surface (Ryan et al., 1975; Hockley and McLaren, 1973). However lung lamellar bodies are also the intracellular site of the accumulation of HCF (Williams, 1982), suggesting that they have a similar role as the lamellar bodies in Calpodes.

In summary, the lamellar bodies that form from MVBs are the intracellular site of accumulation of HCF. Since so many secretory cell types have lamellar bodies they may be of general importance in membrane turnover.

CHAPTER 7

SUMMARY

(1) A method for the microinjection of cells was developed using the tracer horseradish peroxidase that allows light and electron microscope localization of the injected tracer. The horseradish peroxidase reaction-product diffused in the cytoplasm and bound to intracellular surfaces. It is therefore possible to inject protein tracers into intact cells and examine their distribution by electron microscopy without affecting their viability.

(2) The distribution of microinjected ferritin, ranging in charge from anionic to highly cationic, was used to examine the surface charge on the rough endoplasmic reticulum and the Golgi complex of intact cells. Highly cationic ferritins (HCF pI>9) were mostly bound and caused swelling of the rough endoplasmic reticulum. Cationic ferritin (CF pI 7.0-8.0) and anionic ferritin (AF pI 4.0-4.4) caused no abnormal morphology. The distribution of these ferritins in the cytoplasmic space varied with their charge. Significantly more CF was bound to surfaces than was found in the free cytoplasmic space. Conversely, there was significantly more AF in the free cytoplasmic space than close to surfaces. Increases in the isoelectric point of the ferritins were correlated with a greater proportion of

bound ferritin. Therefore the intracellular surfaces are negatively charged.

(3) The distribution of CF (pI 7.0-8.0) was used as a measure of the surface charge of structures in the endoplasmic reticulum/Golgi complex transitional region. Comparison of the different surfaces showed that there was no significant difference in the amount of CF bound to rough endoplasmic reticulum, transition vesicles, Golgi saccules or secretory vesicles. The Golgi complex beads were not distinguished by their charge. This suggests that differences in surface charge are not the mechanism of regulating the hierarchy of membrane interactions in the secretory pathway.

(4) The microinjection of polycationic but not anionic molecules causes swelling of the rough endoplasmic reticulum. Calcium buffers, lanthanum chloride, lysozyme, bovine serum albumin, highly cationic and anionic ferritin were microinjected into salivary gland cells and their effects observed by light and electron microscopy. Immediately after the microinjection of polycationic molecules, the cytoplasm changed from transparent to opaque as the rough endoplasmic reticulum became swollen. Binding of polycationic molecules to the rough endoplasmic reticulum may cause the membrane to become permeable to some solutes and swell due to osmotic forces.

(5) The distribution of anionic sites on the basal lamina of fat body cells was examined with HCF. Clusters of anionic sites are present throughout the basal lamina. The penetration of ferritins, with a range of charges from anionic to highly cationic, through the basal lamina into the spaces between fat body cells is correlated with the charge of the tracer. Negatively but not positively charged ferritins are mostly prevented from crossing the basal lamina. The anionic sites of the basal lamina may therefore affect the composition of the lymph that bathes the fat body cells.

(6) There was significantly more CF bound to the membranes of plasma membrane reticular system than to the lateral plasma membranes, suggesting that there may be regional differences in surface charge at the cell surface. Since it has been proposed that the plasma membrane reticular system is a reaction chamber for the unloading of lipids from hemolymph proteins, the anionic sites may have a role in this function.

(7) Analysis of the time course of HCF uptake by the fat body cells has shown that the tracer bound to the plasma membrane and was pinocytosed by coated vesicles. The first sites of intracellular accumulation were multivesicular bodies which became filled with HCF between 30-60 min after the cells were exposed to the tracer. At no time during

the experiments were any parts of the Golgi complex labeled with the tracer. By 60 min, the HCF was increasingly found in lamellar bodies. The different types of "light" and "dark" multivesicular bodies suggest that lamellar bodies formed from multivesicular bodies as they filled with tracer. The occurrence of lamellar bodies in many different cell types suggests an important role in membrane dynamics.

References

Abe, H., M. A. Moscarello and J. M. Sturgess. 1976. The distribution of anionic sites on the surface of the Golgi complex. J. Cell Biol. 71:973-979.

Ainsworth, S. K. and M. J. Karnovsky. 1972. An ultrastructural staining method for enhancing the size and electron opacity of ferritin in thin sections. J. Histochem. Cytochem. 20:225-229.

Alberts, B., D. Bray, J. Lewis, M. Raff, M. Roberts and J. D. Watson. 1983. Molecular Biology of the Cell. Garland Pub., New York. pp. 1143.

Allan, D., M. Billah, J. B. Finean and R. H. Michell. 1976. Release of diacylglycerol-enriched vesicles from erythrocytes with increased intracellular calcium. Nature (Lond.) 261:58-60.

Andersson, K., B. Bjorkroth and B. Daneholt. 1980. The in situ structure of the active 75S RNA genes in Balbiani rings of Chironomus tentans. Exp. Cell Res. 130:313-326.

Arstila, A., O. Jauregui, J. Chang and B. F. Trump. 1971. Studies on cellular autophagocytosis. Lab. Invest. 24:162-174.

Ashhurst, D. E. 1982. The structure and development of insect connective tissue. In Insect Ultrastructure. R. C. King and H. Akai (eds.). Plenum Press, New York. pp. 313-350.

Banerjee, S., R. Cohn and M. Bernfield. 1977. The basal lamina of embryonic salivary epithelia: production by the epithelium and role in maintaining lobular morphology. J. Cell Biol. 73:445-463.

Bangham, A. D. 1981. Interactions of biological membranes with their environment. In Interaction of the Blood with Natural and Artificial Surfaces. E, W. Salzman (ed.). Marcel Dekker, Inc., New York. pp. 61-101.

Barber, J. 1980. Membrane surface charges and potentials in relation to photosynthesis. Biochim. Biophys. Acta 594:253-308.

Behnke, O. and T. Zelander. 1970. Preservation of intracellular substances by the cationic dye alcian blue in preparative procedures for electron microscopy. J. Ultrastruct. Res. 31:424-438.

Ben-Ishay, Z., F. Reichart and R. Gallily. 1975. Crystallin-like surface charge array of murine macrophages and lymphocytes: visualization with cationized ferritin. J. Ultrastruct. Res. 53:119-127.

Bernfield, M. and S. Banerjee. 1972. Acid mucopolysaccaride (glycosaminoglycans) at the epithelial-mesenchymal interface of mouse embryo salivary glands. J. Cell Biol. 52:664-673.

Bernfield, M. and S. Banerjee. 1978. The basal lamina in epithelial-mesenchymal morphogenetic interactions. In First International Symposium on the Biology and Chemistry of Basement Membranes. N. A. Kefalides (ed.). Academic Press, New York. pp. 137-148.

Bierman, A. 1955. Electrostatic forces between non-identical colloidal particles. J. Colloid Sci. 10:231-245.

Bittiger, H. and J. Heid. 1977. The subcellular distribution of particle bound negative charges in rat brain. J. Neurochem. 28:917-922.

Black, B. L., L. Jarett and J. McDonald. 1981. The regulation of endoplasmic reticulum calcium uptake of adipocytes by cytoplasmic calcium. J. Biol. Chem. 256:322-329.

Blad-Holmberg, D. 1979. Study of electrophoretic mobility of cellular membranes isolated from rat liver. Biochim. Biophys. Acta 553:25-39.

Bock, P. 1972. Adsorption of horseradish peroxidase to negatively charged groups. Acta. Histochem. 43:8-14.

Boggs, J. 1980. Intermolecular hydrogen bonding between lipids: influence on organization and function of lipids in membranes. Can. J. Biochem. 58:755-770.

Borysenko, J. Z. and W. Woods. 1979. Density, distribution and mobility of surface anions on normal/transformed cell pair. Exp. Cell Res. 118:215-227.

Brac, T. 1981. Intracellular charge distribution investigated by microinjection of charged tracers. J. Cell Biol. 91 (2, Pt.2):411a (Abstr.).

Brodie, D. A. 1981. Bead rings at the endoplasmic reticulum Golgi complex boundary: morphological

changes accompanying inhibition of intracellular transport of secretory proteins in Arthropod fat body tissue. J. Cell Biol. 90:92-100.

Brodie, D. A. 1982a. The arrangement of the Golgi complex beads is not controlled by the cytoskeleton. Tissue and Cell 14:263-271.

Brodie, D. A. 1982b. Golgi complex beads in vertebrates and their relationship with clathrin coats. Tissue and Cell 14:253-262.

Brodie, D., M. Locke and F. P. Ottensmeyer. 1982. High resolution microanalysis for phosphorus in Golgi complex beads of insect fat body tissue by electron spectroscopic imaging. Tissue and Cell 14:1-11.

Burry, R. W. and J. G. Wood. 1979. Contribution of lipids and proteins to the surface charge of membranes. J. Cell Biol. 82:72-741.

Busch, H. 1965. Histones and Other Nuclear Proteins. Academic Press, New York. pp. 266.

Butman, B., G. Bourguignon and L. Bourguignon. 1980. Lymphocyte capping induced by polycationized ferritin. J. Cell. Physiol. 105:7-15.

Caulfield, J. and M. G. Farquhar. 1976. Distribution of anionic sites in the glomerular basement membrane; their possible role in filtration and attachment. Proc. Natl. Acad. Sci. USA 73: 1646-1650.

Caulfield, J. P. and M. G. Farquahar. 1978. Loss of anionic sites from the glomerular basement membrane in aminonucleoside nephrosis. Lab Invest. 39:505-512.

Chakrabarti, B. and J. Park. 1980. Glycosaminoglycans: structure and interactions. CRC Rev. Biochem. 8:225-313.

Cheung, W. Y. 1980. Calmodulin plays a pivotal role in cellular regulation. Science (Wash. D.C.) 207:19-27.

Chwang, W. K., A. Pawagi and I. M. Campbell. 1979. Changes in the osmotic behaviour of phosphatidylcholine vesicles induced by interaction with polyamino acids. Can. J. Biochem. 57:302-307.

Cohn, R., S. Banerjee and M. Bernfield. 1977. Basal lamina of embryonic salivary epithelia. Nature of glycosaminoglycan and organization of extracellular

materials. J. Cell Biol. 73:464-478.

Comper, W. and T. Laurent. 1978. Physiological function of connective tissue polysaccharides. Physiol. Rev. 58:255-315.

Cornelisse, C. J. and P. Van Duijn. 1973a. A new method for the investigation of the kinetics of the capture reaction in phosphatase cytochemistry. I Theoretical aspects of the local formation of crystalline precipitates. J. Histochem. Cytochem. 21:607-613.

Cornelisse, C. J. and P. Van Duijn. 1973b. A new method for the investigation of the kinetics of the capture reaction in phosphatase cytochemistry. II Theoretical and experimental studies of phosphate diffusion from thin polyacrylamide films. J. Histochem. Cytochem. 21:614-622.

Crow, T., E. Heldman, V. Hagopian, T. Enos and D. Alkon. 1979. Ultrastructure of photoreceptors in the eye Hermissenda labeled with intracellular injection of horseradish peroxidase. J. Neurocytol. 8:181-195.

Cullis, P. R. and B. DeKruijff. 1979. Lipid polymorphism and the functional roles of lipids in biological membranes. Biochim. Biophys. Acta. 559:399-420.

Danon, D., L. Goldstein, Y. Marikovsky, and E. Skutlsky. 1972. Use of cationized ferritin as a label of negative charges on cell surfaces. J. Ultrastruct. Res. 38:500-510.

D'Arrigo, J. 1975. Axonal surface charges: evidence for phosphate structure. J. Membr. Biol. 22:255-263.

Davies, P. F., H. G. Rennke and R. S. Cotran. 1981. Influence of molecular charge upon the endocytosis and intracellular fate of peroxidase activity in cultured arterial endothelium. J. Cell Sci. 49:69-86.

Dean, P. M. 1974. The electrokinetic properties of isolated secretory particles. In Secretory Mechanisms of Exocrine Glands. N. A. Thorn and O. H. Peterson (eds.). Munksgaard, Copenhagen. pp. 152-161.

Dean, P. M. 1975. Exocytosis modelling: an electostatic function for calcium in stimulus-secretion coupling. J. Theor. Biol. 54:289-308.

Dean, P. M. and E. K. Matthews. 1974. Calcium ion binding to the chromaffin granule surface. Biochem. J. 142:637-640.

Dean, P. M. and E. K. Matthews. 1975. The London Van der Waals attraction constant of secretory granules and its significance. J. Theor. Biol. 54:309-321.

Dean, R., W. Bollenbacher, M. Locke, S. Smith and L. Gilbert. 1980. Haemolymph ecdysteroid levels and cellular events in the intermolt/ moult sequence of Calpodes ethlius. J. Insect Physiol. 26:267-280.

Dean, R.L., J. V. Collins and M. Locke. 1984. The structure of fat body. In Comprehensive Insect Physiology, Biochemistry, and Pharmacology. Vol. 3, Chapt. 10. G.A. Kerkut and L.I. Gilbert (eds.). Pergamon Press, Oxford. in press.

Deen, W., C. Bridges and B. Brenner. 1983. Biophysical basis of glomerular permselectivity. J. Membr. Biol. 71:1-10.

Degens, E. T. and V. Ittekkat. 1982. In situ metal staining of biological membrane in sediments. Nature (Lond.) 298: 262-264.

DeKruijff, B. and P. R. Cullis. 1980. The influence of poly (L-lysine) on the phospholipid polymorphism. Biochim. Biophys. Acta 601:235-240.

DeKruijff, B., P. R. Cullis and A. Verkeij. 1980. Non-bilayer lipid structures in model and biological membranes. Trends Biochem. Sci. 5:79-81.

Deman, J. J., E. Bruyneel and M. Marcell. 1974. A study on the mechanisms of intercellular adhesion: effects of neuraminidase, calcium and trypsin on the aggregation of suspended HeLa cells. J. Cell Biol. 60:641-652.

Denef, J.-E. and R. Ekholm. 1980. Membrane labeling with cationized ferritin in isolated thyroid follicles. J. Ultrastruct. Res. 71:203-221.

Derjaguin, B. and L. Landau. 1941. Theory of the stability of strongly charged lyophobic sols and the adhesion of strongly charged particles in solutions of electrolytes. Acta Physicochim. USSR 14:633-692.

Diamond, J. 1975. How do biological systems discriminate physically similar ions? J. Exp. Zool. 194:227-240.

Diamond, J. and E. Wright. 1969. Biological membranes: the physical basis of ion and non-electrolyte selectivity. Ann. Rev. Physiol. 31:588-646.

Doggenweiler, C. and S. Frenk. 1965. Staining properties of lanthanum on cell membranes. Proc. Natl. Acad. Sci. USA 53:425-430.

Dorrscheidt-Kafer, M. 1979a. Excitation contraction coupling in the frog sartorius and the role of the surface charge due to the carboxyl group of the sialic acid. Pflügers Arch. 380:171-179.

Dorrscheidt-Kafer, M. 1979b. The interaction of ruthenium red with surface charges controlling excitation contraction coupling in frog sartorius. Pflügers Arch. 380:181-187.

Douglas, W. W. 1974. Involvement of calcium in exocytosis and the exocytosis-vesiculation sequence. Biochem. Soc. Symp. 39:1-28.

Dow, J., B. Gupta and T. Hall. 1981. Microprobe analysis of sodium, potassium, chloride, phosphorus, calcium, magnesium and water in frozen-hydrated sections of anterior caeca of the locust, Schistocerca gregaria. J. Insect Physiol. 27:629-639.

Duniec, J. T., M. J. Sculley and S. W. Thorne. 1979. An analysis of the effect of mono- and di-valent cations on the forces between charged lipid membranes with special reference to the grana thylakoids of chloroplasts. J. Theor. Biol. 79:473-484.

Dutkowski, A. B. 1977. The ultrastructure and ultracytochemistry of basement membrane of the Galleria mellonella fat body. Cell Tiss. Res. 176:417-429.

Dybowska, H. E. and A. B. Dutkowski. 1977. Ruthenium red staining of the neural lamella of the brain of Galleria mellonella. Cell Tiss. Res. 176:275-284.

Eagles, P. A. M., L. N. Johnston, and C. Van Horn. 1976. The distribution of anionic sites on the surface of the chromaffin granule membrane. J. Ultrastruct. Res. 55: 87-95.

Earnshaw, W. C., B. Honda, R. A. Laskey and J. E. Thomas. 1980. Assembly of nucleosomes: the reaction involving X. laevis nucleoplasmin. Cell 21:373-383.

Ebbesen, P. and F. Guttler. 1979. Arrest of cell

membrane movements by in vitro incubation with polycation reversed by polyanion. J. Cell Sci. 37:181-187.

Eckert, H. and C. Boschek. 1980. The use of horseradish peroxidase as a neuronal marker in the arthropod central nervous system. In Neuroanatomical Techniques. N. J. Strausfeld and T. Miller (eds.). Springer-Verlag, New York. pp. 326-339.

Edstrom J. E. and U. Lonn. 1976. Cytoplasmic zone analysis. RNA flow studied by micromanipulation. J. Cell Biol. 70:562-572.

Edstrom, J. E., L. Rylander and C. Francke. 1980. Concomitant induction of a Balbiani ring and a giant secretory protein in Chironomus salivary glands. Chromosoma (Berl.) 81:115-124.

Eggleton, K. H., and L. C. Norkin. 1981. Cell killing by SV40: the sequence of ultrastructural alterations leading to cell degeneration and death. Virology 110:73-86.

Egyhazi, E., A. Ossoinak, M. Holst, K. Rosendahl and U. Tayip. 1980. Kinetic analysis of uptake and phosphorylation of 5,6-dichlororibofurandsylbenzimidazole (DRB) by salivary glands cells of Chironomus tentans. J. Biol. Chem. 255:7807-7812.

Ekerdt, R., G. Dahl and M. Gratzl. 1981. Membrane fusion of secretory vesicles and liposomes. Biochim. Biophys. Acta 646:10-22.

Essner, E. 1974. Hemoproteins. In Electron Microscopy of Enzymes. M. Hayat (ed.). Van Nostrand Reinhold Co., New York. pp. 1-33.

Famulski, K., M. Nalecz and L. Wojtczak. 1979. Effect of phosphorylation on microsomal proteins on the surface potential and enzymes activities. FEBS Letters 103:260-264.

Farquhar, M. G. 1978. Recovery of surface membrane in anterior pituitary cells. Variations in traffic detected with anionic and cationic ferritin: J. Cell Biol. 78:R35-R42.

Farquhar, M. G. and G. E. Palade. 1981. The Golgi apparatus (complex)-(1954-1981) from artifact to center stage. J. Cell Biol. 91 (3, Pt. 2) 91:77s-103s.

Feder, J. and I. Giaever. 1980. Adsorption of ferritin. J. Colloid. Interf. Sci. 78:144-154.

Feria-Velasco, A., S. Sanchez-de-la Pena and V. Magdalena. 1976. Labeling of electrical surface charges at synaptosome membrane: an electron cytochemical and biochemical study. Brain Res. 112:214-220.

Friend, D. and M. G. Farquhar. 1967. Function of coated vesicles during protein absorption in rat vas deferens. J. Cell Biol. 35:357-376.

Gad, A. E., B. L. Silver and G. D. Eytan. 1982. Polycation induced fusion of negatively-charged vesicles. Biochim. Biophys. Acta 690:124-132.

Gasic, G., L. Berwick and M. Sorrephino. 1968. Positive and negative colloidal iron as cell surface electron stain. Lab. Invest. 18:63-71.

Gil, J., and O. K. Reiss. 1973. Isolation and characterization of lamellar bodies and tubular myelin from rat lung homogenates. J. Cell Biol. 58:152-171.

Gingell, D. and L. Ginsberg. 1978. Problems in the physical interpretation of membrane interaction and fusion. Cell Surf. Rev. 5:792-833.

Graham, R. and M. J. Karnovsky. 1966. The early stages of absorption of injected horseradish peroxidase in the proximal tubule of mouse kidney. Ultrastructural cytochemistry by a new technique. J. Histochem. Cytochem. 14:291-302.

Grinnell, F., R. Anderson and C. Hackenbrock. 1976. Glutaraldehyde induced alterations of membrane anionic sites. Biochim. Biophys. Acta 426:772-775.

Grinnell, F. and D. Hays. 1979. Measurement of anionic sites on the surfaces of baby hamster kidney cells using radiolabeled polycationic ferritin. Analyt. Biochem. 97:400-402.

Grinnell, F., M. Q. Tobleman, and C. R. Hackenbrock. 1975. The distribution and mobility of anionic sites on the surfaces of baby hamster kidney cells. J. Cell Biol. 66: 470-479.

Grossbach, U. 1977. The salivary gland of Chironomus (Diptera): A model system for the study of cell differentiation. In Results and Problems in Cell

Differentiation, Vol. 8. W. Beerman (ed.). Springer Verlag, Berlin. pp. 147-196.

Gupta, B. L., T. A. Hall and R. B. Moreton. 1977. Electron probe x-ray microanalysis. In Transport of Ions and Water in Animals. B. L. Gupta, R. B. Moreton, J. L. Oschman and B. L. Wall (eds.). Academic Press, London. pp. 83-143.

Gupta, B. L. and T. A. Hall. 1979. Quantitative electron probe x-ray microanalysis of electolytes elements within epithelial tissue compartments. Fed. Proc. 38:144-153.

Hackenbrock, C. R. and K. Miller. 1975. The distribution of anionic sites on the mitochondrial membranes. Visual probing with polycationic ferritin. J. Cell Biol. 65:615-630.

Hammoudah, M. W., S. Nir, T. Isac, R. Kornhauser, T. P. Stewart, S. W. Hui and W. L. Vaz. 1979. Interactions of lanthanum with phosphatidylserine vesicles binding, phase transition, leakage and fusion. Biochim. Biophys. Acta 558:338-343.

Hannig, K. and H. G. Heidrich. 1974. The use of continuous preparative free-flow electrophoresis for dissociating cell fractions and isolation of membraneous components. Methods Enzymol. 31:746-761.

Harrison, P., F. Fishbach, T. Hoy and G. Haggis. 1967. Ferric oxyhydroxide core of ferritin. Nature (Lond.) 216:1188-1190.

Harrod, M. and C. Kastritsis. 1972. Developmental studies in Drosophila II Ultrastructural analysis of the salivary glands of Drosophila pseudoobscura during some stages of development. J. Ultrastruct. Res. 38:482-499.

Haynes, D. H., M. Kobler and S.J. Morris. 1979a. Short and long-range forces involved in cation-induced aggregation of chromaffin granule membranes. J. Theor. Biol. 81:713-743.

Haynes, D. H., J. Lansman, A. E. Cahill and S. J. Morris. 1979b. Kinetics of cation-induced aggregation of Torpedo electric organ synaptic vesicles. Biochim. Biophys. Acta 557:340-353.

Heathcote, J. and M. Grant. 1981. The molecular organization of basement membranes. Int. Rev. Connect. Tiss. Res. 9:191-264.

Heidrich, H., R. Kinne, E. Kinne-Saffran and K. Hannig. 1972. Polarity of proximal tubule cell in rat kidney. Different surface charges for brush border and plasma membrane of basal infoldings. J. Cell Biol. 54:232-245.

Hertner, T., B. Meyer, H. Eppenberger and R. Mahr. 1980. The secretion proteins in Chironomus tentans salivary glands: electrophoretic characterization and molecular weight estimation. W. Roux's Arch. 189:69-72.

Herzog, V. and F. Miller: 1979. Membrane retrieval in epithelial cells of isolated thyroid follicles. Eur. J. Cell Biol. 19:203-215.

Heuser, J. and R. Miledi. 1971. Effect of lanthanum ions on the function and structure of frog neuromuscular junction. Proc. R. Soc. Lond. B 179:247-260.

Hoare, D. G. and D. E. Koshland Jr. 1967. Method for the quantitative modification and estimation of carboxylic acid groups in proteins. J. Biol. Chem. 242:2447-2453.

Hochli, M. and C. Hackenbrock. 1977. Thermotropic lateral motion of intramembrane particles in the inner mitochondrial membrane and its inhibition by artificial peripheral proteins. J. Cell Biol. 72:278-291.

Hockley, D. J. and D. J. McLaren. 1973. Schistosoma mansoni: changes in the outer membrane of the tegument during development from cercaria to adult form. Int. J. Parasitol. 3:13-25.

Holtzman, E. 1976. Lysosomes; A Survey. Cell Biology Monogragh Vol. 3. Springer-Verlag, New York. pp. 298.

Holtzman, E. and R. Dominitz. 1968. Cytochemical studies of lysosomes, Golgi apparatus and endoplasmic reticulum in secretion and protein uptake by adrenal medulla of the rat. J. Histochem. Cytochem. 16:320-336.

Hope, M. J. and P. R. Cullis. 1979. The bilayer stability of inner monolayer lipids from the human erythrocyte. FEBS Letters 107:323-326.

Howell, S. and M. Tyhurst. 1977. Distribution of anionic sites on surface of B cell granule and plasma

membranes: a study using cationic ferritin. J. Cell Sci. 27:289-300.

James, A. 1979. Molecular aspects of biological surfaces. Chem. Soc. Rev. 8:389-418.

Jamieson, J. D. and G. E. Palade. 1977. Production of secretory proteins in animal cells. In International Cell Biology 1976-1977. B.R. Brinkley and K.R. Porter (eds.). Rockefeller University Press, New York. pp. 308-317.

Jones, M. 1975. Biological Interfaces. Elsevier Pub. Co., Amsterdam. pp. 240.

Kahane, I., A. Polliack, E. A. Rachmilewitz, E. A. Bayer and E. Skutelsky. 1978. Distribution of sialic acids on the red blood cell membrane in B thalassaemia. Nature (Lond.) 271:674-675.

Kanwar, Y. S. and M. G. Farquhar. 1979a. Anionic sites in the glomerular basement membrane. In vivo and in vitro localization to the laminae rarae by cationic probes. J. Cell Biol. 81:137-153.

Kanwar, Y. S. and M. G. Farquhar. 1979b. Presence of heparan sulphate in the glomerular basement membrane. Proc. Natl. Acad. Sci. USA 76:1303-1307.

Kanwar, Y. S. and M. G. Farquhar. 1979c. Isolation of glycosaminoglycans (heparan sulfate) from glomerular basement membranes. Proc. Natl. Acad. Sci. USA 76:4493-4497.

Kanwar, Y. S., A. Linker and M. G. Farquahar. 1980. Increased permeability of the glomerular basement membrane to ferritin after removal of glycosaminoglycans (heparan sulphate) by enzyme digestion. J. Cell Biol. 86:688-693.

Kenny, T. and R. R. Shivers. 1974. The blood-brain barrier in a reptile Anolis carolinensis. Tissue and Cell 6:319-333.

Kessel, R. and L. Ganion. 1979. Localization of horseradish peroxidase in the panoistic dragonfly ovary. J. Submicr. Cytol. 11:313-324.

King, B. 1982. The role of coated vesicles in selective transfer across yolk sac epithelium. J. Ultrastruct. Res. 79:273-284.

King, C. and T. Preston. 1977. Studies of anionic sites

on the cell surface of the amoeba Naegleria gruberi using cationized ferritin. J. Cell Sci. 28:133-149.

Lamb, M. and B. Daneholt. 1979. Characterization of active transcription units in Balbiani rings of Chironomus tentans. Cell 17:835-848.

Lambert, B. and B. Daneholt. 1975. Microanalysis of RNA from defined cellular components. Meth. Cell Biol. 10:17-47.

Larsen, W. J. 1976. Cell remodeling in the fat body of an insect. Tissue and Cell 8:73-92.

Laurent, T. 1977. Interaction between proteins and glycosaminoglycans. Fed. Proc. 36:24-27.

Laurie, G., C. LeBlond and G. Martin. 1982. Localization of type IV collagen, laminin, heparan sulfate proteoglycan and fibronectin to the basal lamina of basement membranes. J. Cell Biol. 95:340-344.

Leivo, I. 1983. Basement membrane-like matrix of teratocarcinoma derived endodermal cells. J. Histochem. Cytochem. 31:35-45.

Levine, I. 1978. Physical Chemistry. McGraw Hill Book Co., New York. pp. 847.

Lis, L., W. Lis, V. A. Parsegian and R. P. Rand. 1981a. Adsorption of divalent cations to a variety of phosphtidylcholine bilayers. Biochemistry 20:1771-1777.

Lis, L., V. A. Parsegian and R. P. Rand. 1981b. Binding of divalent cations to dipalmitoylphosphatidylcholine bilayers and its effect on bilayer interaction. Biochemistry 20:1761-1770.

Locke, J., H. McDermid, T. Brac and B. G. Atkinson. 1982. Developmental changes in the synthesis of hemolymph polypeptides and their sequestration by the prepupal fat body in Calpodes ethlius stöll (Lepidoptera:Hesperiidae). Insect Biochem. 12:431-440.

Locke, M. 1969. The structure of an epidermal cell during development of the protein epicuticle and the uptake of molting fluid in an insect. J. Morph. 127:7-40.

Locke, M. 1970. The molt/intermolt cycle in the epidermis and other tissues of an insect Calpodes ethlius

(Lepidoptera; Hesperiidae). Tissue and Cell 2:197-223.

Locke, M. 1983. The structure and development of vacuoles in the fat body of insects. In Insect Ultrastructure. Vol. 2. H. Akai and R. C. King (eds.). Plenum Press, New York. in press.

Locke, M. 1984. A structural analysis of post-embryonic development. In Comprehensive Insect Physiology, Biochemistry and Pharmacology. Vol. 2, Chapt. 2. G.A. Kerkut and L.I. Gilbert (eds.). Pergamon Press, Oxford. in press.

Locke, M. and J. V. Collins. 1967. Protein uptake in multivesicular bodies in the molt-intermolt cycle of an insect. Science (Wash. D.C.) 155:467-469.

Locke, M. and J. V. Collins. 1968. Protein uptake into multivesicular bodies and storage granules in the fat body of an insect. J. Cell Biol. 36:453-483.

Locke, M. and J. V. Collins. 1980. Organelle turnover. In Pathobiology of Cell Membranes. Vol. 2. B. T. Trump and A. U. Arstila (eds.). Academic Press, New York. pp. 223-248.

Locke, M. and P. Huie. 1975. Golgi complex-endoplasmic reticulum transition region has rings of beads. Science (Wash. D. C.) 188:1219-1221.

Locke, M. and P. Huie. 1976a. The beads in the Golgi complex-endoplasmic reticulum region. J. Cell Biol. 70:384-394.

Locke, M. and P. Huie. 1976b. Vertebrate Golgi complexes have beads in a similar position to those found in arthropods. Tissue and Cell 8:739-743.

Locke, M. and P. Huie. 1977. Bismuth staining for light and electron microscopy. Tissue and Cell 9:347-371.

Locke, M. and P. Huie. 1980. Ultrastructural methods in cuticle research. In Cuticle techniques in Arthropods. T. A. Miller (ed.). Springer-Verlag, New York. pp.91-144.

Locke, M. and N. Krishnan. 1973. The formation of the ecdysial droplets and the ecdysial membrane in an insect. Tissue and Cell 5:441-450.

Locke, M. and A. Sykes. 1975. The role of the Golgi complex in the isolation and digestion of organelles.

Tissue and Cell 7:143-158.

Lonn, U. and J. E. Edstrom. 1976. Movements and association of ribosomal subunits in a secretory cell during growth inhibition by starvation. J. Cell Biol. 73:696-704.

Luft, J. H. 1971a. Ruthenium red and violet I Chemistry, purification, methods of use for electron microscopy and mechanism of action. Anat. Rec. 171:347-368.

Luft, J. H. 1971b. Ruthenium red and violent II Fine structural localization in animal tissues. Anat. Rec. 171:369-416.

Mahr, R., B. Meyer, B. Daneholt and H. Eppenberger. 1980. Activation of Balbiani ring genes in Chironomus tentans after pilocarpine induced depletion of the secretory products from the salivary gland lumen. Devel. Biol. 80:409-418.

Mandersloot, J. G., W. J. Gerritsen, J. Leunissen-Bijvett, C. J. Van Echteld, P. C. Noordan and J. Geir. 1981. Calcium-induced changes in the barrier properties of cardiolipin/phosphatidylcholine bilayers. Biochim. Biophys. Acta 640:106-113.

McClintock, J. 1982. Lead staining and phosphatase localizations in the vacuolar system. Thesis, University of Western Ontario, London. pp. 67.

McDermid, H. and M. Locke. 1983. Tyrosine storage vacuoles in insect fat body. Tissue and Cell 15:137-158.

McDiarmid, S., R. Podesta and S. Rahman. 1982. Preparation and partial characterization of a multilamellar body fraction from Schistosoma mansoni. Mol. Biochem. Parasit. 5:93-105.

McLaughlin, S. 1977. Electrostatic potentials of membrane-solution interfaces. Curr. Top. Membr. Trans. 9:71-144.

McNeil, P., T. Hohman and L. Muscatine. 1981. Mechanisms of nutritive endocytosis II The effect of charged agents on phagocytosis recognition by digestive cells. J. Cell Sci. 52:243-269.

Meldolesi, J., N. Borgese, P. DeCamilli and B. Ceccarelli. 1978. Cytopasmic membranes and the secretory process. Cell Surf. Rev. 5:509-627.

Moller, P. and J. Chang. 1978. Internalization of cationized ferritin receptors by rat hepatoma ascites cells. Exp. Cell Res. 114:39-45.

Morris, S. J., V. Chiu and D. H. Haynes. 1979. Divalent cation-induced aggregation of chromaffin membranes. Membrane Biochem. 2:163-201.

Morris, S. J. and R. Schober. 1977. Demonstration of binding sites for divalent and trivalent ions on the outer surface of chromaffin granule membranes. Eur. J. Biochem. 75:1-12.

Muller, K. and U. McMahan. 1976. The shapes of sensory and motor neurons and the distribution of their synapses in ganglia of the leech: a study using intracellular injection of horseradish peroxidase. Proc. R. Soc. Lond. Ser. B 194:481-499.

Mussett, T. 1977. Characterization of hemolymph and fat body related proteins of Calpodes ethlius by isoelectric focussing and the relation of calcium to the control of their secretion from the fat body. Thesis, Dalhousie University, Halifax.

Nalecz, M., Z. Borowski, K. Famulski and L. Wojtczak. 1980. Effect of phospholipid composition on the surface potential of liposomes and the activity of enzymes incorporated. Eur. J. Biochem. 112:75-80.

Nardi, J. 1983. Neuronal pathfinding in developing wings of the moth Manduca sexta. Devel. Biol. 95:163-174.

Nayler, W. G. and J. Harris. 1976. Inhibition by lanthanum of Na^+,K^+-activated, oubain sensitive ATPase enzyme. J. Mol. Cell. Cardiol. 8:811-822.

Neale, E., R. MacDonald and P. Nelson. 1978. Intracellular horseradish peroxidase injection for correlation of light and electron microscopic anatomy with synaptic physiology of cultured mouse spinal cord neurons. Brain Res. 152:265-282.

Nielsen, E. H., J. Clausen and P. Bytzer. 1981. Membrane retrieval in non-exocytic and exocytic rat peritoneal mast cells. Exp. Cell Res. 135:291-298.

Nilsson, J., T. Ksiazek and J. Thyberg. 1983. Endocytosis of cationic and anionic proteins in cultivated arterial smooth muscle cells. Exp. Cell Res. 143:359-365.

Nordt, F. 1980. Alterations in surface charge density

versus changes in surface charge topography in aging red blood cells. Blut 40:233-238.

Novikoff, A. 1980. DAB cytochemistry: artifact problem in its current uses. J. Histochem. Cytochem. 28:1036-1038.

Novikoff, A., P. Novikoff, N. Quintana and C. Daves. 1972. Diffusion artifacts in diaminobenzidene cytochemistry. J. Histochem. Cytochem. 20:745-749.

Olins, A., D. Olins and W. W. Franke. 1980. Stereo electron microscopy of nucleoli, Balbiani rings and endoplasmic reticulum in Chironomus salivary gland cells. Eur. J. Cell Biol. 22:714-723.

Olson, J. L., H. G. Rennke and M. A. Venkatachalam. 1981. Alterations in the charge and size selectivity barrier of the glomerular filter in aminonucleoside nephrosis in rats. Lab. Invest. 44:271-279.

Ottosen, D., P. Courtoy and M. G. Farquhar. 1980. Pathways followed by membrane recovered from the surface of plasma cells and myeloma cells. J. Exp. Med. 152:1-19.

Paine, P. 1975. Nucleocytoplasmic movement of fluorescent tracers microinjected into living salivary gland cells. J. Cell Biol. 66:652-657.

Palade, G. E. 1959. Fuctional changes in the structure of cell components. In Subcellular Particles. T. Hayashi (ed.). Ronald Press Co., New York. pp. 64-83.

Palade, G. E. 1975. Intracellular aspects of the process of protein synthesis. Science (Wash. D.C.) 189:347-358.

Papahadjopoulos, D. 1978. Calcium-induced phase changes and fusion in natural and model membranes. Cell Surf. Rev. 5:766-790.

Parsegian, V. A. 1973. Long range physical forces in the biological milieu. Ann. Rev. Biophys. Bioeng. 2:221-255.

Parsegian, V. A., R. Rand, N. Fuller, M. McAlister, and L. J. Lis. 1979. Molecular forces between and within lipid membranes. Biorheology 16:293-295.

Petty, H. 1980. Response of the resident macrophage to Concanavalin A. Exp. Cell Res. 128:439-454.

Pilar, G. and L. Landmesser. 1976. Ultrastructural differences during embryonic cell death in normal and peripherally derived ciliary ganglia. J. Cell Biol. 68:339-356.

Pinto da Silva, P., P. Moss and H. Fudenberg. 1973. Anionic sites on the membrane intercalated particles of human erythrocyte ghost membranes. Exp. Cell Res. 81:127-138.

Pinto da Silva, P., C. Parkinson and N. Dwyer. 1981. Freeze-fracture cytochemistry: thin section of cells and tissues after labelling of fracture faces. J. Histochem. Cytochem. 29:917-928.

Plattner, H. 1978. Fusion of cellular membranes. In Transport of macromolecules in cellular systems. S. G. Silverstein (ed.). Dahlem Konferenzen, Berlin. pp. 465-488.

Portis, A., C. Newton, W. Pangborn, and D. Papahadjopoulos. 1979. Studies on the mechanism of membrane fusion: evidence for an intermembrane calcium-phospholipid complex, synergism with magnesium and inhibition by spectrin. Biochemistry 18:780-790.

Poste, G. and C. A. Pasternak. 1978. Virus-induced cell fusion. Cell Surf. Rev. 5:306-367.

Rand, R. P. 1981. Interacting phospholipid bilayers: measured forces and induced structural changes. Ann. Rev. Biophys. Bioeng. 10:227-314.

Rennke, H. G., R. S. Cotran and M. A. Venkatachalam. 1975. Role of molecular charge in glomerular permeability. Tracer studies with cationized ferritins. J. Cell Biol. 67:638-646.

Rennke, H. G., Y. Patel and M. A. Venkatachalam. 1978. Glomerular filtration of proteins: clearance of anionic, neutral and cationic horseradish peroxidase in the rat. Kidney Int. 13:324-328.

Rennke, H. G. and M. A. Venkatachalam. 1977. Glomerular permeability: in vivo tracer studies with polyanionic and polycationic ferritins. Kidney Int. 11:44-53.

Rennke, H. G. and M. A. Venkatachalam. 1979. Chemical modification of horseradish peroxidase. J. Histochem. Cytochem. 27:1352-1353.

Rose, B. and R. Rick. 1978. Intracellular pH,

intracellular free calcium and junctional cell-cell coupling. J. Membr. Biol. 44:377-415.

Ryan, K., H. Kalant and E. L. Thomas. 1971. Free flow electrophoresis and electrical surface properties of subcellular particles from guinea pig brain. J. Cell Biol. 49:235-246.

Ryan, U., J. Ryan and D. S. Smith. 1975. Alveolar type II cells: studies on the mode of release of lamellar bodies. Tissue and Cell 7:587-599.

Rylander, L. and J. Edstrom. 1980. Large-sized nascent protein as dominating component during protein synthesis in Chironomus salivary glands. Chromosoma (Berl.) 81:85-99.

Rylander, L., A. Pigon and J. Edstrom. 1980. Sequences translated Balbiani ring 75S RNA in vitro are present in giant secretory protein from Chironomus tentans. Chromosoma (Berl.) 81:101-113.

Sauerheber, R. D., T. S. Zimmermann, J. A. Esgate, W. P. VanderLaan and L. M. Gordon. 1980. Effects of calcium, lanthanum and temperature on the fluidity of spin labeled human platelets. J. Membrane Biol. 52:201-219.

Seligman, A., W. Shannon, Y. Hosino and R. Plapinger. 1973. Some important principles in diaminobenzidene ultrastructural cytochemistry. J. Histochem. Cytochem. 21:756-758.

Shea, S., M. 1971. Lanthanum staining of the surface coat of cells: its enhancement by the use of fixatives containing alcian blue or cetylpyridinium chloride. J. Cell Biol. 51:611-620.

Sherbet, G. V. 1978. The Biophysical Characterization of the Cell Surface. Academic Press, London. pp. 298.

Shinitzky, M. and P. Henkart. 1979. Fluidity of cell membranes: current concepts and trends. Int. Rev. Cytol. 60:121-147.

Shaklai, M. and M. Tavassoli. 1982. Lanthanum as an electron microscope stain. J. Histochem. Cytochem. 30:1325-1330.

Siegal, D. P. and B. R. Ware. 1980. Electokinetic properties of synaptic vesicles and synaptosomal membranes. Biophys. J. 30:159-171.

Simionescu, M., N. Simionescu and G. E. Palade. 1982. Preferential distribution of anionic sites on the basement membrane and abluminal aspect of the endothelium in fenestrated capillaries. J. Cell Biol. 95:425-434.

Simonneau, M., G. Baux and L. Tauc. 1980. Sialic acid containing substrates as intracellular calcium receptors involved in transmitter release. J. Physiol. (Paris) 76:427-433.

Skutelsky, E., S. Hoglund, B. Morein and E. A. Bayer. 1978. On the ultrastructural localization of cell surface sialyl residues versus anionic sites. Ninth International Congress on Electron Microscopy, Toronto, Vol. 2, 294-295.

Skutelsky, E. and E. A. Bayer. 1979. The ultrastructural localization of cell surface glycoconjugates: affinity cytochemistry via avidin-biotin complex. Biol. Cellulaire 36:237-252.

Smith, W. and H. F. Nijhout. 1982. In vitro stimulation of cell death in moulting glands of Oncopeltus fasciatus by 20-hydroxyecdysone. J. Insect Physiol. 29:169-176.

Sohal, R., P. Peters and T. Hall. 1976. Fine structure and x-ray microanalysis of mineralized concretions in the malpighian tubules of the housefly, Musca domestica. Tissue and Cell 8:447-458.

Sohal, R., P. Peters and T. Hall. 1977. Origin, structure, composition and age-dependence of mineralized dense bodies (concretions) in the midgut epithelium of the adult housefly Musca domestica. Tissue and Cell 9:87-102.

Steinman, R., I. Mellman, W. Muller and Z. A. Cohn. 1983. Endocytosis and the recycling of plasma membrane. J. Cell Biol. 96:1-27.

Stratton, C. 1978. The ultrastructure of multilamellar bodies and surfactant in the human lung. Cell Tiss. Res. 193:219-229.

Straus, W. 1964. Factors affecting the state of injected horseradish peroxidase in animal tissues and procedures for the study of phagosomes and phagolysosomes. J. Histochem. Cytochem. 12:470-479.

Sturgess, J., M. Moscarello and H. Schachter. 1978. The

structure and biosynthesis of membrane glycoproteins. Curr. Top. Membr. Transp. 11:16-105.

Tanford, C. 1979. The Hydrophobic Effect: formation of Micelles and Biological Membranes. J. Wiley and Sons, New York. pp.233.

Tartakoff, A., P. Vassali and R. Montesano. 1981. Plasma cell endocytosis: is it related to immunoglobulin secretion? Eur. J. Cell Biol. 26:188-197.

Tedeschi, H., J. M. James and W. Anthony. 1963. Photometric evidence for the osmotic behaviour of rat liver microsomes. J. Cell Biol. 18:503-513.

Telfer, W., E. Huebner and D. S. Smith. 1982. The cell biology of vitellogenic follicles in Hyalophora and Rhodnius. In Insect Ultrastructure. R. King and H. Akai (eds.). Plenum Press, New York. pp. 118-149.

Thyberg, J. 1980. Internalization of cationized ferritin into the Golgi complex of cultured mouse peritoneal macrophages. Effects of colchicine and cytochalasin B. Eur. J. Cell Biol. 23:95-103.

Thyberg, J., J. Nielsson and D. Hellgren. 1980. Recirculation of cationized ferritin in cultured mouse peritoneal macrophages. Electron microscopic and cytochemical studies with double labeling technique. Eur. J. Cell Biol. 23:85-94.

Ting-Beall, H. 1979. Interaction of uranyl ions with lipid bilayer membrane. J. Microscop. (Oxf.) 118:221-227.

Van Deurs, B. and K. Nilausen. 1982. Pinocytosis in mouse L-fibroblasts: ultrastructural evidence for a direct membrane shuttle between the plasma membrane and the lysosomal compartment. J. Cell Biol. 94:279-286.

Van Deurs, B., K. Nilausen, O. Faergeman and H. Meinertz. 1982. Coated pits and pinocytosis of cationized ferritin in human skin fibroblasts. Eur. J. Cell Biol. 27:270-278.

Van Deurs, B., F. Von Bulow and M. Moller. 1981. Vesicular transport of cationized ferritin by the epithelium of the rat choroid plexus. J. Cell Biol. 89:131-139.

Verwey, E. J. W. and J. Th. G. Overbeek. 1948.

Theory of the Stability of Lyphobic Colloids. Elsevier, Amsterdam. pp. 205.

Vincent, M. and R. Tanguay. 1979. Heat shock induced proteins present in the cell nucleus of Chironomus tentans. Nature (Lond.) 281:501-503.

Virtanen, I. 1978. Asymmetric distribution of anionic sites on rat liver nuclear membranes. Cell Biol. Int. Rep. 2:33-39.

Virtanen, I. and J. Wartiovaara. 1974. Visualization of charged groups on the surface of rat liver nuclei. J. Cell Sci. 16:665-675.

Wagner, S., A. Keith and W. Snipes. 1980. Interaction of divalent cations and proteins with phospholipid vesicles. Biochim. Biophys. Acta 600:367-375.

Walker, D. 1981. Cationic ferritin binding sites and surface charge densities of transformed cells. J. Histochem. Cytochem. 29:255-265.

Wallach, D. F. H., V. B. Kamat, and M. Gail. 1966. Physico-chemical differences between fragments of plasma membrane and endoplasmic reticulum. J. Cell Biol. 30:601-621.

Webster, D. 1982. The major hemolymph proteins of an insect. Thesis, University of Wester Ontario, London.

Weinberger, C. and I. Brick. 1980. Locomotion and adhesion of amphibian gastrula and neurula cells cultured on substrata of varied surface charge. Exp Cell Res. 130:251-263.

Weiss, G. B. 1974. Cellular pharmacology of lanthanum. Ann. Rev. Pharmacol. 14:343-354.

Weiss, L. 1969. The cell periphery. Int. Rev. Cytol. 26:63-105.

Wick, S. M. and P. K. Hepler. 1980. Localization of calcium containing antimonate precipitates during mitosis. J. Cell Biol. 86:500-513.

Williams, D. and A. D. Blest. 1980. Extracellular shedding of photoreceptor membrane in the open rhabdom of a tipulid fly. Cell Tiss. Res. 205:423-438.

Williams, M. A. 1977. Quantitative Methods in Biology. Elsevier/North Holland Biomedical Press, Amsterdam. pp. 234.

Williams, M. C. 1982. A possible endocytic pathway for the return of secreted surfactant to lamellar bodies. J. Cell Biol. 95 (2 Pt.2):388a (Abstr.).

Wojtczak, L. and M. Nalecz. 1979. Surface charge of biological membranes as a possible regulator of membrane bound enzymes. Eur. J. Biochem. 94:99-107.

Woodruff, R. and W. H. Telfer. 1973. Polarized intercellular bridges in ovarian follicles of the Cecropia moth. J. Cell Biol. 58:172-188.

Woodruff, R. and W. H. Telfer. 1980. Electrophoresis of proteins in intercellular bridges. Nature (Lond.) 286:84-86.

Wright, T., B. Smith, B. Ware and M. J. Karnovsky. 1980. The role of negative charge in spontaneous aggregation of transformed and untransformed cell lines. J. Cell Sci. 45:99-117.

Wyatt, G. 1980. The fat body as a protein factory. In Insect Biology in the Future "VBW 80". M. Locke and D. S. Smith (eds.). Academic Press, New York. pp. 201-225.

Zar, J. H. 1974. Biostatistical Analysis. Prentice-Hall Inc., Englewood Cliffs N. J. pp. 620.

END

20103184

FIN